Cancer Cell Behaviour Following Parasite Exposure

Brittany-Amber Jacobs

Supervisor: Dr Katherine Smith

Co-supervisor: Professor Sharon Prince

Division of Immunology

Department of Pathology

Presented for MSc Med in Clinical Science and Immunology

Faculty of Health Sciences

University of Cape Town

August 2018

Acknowledgements

Dr Katherine Smith, thank you for always encouraging and supporting me. I am grateful for your endless patience and for regularly reminding me that Science does not have to be so serious. Someday I hope to be as inspirational to one of my students.

Professor Sharon Prince, thank you for accepting me into your laboratory. From day one I have felt extremely welcome and appreciated. Your enthusiasm for your research has inspired me to find something that I feel as passionate about. I truly value the time and effort you put into helping me become better student, scientist and person.

I would like to thank the **Prince Lab** and **Dr Jade Peres** for being so accommodating of me and creating an environment where Science is both fun and challenging. Most importantly, thank you **Jenna Bleloch**, **Alexis Neumann** and **Brunette Katsandegwaza**. I am tremendously grateful for the time you took out of your busy PhD schedules to help me. The past two years year would not have been the same without your friendship.

To **Associate Professor William Horsnell, Dr Matthew Darby, Dr Tarryn Willmer, Alisha Chetty** and **Dr Georgia Shäfer** thank you for your contributions to this project and for the much-needed advice you have given me.

Thank you to **Professor Awen Gallimore**, **Dr Sarah Lauder**, **Michelle Somerville** and **Kathryn Smart** for welcoming me to Cardiff University and for making me feel at home for the 4 months that I was with you.

Lastly, to **my family**, thank you for being my biggest supporters. **Mom** and **Dad**, you always taught me to never give up and I hope that I have made you proud.

This work was generously supported by the Oppenheimer Memorial Trust, The National Research Foundation and The National-Research Foundation – Deutscher Akademischer Austausch Dienst Scholarship. Opinions expressed, and conclusions arrived at, are those of the author and are not necessarily to be attributed to the NRF.

Research Outputs

Publications

Jacobs B-A, Chetty A, Horsnell WGC, Schäfer G, Prince S, Smith KA. 2018. Hookworm exposure decreases human papillomavirus uptake and cervical cancer cell migration through systemic regulation of epithelial-mesenchymal transition marker expression. Scientific Reports **8:**11547. http://www.nature.com/articles/s41598-018-30058-9

Conferences

Presenter at the South African Society of Biochemistry and Molecular Biology (SASBMB) and the Federation of African Societies of Biochemistry and Molecular Biology (FASBMB) conference (8-11 July 2018), North West University. Talk title (9 July 2018): Cancer Cell Behaviour Following Parasite Exposure

Presenter/Poster Presentation (TBA) at Molecular and Cellular Biology of Helminth Parasites VI conference (2-7 September 2018), Hydra, Greece. Talk title: Cancer Cell Behaviour Following Parasite Exposure

Research Presentations

Presenter at a Co-Infection Seminar: Helminth-Mediated Modulation of Bystander Immune Responses (7-8 March), University of Cape Town. Talk title (8 March): Cancer Cell Behaviour Following Parasite Exposure

Poster presentation at the University of Cape Town Human Biology/Integrative Biomedical Sciences/Pathology Postgraduate Research Day (27 September)

Presenter at a Cell Biology Seminar: Division of Cell Biology Lunchtime Research Seminars, University of Cape Town. Talk title (28 September 2017 and 27 February 2018): Cancer Cell Behaviour Following Parasite Exposure

Plagiarism Declaration

This thesis/dissertation has been submitted to the Turnitin module and I confirm that my supervisor has seen my report and any concerns revealed by such have been resolved with my supervisor.

Signature

Signed by candidate

Date: 6 August 2018

Table of Contents

List of Abbreviations

AAMΦ – Alternatively-activated macrophages
AOM – Azoxymethane
APC – Adenomatous polyposis coli
Apc – allophycocyanin
ATCC – American Type Culture Collection
BrdU – Bromodeoxyuridine
Brev A – Brefaldin A
BV – Brilliant Violet
BSA – Bovine Serum Albumin
CAC – Colitis-Associated Colorectal Cancer
CAMΦ – Classically-activated macrophages
CCA – Cholangiocarcinoma
CD – Crohn's Disease
CFSE - Carboxyfluorescein Succinimidyl Ester
CHO – Chinese Hamster Ovary
CRC – Colorectal Cancer
DALY – Disability-Adjusted Life Years
DAPI - 4',6-diamidino-2-phenylindole
DC – Dendritic Cell
dLN – Draining Lymph Node
DSS – Dextran Sulphate Sodium
DMEM – Dulbecco's Modified Eagle Medium
DNBS – Dinitrobenzene Sulfonic Acid
EBV – Epstein Barr Virus
ECL – Enhanced Chemiluminescence
ECM – Extracellular Matrix
EDTA – Ethylenediaminetetraacetic acid
EMT – Epithelial-Mesenchymal Transition
ES – Excretory-Secretory
FBS – Foetal Bovine Serum
FGS – Female Genital Schistosomiasis
FGT – Female Genital Tract
FITC – Fluorescein isothiocyanate
Foxp3 – Forkhead box p3
HBV – Hepatitis B Virus

HCV – Hepatitis C Virus

HES – *Heligmosomoides polygyrus* excretory-secretory product

HEV – High Endothelial Venule

HIC – High-Income Countries

HPV – Human Papillomavirus

HTLV-1 – Human T-Cell Leukemia/Lymphoma Virus Type 1 (HTLV-1)

IBD – Inflammatory Bowel Disease

IL-4Rα – IL-4 Receptor Alpha

ILC – Innate Lymphoid Cells

ILC-2 – Group 2 Innate Lymphoid Cells

IP injection – Intraperitoneal Injection

LAL - *Limulus* Amoebocyte Lysate

LMIC – Low- and middle-income countries

LPS – Lipopolysaccharide

MALT – Mucosal Associated Lymphoid Tissue

MC – Mast cell

MCPyV – Merkel Cell Polyomavirus (MCPyV)

miRNA – microRNA

MLN – Mesenteric Lymph Node

MTT – Methylthiazol Tetrazolium

ndLN – Non-Draining Lymph Node

OD – Optical Density

PBS and PBS/T – Phosphate Buffered Saline and Phosphate Buffered Saline/Tween

pRB – Phosphorylated Retinoblastoma

PE – Phycoerythrin

PerCp – Peridinin Chlorophyll Protein

PerCpCy5.5 – Peridinin Chlorophyll Protein Cyanine 5.5

PeCy7 – Phycoerythrin Cyanine 7

PMA – Phorbol Myristate Acetate

Rpm – Revolutions per minute

RPMI – Roswell Park Memorial Institute Medium

RSV – Respiratory Syncytial Virus

SCC – Squamous Cell Carcinoma

SDS-PAGE – Sodium-Dodecyl-Sulphate Polyacrylamide Gel Electrophoresis

SEA – *Schistosoma mansoni* Egg Antigen

STH - Soil-Transmitted Helminths

T1D – Type 1 Diabetes

T2D – Type 2 Diabetes

TBS and TBS/T – Tris-Buffered Saline and Tris-Buffered Saline/Tween

TcES – *Taenia crassiceps* excretory-secretory product

TGF-β – Transforming Growth Factor β

Th1 – Type-1 immune response

Th2 – Type-2 immune response

Th17 – Type-17 immune response

TNBS – Trinitrobenzene Sulphonic Acid

Tregs – Regulatory T cells

TspES – *Trichinella spiralis* excretory-secretory product

UC – Ulcerative Colitis

UGS – Urogenital Schistosomiasis

UV – Ultraviolet

List of Figures

Abstract

Infectious diseases, including helminthiases, are estimated to cause 16.1% of global cancer cases. While certain helminths are conclusive causes of cancer, others have been shown to reduce the disease. It is currently unknown why differing helminth infections promote or prevent cancer development and progression, or which cellular mechanisms are altered following exposure. Using several *in vitro* and *in vivo* techniques, this study aimed to determine the effect that certain helminths have on the progression of cervical and colorectal cancer. The results revealed that antigen from the hookworm *Nippostrongylus brasiliensis* significantly reduced cervical cancer cell migration and the expression of two markers of metastasis: vimentin and N-cadherin. Importantly, *N. brasiliensis* antigen significantly lowered the expression of cell-surface vimentin, while decreasing Human Papillomavirus type16 pseudovirion internalization. *In vivo* infection with *N. brasiliensis* significantly decreased vimentin expression within the female genital tract, confirming the relevance of these *in vitro* findings. Furthermore, exposure to antigen from the gastrointestinal nematode *Heligmosomoides polygyrus* decreased the *in vitro* proliferation of human and mouse colorectal cancer cells and simultaneously increased the expression of cell cycle regulator proteins, p53 and p21. Surprisingly, while antigen from *H. polygyrus* inhibited human colorectal cancer cell migration, it had the opposite effect on mouse colorectal cancer cells, suggesting that its impact on colorectal cancer migration may be, at the very least, species dependent. Using a syngeneic tumour model, the excretory-secretory product from *H. polygyrus* was shown to significantly increase tumour growth and the expansion of regulatory T cells and neutrophils in the tumour. Similarly, in a model of colitis-associated colorectal cancer this antigen significantly worsened pathology in a TGF-β dependent manner. Undoubtedly, the knowledge gained from this study will contribute to the limited understanding about helminths and the effect that these parasites have on cancer progression.

1. Introduction

1.1 Cancer

Cancer is a disease characterised by uncontrolled cell proliferation which has the potential to spread throughout the body (National Health Service, 2016). Importantly, over recent years, inflammation has been shown to play a critical role in tumour progression (1). Cancer causes significant worldwide morbidity and mortality with an estimated 14.1 million new cases and 8.2 million deaths occurring in 2012 alone (2). Notably, the cancer burden is more prominent in low- and middle-income countries (LMIC) where it accounts for 57% of cases and 65% of deaths. It is estimated that over the next two decades the incidence of cancer will increase by 45.6% in LMIC, whereas it will increase by 23.7% in High Income Countries (HIC) (**Figure 1.1**) (GLOBOCAN, 2012).

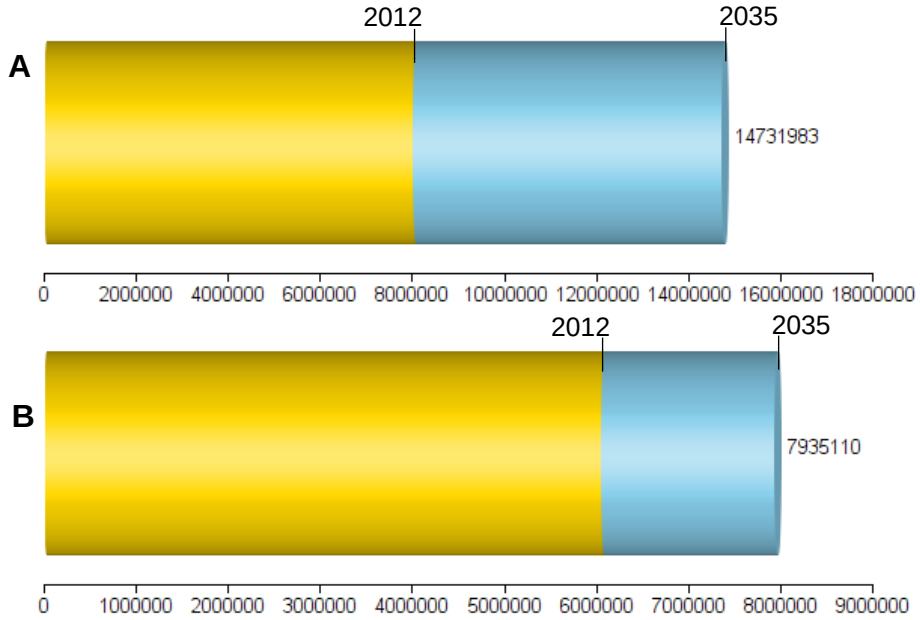

Figure 1.1: The predicted cancer incidence in 2035 in **A.** LMIC compared to **B.** HIC, adapted from GLOBOCAN 2012. Yellow areas indicate the worldwide cancer incidence in 2012 and blue areas indicate the predicted increase in cancer incidence between 2012 and 2035. The x-axis represents the number of individual cancer cases.

It has been predicted that four in ten cancer cases could be prevented by reducing specific risk factors. These include smoking, exposure to ultraviolet (UV) radiation, an unbalanced diet and overeating, minimal physical exercise, excessive alcohol consumption and contact with certain infectious diseases (Cancer Research UK).

In developing regions significantly more cancer cases are attributable to chronic infectious diseases. Astoundingly, more than a third of new cancer cases in sub-Saharan Africa are attributable to chronic infectious disease (**Figure 1.2**) (3, 4). Epstein Barr Virus (EBV), Hepatitis B and C Viruses (HBV and HCV), Kaposi Sarcoma-Associated Herpesvirus, Human

Papillomavirus (HPV), Merkel Cell Polyomavirus (MCPyV) and Human T-Cell Leukaemia/Lymphoma Virus Type 1 (HTLV-1) are all strongly associated with an increased risk of cancer development. Furthermore, the bacterium *Helicobacter pylori*, which the Centre for Disease Control estimates to be present within two-thirds of the population, can cause gastric cancer as well as Mucosal Associated Lymphoid Tissue (MALT) lymphoma (3, 4).

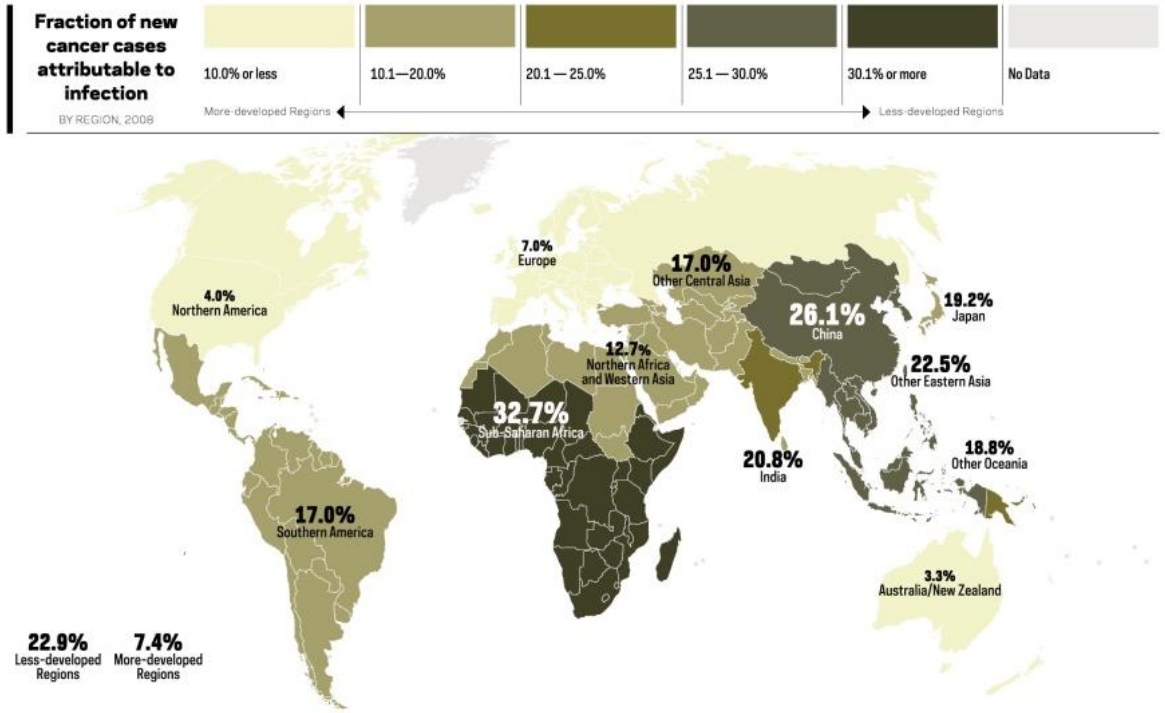

Figure 1.2: The proportion of worldwide cancer cases caused by infectious diseases, adapted from American Cancer Society 2017 (4).

While less thoroughly understood, some helminth infections have also been linked to an elevated risk of developing certain cancers. For example, *S. haematobium, Opisthorchis viverrini* and *Clonorchis sinensis* are all classified as group one biological carcinogens and are conclusive causes of cancer (5-7).

1.2 Helminths

Helminths are one of the most common infectious agents in LMIC, infecting over a billion people in sub-Saharan Africa, Asia and the Americas (**Figure 1.3**) (8, 9). These large, multicellular parasitic worms have a considerable disease burden resulting in the loss of 14 million disability-adjusted life years (DALY - the amount of years lost due to illnesses, disability or premature death) (8). The gastrointestinal tract of an individual living in a developing country is likely to be parasitised by one if not all three of the leading soil-transmitted helminths (STH): roundworms (*Ascaris lumbricoides*), hookworms (*Necator americanus* or *Ancylostoma*

duodenale) and whipworms (*Trichuris trichiura*) (10). Globally, 807 million people are infected with roundworms, 700 million are infected with hookworms and 604 million are infected with whipworms (The End Fund, 2016). Furthermore, each year an estimated 240 million people are infected with the vascular trematode Schistosoma. Schistosomiasis ranks second to malaria as the most prevalent parasitic disease (Global Network – Neglected Tropical Diseases, 2016).

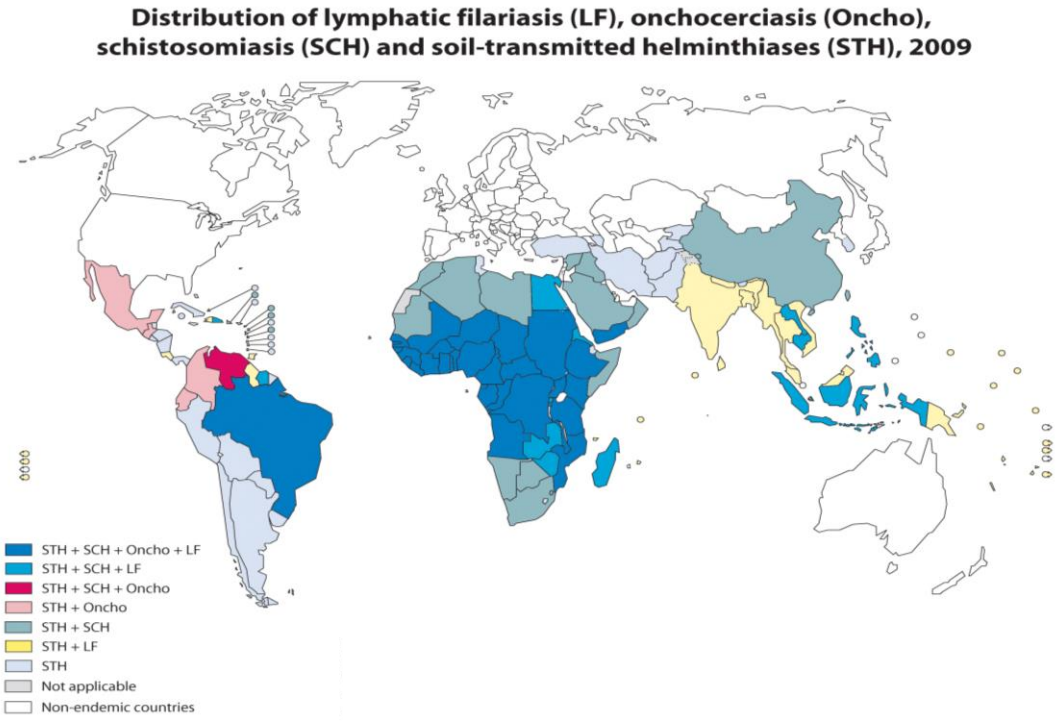

Figure 1.3: Worldwide helminth prevalence, adapted from the World Health Organisation 2009.

1.3 The Immune Response to Helminths

As seen in **Figure 1.4**, helminth infections are typically characterised by a type-2 (Th2) immune response (11). This response centres around the production of specific cytokines (IL-4, IL-5, IL-9, IL-10 and IL-13), which limit type-1 (Th1) immune responses while amplifying Th2 immunity (12). In addition, the action of B cells and cells of the innate immune system, including dendritic cells (DCs), eosinophils, mast cells (MCs), type 2 innate-lymphoid cells (ILC-2s) and basophils all contribute to efficiently expelling the parasite (13).

The differentiation of Th2 cells depends on the activation of transcription factors STAT6 and STAT5 by cytokines IL-4 and IL-2 respectively. Activation of STAT6 results in the expression of GATA3, which together with STAT5 causes the expression of Th2 specific genes. Following infection with the murine gastrointestinal nematode *Heligmosomoides polygyrus,* transgenic mice overexpressing GATA3 produced significantly higher amounts of IL-5 and IL-13

highlighting the critical role of GATA3 in controlling the production of Th2 cytokines (14). Importantly, helminths, including *H. polygyrus,* are understood to promote the development of an anti-inflammatory immune tolerant environment in order to facilitate their survival in the host (15). This involves the amplification of regulatory cell populations including regulatory T cells (Tregs), regulatory B cells and alternatively activated macrophages (AAMΦ). Moreover, helminth infections favour the production of anti-inflammatory cytokines (IL-4, IL-10 and Transforming Growth Factor β) over the pro-inflammatory cytokines (IL-17 and IFN-ɣ) (13, 16, 17).

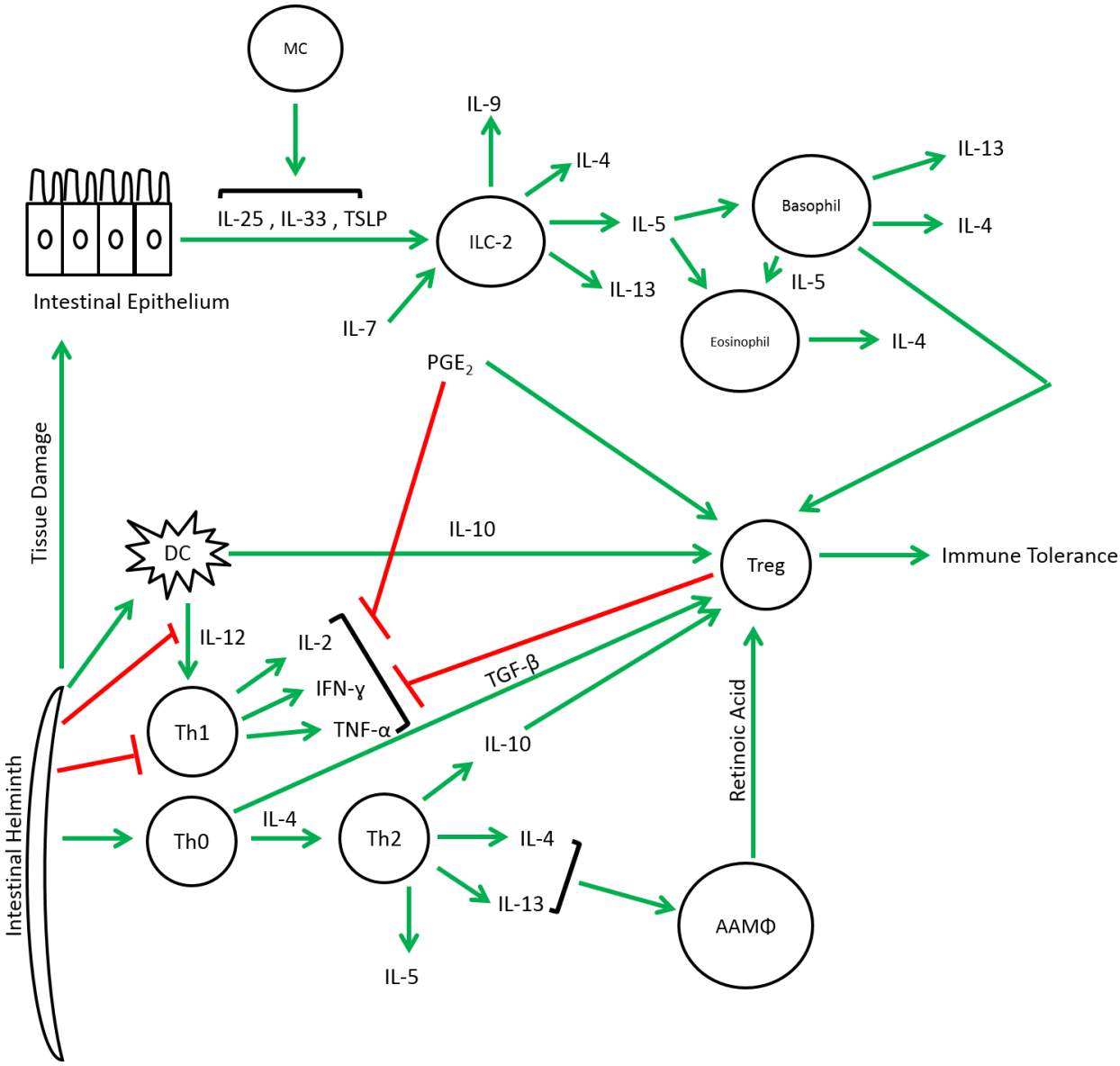

Figure 1.4: The immune response induced by intestinal helminths.

Tregs play a crucial role in immune suppression and limiting the development of autoimmune diseases (18, 19). This cell population is made up of natural Tregs, which are produced in the

thymus, and inducible Tregs, which are derived from circulating conventional T cells in the presence of IL-10, TGF-β and retinoic acid (20-22). Notably, both subsets constitutively express the transcription factor Forkhead Box P3 (Foxp3) (23). Certain helminths, including *H. polygyrus, Brugia malayi, Echinococcus granulosus*, *Schistosoma mansoni* and *Trichinella spiralis*, expand the Foxp3+ T cell population thereby contributing to immune suppression, limiting damage to the host and favouring survival of the parasite (16, 24-27). Unsurprisingly, several studies have shown that due to an enhanced Th2 response, Treg depletion in the host promotes parasite expulsion (28-30). The excretory-secretory (ES) products secreted by helminths similarly contributes towards suppression of the host immune response (27, 31, 32). Of particular relevance to the current study is *H. polygyrus* ES (HES), which contains an equivalent of the mammalian TGF-β and induces *de novo* Foxp3+ T cell population expansion in mice and humans (16, 33).

In addition to Tregs, helminths promote the AAMΦ populations. In response to pro-inflammatory cytokines such as IFN-ɣ, bone-marrow derived macrophages differentiate into classically activated macrophages (CAMΦs) and in contrast, anti-inflammatory cytokines cause bone-marrow derived macrophages to differentiate into AAMΦs (34). In response to intestinal helminth infection, IL-4 and IL-13 stimulate the production of AAMΦs which function to dampen the inflammatory response to the parasite, repair tissue damage and, through their production of retinoic acid, induce the differentiation of Tregs (35, 36). However, AAMΦs can also play a role in parasite expulsion in part by causing morphological and functional changes to the smooth muscle of the host intestinal lumen and by limiting larvae motility, thus further reducing host tissue damage (37-40).

ILCs are a critical component of innate immunity, regulating inflammation and tissue homeostasis (41). ILCs depend on IL-7 for their development and maintenance and can be further divided into three subsets depending on effector functions, cytokine expression and transcriptional profile (42). Fully matured Group 2 ILCs (ILC-2s) play a crucial role in initiating and amplifying *in vivo* Th2 responses which are important for helminth expulsion (43). Following helminth-induced tissue damage, ILC-2s are activated by epithelial cytokine alarmins IL-25, thymic stromal lymphopoietin (TSLP) and IL-33 and release IL-5, IL-9, IL-13 and a small amount of IL-4 (44, 45). Furthermore, IL-25 release by intestinal tuft cells (a chemosensory cell population located in the intestinal epithelium) induces IL-13 production by ILC-2s, which expands the tuft cell population, and further promotes the development of a Th2 response and parasite expulsion (46, 47). Naturally, ILC-2 activation is targeted as a mechanism for immune evasion by helminths. MHCII-expressing ILC-2s interact with antigen-specific T cells and thereby initiate and amplify IL-13 production (48). For this reason, depletion of MHCII on ILC-2s in *N. brasiliensis* infected mice decreased the potential for

helminth elimination and was associated with decreased IL-13 levels. Similarly, *H. polygyrus* promotes the release of host-derived IL-1β, causing decreased IL-33 and IL-25 production, and ultimately reduced ILC-2 activation and impaired helminth elimination (49). *H. polygyrus* derived HES has also been shown to decrease IL-33 production and ILC-2-derived Th2 cytokine release in order to prevent the development of a Th2 response (50).

In addition to the responses mentioned above, helminth infections have multiple other effects on the cells of the host immune system. Antigen-presenting cells, including DCs, have likewise been implicated in contributing towards the Th2 response to helminthiases (51). CD11c (hi) and CD11c (lo) DCs induce antigen-specific CD4+ T cell activation and Treg production respectively (52, 53). Furthermore, helminth-activated DCs produce IL-10 and in doing so, further stimulate the development of Tregs (54). Basophils are similarly central to the effector phase of the Th2 immune response by releasing IL-4, IL-5 and IL-13 which promote AAMΦ differentiation and eosinophilia (55). MCs play a role in orchestrating a Th2 immune response via the regulation of tissue-derived cytokines and prostaglandin E_2 contributes to a Th2 immune response by inhibiting pro-inflammatory cell attraction and the production of Th1 cytokines (56, 57).

1.4 Systemic Immune Suppression Caused by Helminth Infection

In addition to the local response induced by helminths, these parasites can also have systemic effects on the immune system. There is epidemiological evidence to suggest that helminth infections can dampen the efficacy of vaccination. In sub-Saharan Africa, vaccinated infants born to woman who had lymphatic filariasis, schistosomiasis, or hookworm infection during pregnancy had an impaired ability to develop an IgG response to *Haemophilus influenza*, diphtheria, hepatitis B and tetanus toxoid antigen (58). Moreover, tetanus toxoid-specific antibody titres and IFN-ɣ levels were found to be lower in vaccinated individuals previously infected with the nematode *Onchocerca volvulus* (59).

These parasitic worms are also able to alter the immune response to co-infection with viruses. An epidemiological study in Uganda revealed that 35% of HIV-positive participants were infected with the hookworm *N. americanus* and consequently, had further reduced CD4+ T cell counts (60). Furthermore, mice co-infected with *Vaccinia* virus and the roundworm *A. lumbricoides* had an increased mortality rate and elevated lung viral titres compared to virus-only infected mice (61). This correlated with a reduced virus-specific immune response involving CD8+ T cells and IFN-ɣ producing CD4+ T cells. In contrast, *H. polygyrus* infection lessened lung inflammation and viral load in mice co-infected with Respiratory Syncytial Virus

(RSV) in a Th2 independent manner involving type 1 interferon signalling and the microbiome (62).

Helminth infection likewise alters the immune response to bacterial co-infection. Individuals with latent tuberculosis who were co-infected with the roundworm *Strongyloides stercoralis* had reduced levels of all B cell subsets, and subsequently lowered IgG and IgM, which was reversed following anthelmintic treatment (63). *H. polygyrus* and *Citrobacter rodentium* co-infected mice had increased morbidity and mortality accompanied by *C. rodentium*-associated intestinal injury, elevated TNF-α and reduced IFN-ɣ levels. Significantly, co-infected STAT6 knockout mice did not establish a robust *C. rodentium* infection highlighting the Th2 mechanism that helminths employ to influence host susceptibility to bacterial infections (64). In the same way, mice infected with *H. polygyrus* and *S. typhimurium* establish advanced colonic inflammation, compared to *S. typhimurium* only infected mice, and have increased morbidity relating to elevated IL-10 and lowered neutrophil recruitment (65). *H. polygyrus* infection has also been shown to alter the intestinal metabolome leading to an enhanced susceptibility to *S. typhimurium* co-infection (66).

Of significant interest is that helminth infections can benefit the host, limiting autoimmune and allergic symptoms in infected hosts. Short-term infection with *H. polygyrus* prevented the onset of disease in a murine model of type 1 diabetes (T1D), which was associated with reduced STAT6 expression, decreased Foxp3+ T cell population expansion and elevated IL-10 levels (67). Blocking IL-10 signalling in non-obese diabetic (NOD) IL-4 knockout mice (IL-$4^{-/-}$) reversed this effect and caused pancreatic β-cell destruction and the onset of T1D. However, CD4+ T cell transfer from infected mice to NOD IL-$4^{-/-}$ mice did not result in the development of T1D, highlighting the possibility that *H. polygyrus* protects against T1D in an IL-10 dependent but Th2 independent manner. The Th2 immune response elicited by infection with *H. polygyrus* has also been shown to contribute towards the control of type 2 diabetes (T2D) (68). Using a murine model of T2D (KK-Ay/TaJcl mice), *H. polygyrus* infection resulted in improved blood glucose levels and decreased the levels of markers associated with T2D in the liver. This seemingly protective effect of helminth exposure on the risk of developing diabetes was also observed in a large cohort in southern India. This study revealed that 2.6% of glucose tolerant individuals had a lymphatic filariasis infection compared to 0% in individuals with T1D (69). Additionally, filarial-specific antibodies were present in 28% of healthy participants compared to only 2% in T1D individuals.

Treatment with *Trichuris suis* ES before onset of autoimmune encephalomyelitis, a murine model of multiple sclerosis, decreased the inflammatory Th1 and type-17 (Th17) immune responses in the spinal cord and spleen and ultimately lowered disease severity (70). In two

independent models of arthritis, *N. brasiliensis* and *H. polygyrus* infection prevented bone loss and arthritis severity associated with an elevated Th2 response and diminished levels of pro-inflammatory cytokines in the joints (71, 72). In a murine model of atopic asthma, *H. polygyrus* infection suppressed allergen-induced bronchial hyper-reactivity associated with lowered airway eosinophilia and increased IL-10 dependent Treg production (73). A similar result can be observed when sensitized mice are treated with HES, however this effect was associated with lowered ILC-2 activation (74, 75). Furthermore, in a murine model of allergic airway inflammation, compared with sensitized and airway challenged controls *H. polygyrus* infected mice had reduced eosinophil and lymphocyte recruitment into the lungs and decreased allergen-specific IgE levels and airway hyper-reactivity (76).

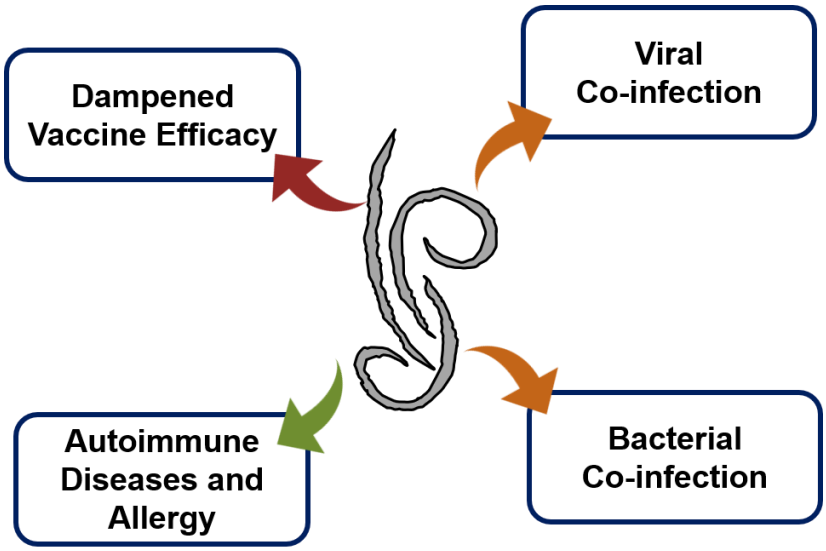

Figure 1.5: Summary of the effect of helminth infection on vaccine efficacy, autoimmune diseases and allergy and viral and bacterial co-infection. Beneficial outcomes are depicted with green arrows, detrimental outcomes with red arrows and both beneficial and detrimental outcomes with orange arrows.

The immune-regulatory properties demonstrated following helminth infection could suggest a favourable outcome when used in the treatment of chronic inflammatory diseases. Cancer is an inflammatory condition accompanied by an immune response mediated mostly by INF-ɣ (77-79). As previously described, the Th2 response induced by helminth infections does not favour INF-ɣ production and it is, therefore possible that helminths could exacerbate cancer progression by limiting the anti-tumour immune response (11).

1.5 Helminths and Cancer

While the direct impact of helminths on cancer development and progression is unknown, these parasites have been shown to influence susceptibility to cancer-causing viruses and bacteria. A recent study showed that persistent STH infection, with *S. stercoralis*, hookworm,

A. lumbricoides, and/or *Trichuris trichurid*, alters the immune response to favour HPV infection and as a result significantly increases HPV prevalence and consequently the risk of cervical cancer development (80). Furthermore, STHs are able to activate the oncogenic Kaposi's sarcoma herpesvirus from latency greatly increasing the risk of developing Kaposi's sarcoma in the future (81).

The carcinogenic trematode *O. viverrini* greatly increases the risk of cholangiocarcinoma (CCA) development. However, when co-infected with the bacterium *H. pylori,* which is strongly associated with an increased risk of gastric cancer, increased *H. pylori* growth, liver fibrosis and expression of pro-inflammatory cytokines was observed (82, 83). In contrast, *S. mansoni* and several other STHs have been shown to reduce the risk of *H. pylori*-induced gastric cancer by dampening the Th1 response initiated by the cancer-causing bacterium (84-90).

Currently, a consensus on how STH infections impact cancer development and progression has not been reached.

1.6 Cervical Cancer and Helminths

Globally, cervical cancer is the fourth most common cancer in woman, causing an estimated 266 000 deaths in 2012. Significantly, 87% of cervical cancer-related deaths occur in LMIC and it is estimated that by 2035, the incidence will increase by 58% (from 444 546 to 702 152 cases) in these regions compared to 6% (from 83 078 to 88 041 cases) in HIC (**Figure 1.6**) (91).

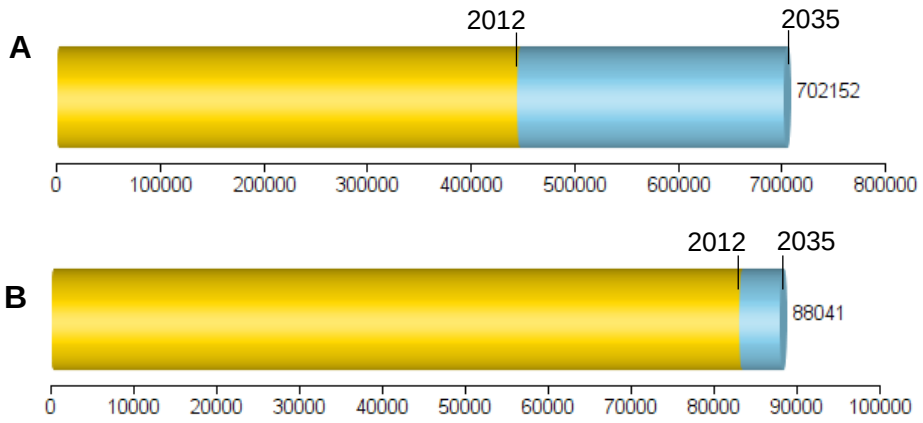

Figure 1.6: The predicted cervical cancer incidence in 2035 in **A.** LMIC compared to **B.** HIC, adapted from GLOBOCAN 2012. Yellow areas indicate the worldwide cervical cancer incidence in 2012 and blue areas indicate the predicted increase in cancer incidence between 2012 and 2035. The x-axis represents the number of individual cancer cases.

Nearly 100% of new cervical cancer cases are attributable to chronic infection with HPV (4). Although recent epidemiological evidence suggests that persistent STH infection alters the immune response to HPV, exactly how STHs and other helminths influence cancer is only fully

understood in a few contexts. For instance, *S. haematobium* is a conclusive cause of bladder cancer and the mechanism is thought to involve unresolved chronic inflammation which leads to genomic instability and tumour formation (7, 92). Indeed, chronic inflammation of the urinary bladder results from the deposition of *S. haematobium* ova in the tissue which causes Female Genital Schistosomiasis (FGS), a tissue reaction resulting in lesions which increase the risk of bleeding and discharge (93). This appears to be associated with an increased risk of cancer at this site, causing urogenital schistosomiasis (UGS)-induced carcinogenesis. Infection with *S. haematobium*, is further associated with cervical dysplasia and invasive squamous cell carcinoma (SCC), both of which predispose a female to cervical cancer (94). Moreover, it has been shown that populations with Schistosome infection have a significantly increased risk of infection with HPV types which are associated with an elevated risk of cervical cancer development (95).

1.7 Colorectal Cancer and Helminths

Globally, colorectal cancer (CRC) is the second and third most commonly diagnosed cancer in females and males respectively and is expected to have nearly doubled in incidence by 2035 (**Figure 1.7**) (2, 91, 96).

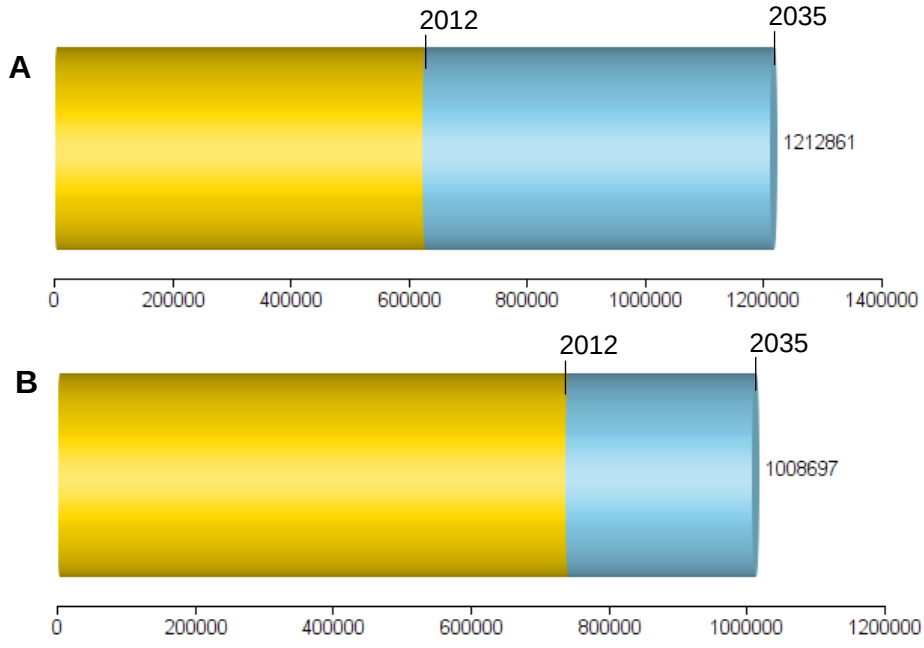

Figure 1.7: The predicted colorectal cancer incidence in 2035 in **A.** LMIC compared to **B.** HIC, adapted from GLOBOCAN 2012. Yellow areas indicate the worldwide colorectal cancer incidence in 2012 and blue areas indicate the predicted increase in cancer incidence between 2012 and 2035. The x-axis represents the number of individual cancer cases.

Of significance, and in contrast to that of cervical cancer, is the fact that 60% of worldwide CRC cases occur in developed regions, with the highest mortality rates occurring in Central

Europe and the lowest in Western Africa (91). It has been suggested that the lifestyle common in more developed countries, including a diet low in fibre, fruits and vegetables, obesity, lack of physical activity, excessive alcohol consumption and a lack of sleep increases the risk of developing CRC (97, 98).

Chronic inflammation associated with Inflammatory Bowel Disease (IDB) has been linked to an increased risk of high-grade dysplasia and cancer known as colitis-associated colorectal cancer (CAC) (99). Although many STH establish life-long infections associated with chronic inflammation within the gastrointestinal tract, it is unclear how these infections directly impact CAC. In mouse models of CAC, infection with the tapeworm *Taenia crassiceps* and treatment with its ES products (TcES) inhibited colonic inflammatory responses and tumour formation (100, 101). More specifically, infection with *T. crassiceps* prevented the loss of intestinal goblet cells, promoted the negative immunomodulation of pro-inflammatory cytokines and prevented an increase in markers associated with CAC-tumorigenesis, β-catenin and CXCR2 (100). TcES-treated mice exhibited a similar result where the expression of pro-inflammatory cytokines, IL-1β, TNF-α and IL-17, were reduced compared to that in untreated mice (101). The generation of an anti-inflammatory environment was further promoted by the decreased expression of tumorigenesis markers COX2, β-catenin and STAT3 in the colon tissue.

While the aforementioned studies suggest a favourable effect of helminth exposure on CAC, chronic and acute infection with the murine gastrointestinal nematode, *Trichuris muris,* enhanced tumour development in a model of spontaneous CRC ($APC^{min/+}$ mice) (102). Moreover, in a model of CAC, infection with *H. polygyrus* exacerbated tumour development and intestinal inflammation characterised by elevated IL-6 and CXCL1 levels (103). Further support of a detrimental role for helminths in CRC development was seen in a cohort of *S. mansoni* infected CRC patients who exhibited early onset of advanced multicentric CRC (104).

As a result of the uncertain role that helminths play in IBD, several recent studies have emerged which investigate their use in the treatment of these inflammation-associated diseases.

1.8 Helminth Therapy

The immune-regulatory tactics employed by helminths to successfully evade expulsion from the host can contribute to the outcome of inflammatory illnesses, including IBD (105-107). However, whether this outcome is an overall amelioration or exacerbation of disease is still unclear.

While the exact cause of IBD, namely Crohn's Disease (CD) and Ulcerative Colitis (UC), remains to be determined, it is presumed to be caused by the dysregulation of the intestinal mucosal immune system and microbiota (12, 108). Individuals with IBD suffer from chronic intestinal inflammation characterised by periods of remission and relapse. As depicted in **Figure 1.8**, CD can affect any part of the gut from the mouth to the rectum causing transmural inflammation, ulceration, granulomas, strictures and fistulae (12). Lymphocytes isolated from the inflamed intestines of individuals with CD secrete a pro-inflammatory Th1 pattern of cytokines including IFN-ɣ and TNF-α (12). In contrast, UC only affects the large intestine with inflammation being the primary cause of discomfort (109). Furthermore, the immune response to UC is characterised by both Th1 (IFN-ɣ and TNF-α) and Th2 (IL-13 and IL-5) typical cytokines (109). Interestingly, IL-17 levels are elevated in both active CD and UC patients (109). Indeed, the Th2 response elicited by intestinal helminth infection may help to abrogate Th1-induced inflammation by reducing Th1 cytokine production and could, therefore be of therapeutic potential in patients with IBD.

To date, data obtained from clinical trials utilising helminths to treat IBD have been contentious. Human studies revealed that prolonged colonization with the human whipworm *T. suis,* as well as treatment with its ova, reduced disease severity in CD and UC patients (110, 111). Moreover, a case-control study in South Africa, dependent on self-reporting, demonstrated evidence for a potential protective effect of childhood helminth infection on the development of IBD later in life (112). However, other studies, which exhibited favourable results early on, ultimately did not show any beneficial effect on IBD patients and were either terminated or left unpublished.

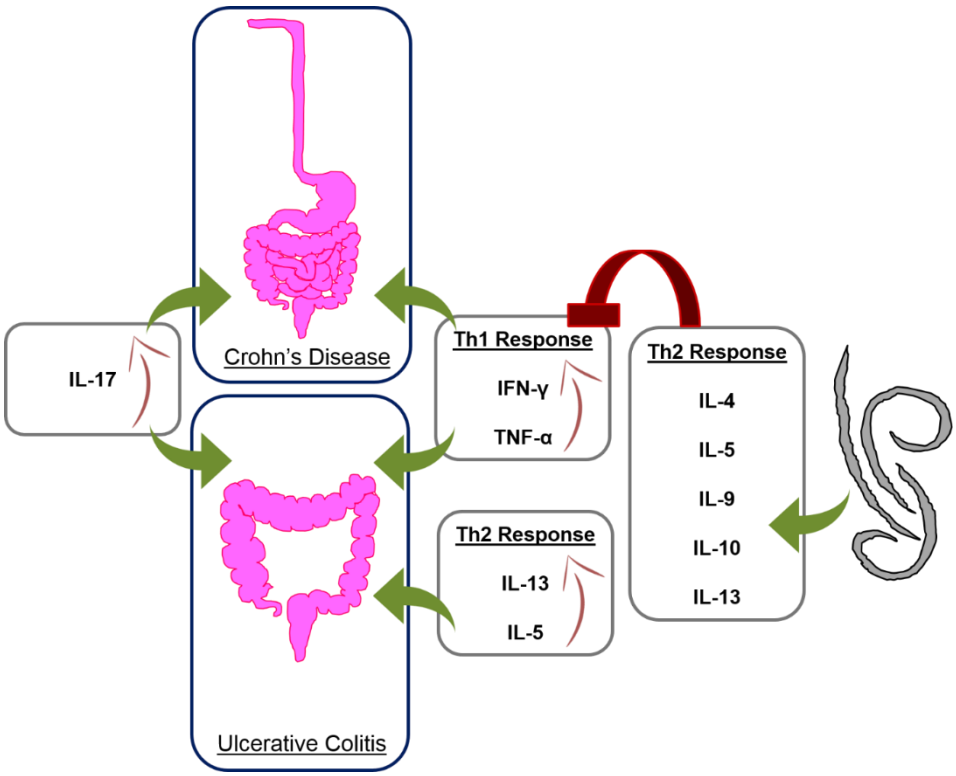

Figure 1.8: The Th2 response elicited by intestinal helminth infection could be of therapeutic potential in patients with IBD by abrogating the characteristic Th1 profile.

In vivo murine models of IBD (113) have been able to provide more reliable and reproducible results pertaining to the effect that helminths may have on IBD. Treatment with antigen derived from the nematode *T. spiralis* and infection with the rat tapeworm *Hymenolepis diminuta* caused a reduction in the severity of Dinitrobenzene Sulfonic Acid (DNBS)-induced colitis. This effect was associated with increased immune-regulatory cytokines, TGF-β, IL-13 and IL-10 and decreased pro-inflammatory molecules iNOS and IL-1β (114-116). In contrast, other studies have shown that infection with *H. diminuta* worsened oxazolone-induced colitis by causing eosinophilia and increasing levels of disease-associated Th2 cytokines (117, 118). Although the role of *T. crassiceps* in CAC has been defined, pre-infecting mice with this tapeworm followed by the exposure to the inflammatory agent dextran sulphate sodium (DSS) significantly decreased signs and symptoms of DSS-induced colitis, weight loss and colon shortening (100, 101, 107). These results were accompanied by reduced pro-inflammatory cytokines (IL-17E and TNF-α) and elevated Th2 immune-regulatory cytokines (IL-4 and IL-10). Interestingly, this beneficial role of helminth exposure on murine models of IBD does not necessarily depend on live infection. Pre-treating mice with *S. japonicum* ova lowered the mortality rate and pathology in Trinitrobenzene Sulfonic acid (TNBS)-induced colitis (119). This was found to result from increased expression of colonic epithelial tight junction proteins, ZO-1 and Occludin, reduced bacterial translocation, and ultimately lowered systemic inflammation.

There is evidence to suggest that the cure of murine colitis depends on Treg accumulation in the intestinal lamina propria (120, 121). Owing to the immunosuppressive effects of Tregs, helminth therapy may prove beneficial in treating IBD due the increase in the Treg population following infection (16). Exposure to adult *S. mansoni* and *S. mansoni* ova beneficially modulated the host immune response to DSS- and TNBS-induced colitis respectively (26, 122). Adult *S. mansoni* protection was associated with Treg population expansion and *S. mansoni* ova treatment decreased pro-inflammatory cytokines (IFN-ɣ, IL-12 and IL-17) and increased immune-regulatory cytokines (IL-10 and TGF-β), leading to elevated Treg numbers (26, 122, 123). Additionally, infection with *H. polygyrus* inhibited colitis in an IBD susceptible mouse model ($IL10^{-/-}$ mice) by reducing pro-inflammatory Th1 cytokine release (IL-12 and IFN-ɣ) and promoting the formation of an anti-inflammatory environment rich in IL-13 and Tregs (124). This beneficial outcome has been further delineated to be caused by the expansion of tolerogenic DCs in infected mice, which block a pro-inflammatory immune response and promote an immune-regulatory one characterised by IL-10 and Tregs (125-127). In vast contrast to this, a more recent study found that *H. polygyrus* infection considerably exacerbated DSS-induced colitis by increasing the expression of inflammation-associated molecules IL-6 and CXCL1 (103). *H. polygyrus* has also been implicated in worsening *S.*

typhimurium enterocolitis as a result of lowered neutrophil recruitment to the intestines and elevated Th2 cytokine expression (65).

While certain studies suggest a beneficial role for Tregs in the cure of murine colitis, studies in human CRC patients show that Tregs may disrupt the tumour-associated antigen-specific immune response. This has been demonstrated by the ability of Tregs, abundant in both the blood and lymph nodes of CRC patients, to suppress CD4+ T cell responses to tumour-associated antigens leading to tumour recurrence (128, 129). Furthermore, Treg depletion from the peripheral blood mononuclear cells of the CRC patients unveiled the CD4+ T cell responses to the tumour-associated antigens (measured by IFN-ɣ release) (129). This would implicate Tregs as a key driver of CRC disease instead of having therapeutic benefits.

It is thought that IBD is contributed to by a dysregulated intestinal microbiota (108). An imbalance in the relationship between the macrobiota (including helminths), microbiota and the host promotes inflammatory responses and predisposes the host to a range of inflammatory and autoimmune diseases (130-132). *T. muris* infection in CD susceptible mice ($NOD2^{-/-}$) prevented intestinal colonization by pro-inflammatory *Bacteroides* species resulting in an environment rich in protective *Clostridia* species (133). However, in a model of *Citrobacter rodentium*-induced colitis, *H. polygyrus* infection significantly altered the microbiome composition of mice by increasing detrimental *Bacteroides* species and decreasing beneficial Firmicutes and Lactobacillales (134). Importantly, mice who received gut microbiota from infected mice had worsened colitis symptoms and increased faecal pathogen shedding associated with increased Tregs and IL-10 levels. Notably, when Tregs were depleted and IL-10 neutralized, the enteropathogen-induced colitis symptoms were alleviated. Interestingly, an abundance in the rodent commensal *L. taiwanensis* has been shown to correlate with *H. polygyrus* infection as well as elevated Treg levels and the presence of a strong Th17 response (135). Moreover, administration of *L. taiwanensis* to *H. polygyrus* infected mice resulted in an increase in Treg levels leading to reduced helminth expulsion.

1.9 Helminths and Cancer Treatment

Tumour cells are able to acquire characteristics which allow them to invade the surrounding tissue and to metastasise to distal sites. Metastasis is associated with a poor outcome and is the major cause of mortality in patients with cancer. Invasion and metastasis is achieved by changes in cell shape and the deregulated expression of extracellular matrix (ECM) attachment proteins (136). These changes promote cell migration, due to an increased level of motility, and often involve reduced expression of the invasion antagonist, E-cadherin, and increased expression of the invasion agonists, N-cadherin and vimentin. While E-cadherin is an adhesion molecule expressed by epithelial cells, N-cadherin and vimentin are adhesion

and type III intermediate filament proteins respectively expressed by mesenchymal cells. The switch in the expression of these invasion proteins is referred to as Epithelial-Mesenchymal Transition (EMT) and while essential in development and wound healing, it also plays a vital role in cancer by promoting the progression of a primary tumour towards a more invasive and metastatic phenotype (**Figure 1.9**) (137).

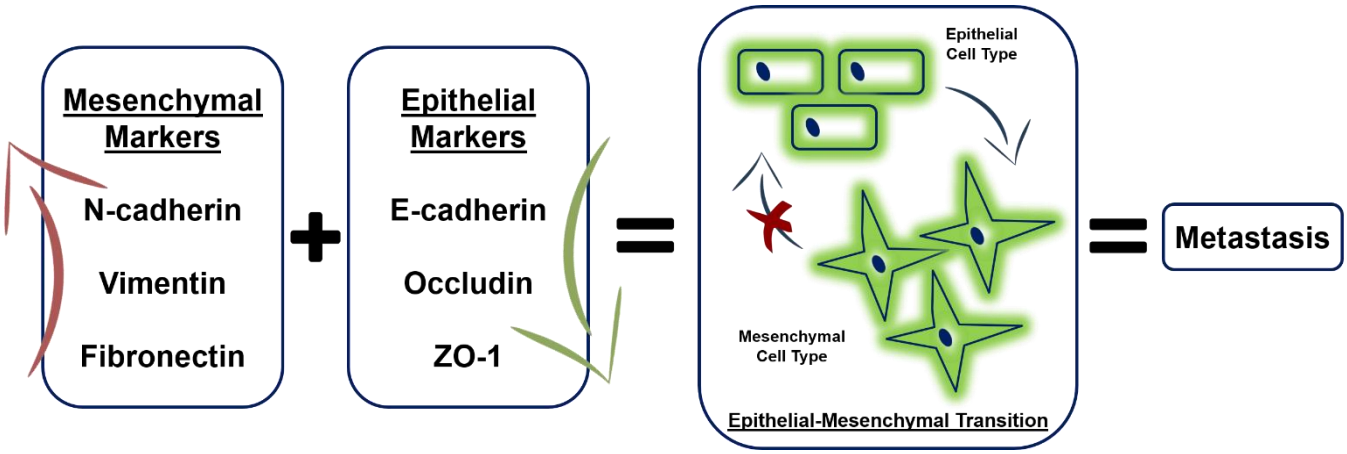

Figure 1.9: Increased expression of mesenchymal markers and decreased expression of epithelial markers leads to Epithelial-Mesenchymal Transition and metastasis.

Besides those which are conclusive causes of cancer, the direct impact that helminths have on invasion and metastasis is largely unclear and only a few studies have started to reveal possible associations (5-7). Compared to untreated tumours, antigen derived from *S. haematobium* accelerated the proliferation of Chinese Hamster Ovary (CHO) tumours with a corresponding increase in the levels of vimentin, suggesting that exposure to parasite derived antigens could drive EMT (138). Furthermore, when co-administered with a chemical carcinogen into the murine bladder wall, treatment with *S. haematobium* eggs reduced E-cadherin expression, elevated vimentin expression and increased the proliferation of urothelial cells (139). Although not used in a cancer model, infection with *H. polygyrus* or *T. spiralis* increased epithelial permeability in the colon due to the decreased expression of E-cadherin and Occludin respectively (140, 141). Similarly, in humans, infection with *T. trichiura* and *S. mansoni* increased the expression of plasma fibronectin, another mesenchymal marker, and cellular vimentin respectively (142, 143).

In addition to altering EMT, helminth infections may also impact cancer progression by causing aberrant changes in the cell cycle which can lead to uncontrolled proliferation and an accumulation of detrimental genetic mutations, both of which are hallmarks of cancer (144, 145). In support of this, treatment with *O. viverrini* ES product or *B. malayi* altered the *in vitro* proliferation of fibroblasts and several human carcinoma cell lines respectively by modifying cell progression through G1 to S of the cell cycle (146, 147).

1.10 Aims and Objectives

In this study, we used antigens derived from two STHs, the hookworm *N. brasiliensis* and the gastrointestinal nematode *H. polygyrus*, to identify how exposure to helminths may influence cancer development and progression.

Hypothesis: Antigens derived from parasitic helminths will promote cancer development and progression *in vitro* and *in vivo.*

Aim: To determine the impact of antigens derived from parasitic helminths on cancer development and progression *in vitro* and *in vivo.*

This aim will be achieved through addressing the following objectives:

Objective 1: Investigate the impact of helminth exposure on cervical cancer progression

Objective 2: Investigate the impact of helminth antigens on CRC progression

Objective 3: Define how helminth antigen alters CRC initiation

2. Materials and Methods

2.1 Helminth Antigen Preparation

2.1.1 *Nippostrongylus brasiliensis* L3 Antigen

N. brasiliensis is a rodent nematode, which is commonly used to model infection with human hookworm. The lifecycle and immune response to this parasite has been well-characterised for use in both *in vivo* and *in vitro* studies (**Figure 2.1**) (148).

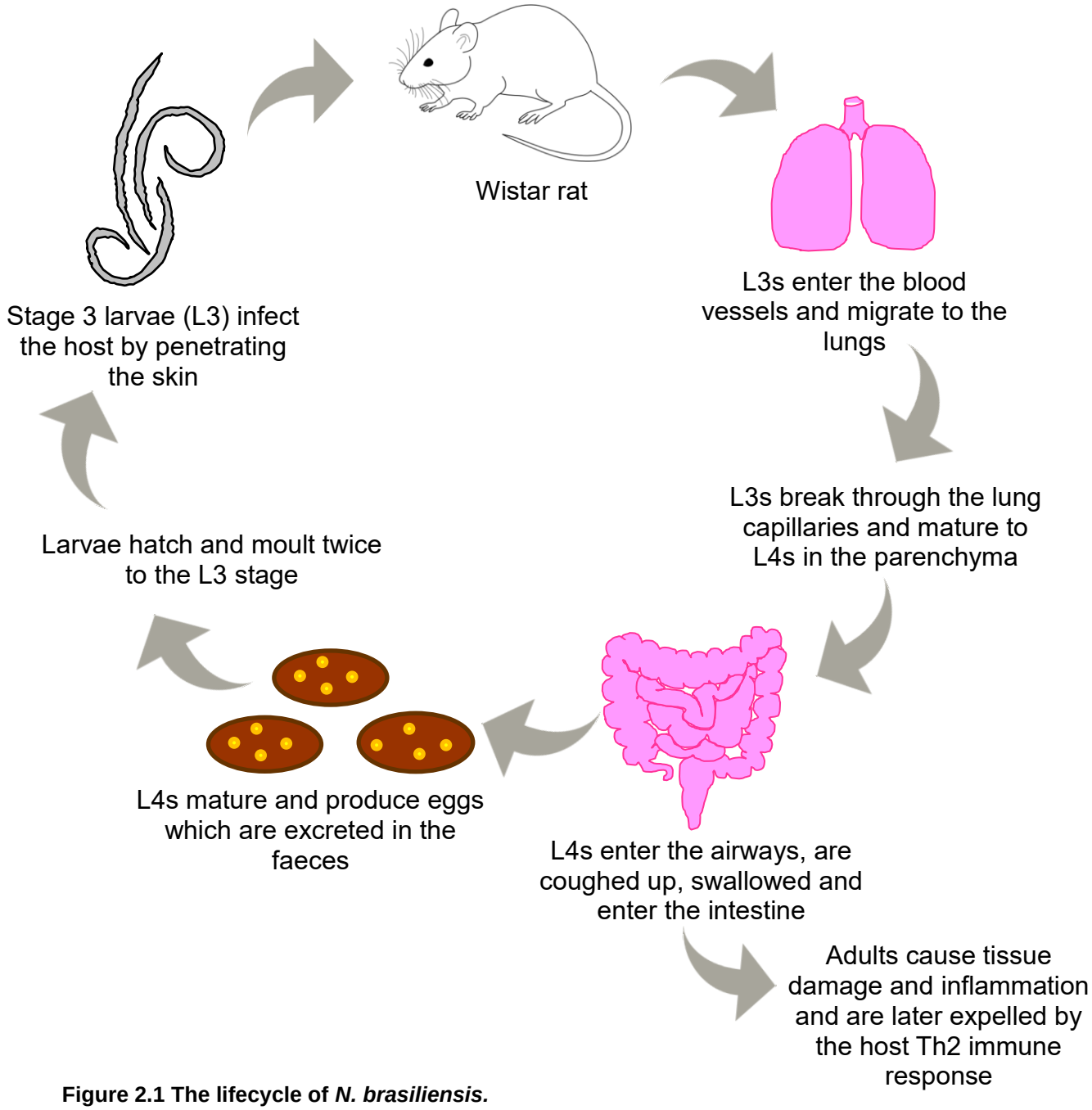

Figure 2.1 The lifecycle of *N. brasiliensis*.

Wistar rats were infected subcutaneously with 500 L3 *N. brasiliensis* larvae and the faecal material collected over the next week. The faeces were mixed with charcoal, smeared onto dampened filter paper and stored in a dark, humid area for two weeks. During this period, the larvae were washed from the edge of the filter paper into distilled water containing 50µg/ml penicillin/streptomycin and fungizone. This mixture was left for one hour allowing the larvae to settle to the bottom of the container. The supernatant was then aspirated off, the larvae washed twice and subsequently concentrated into 2ml of distilled water. In order to disrupt the cellular membranes, the larvae were dipped into liquid Nitrogen (-195°C) before centrifugation at 2500 revolutions per minute (rpm) (700g). The supernatant, containing the water-soluble fraction of the L3 proteins, was collected and the protein concentration quantified using a nanodrop (Nanodrop Spectrophotometer ND-1000). It is undeniable that this preparation contains multiple antigens however for simplicity, it will from here on be referred to as *N. brasiliensis* L3 antigen.

A nanodrop spectrophotometer is used to quantify the concentration and purity of a nucleic acid or protein sample. This is done by exposing it to a specific wavelength of ultraviolet (UV) light, which is absorbed by the sample. The more light absorbed by the sample the higher the concentration of the sample since less light will reach the photo-detector. This will result in a higher optical density (OD) being recorded. In the case of this study, the protein concentration of the helminth derived antigen preparations was measured at a wavelength of 280nm (A280) because this is the wavelength at which protein best absorbs UV light.

2.1.2 *Heligmosomoides polygyrus* Antigen and HES

H. polygyrus is a murine nematode which has been well-defined for use in both *in vivo* and *in vitro* murine studies (**Figure 2.2**) (148). Infection with *H. polygyrus* closely resembles that of human gastrointestinal nematode infections and was, therefore chosen for use in this study.

H. polygyrus somatic antigen and *H. polygyrus* excretory-secretory products (HES) were prepared using the method described by Johnston *et al* (149). Male, 8-week-old, C57BL/6 mice were infected with 400 L3 *H. polygyrus* larvae by gavage and on day 14 the mice were sacrificed. The upper portion of the gut, from the bottom of the stomach to the beginning of the cecum, was removed and drawn out to its full length. The gut was then cut along its length and scraped to remove the intestinal contents, including the adult *H. polygyrus*. As seen in **Figure 2.3**, the worms were then placed into muslin bags and secured to the edge of a funnel attached to a collection tube.

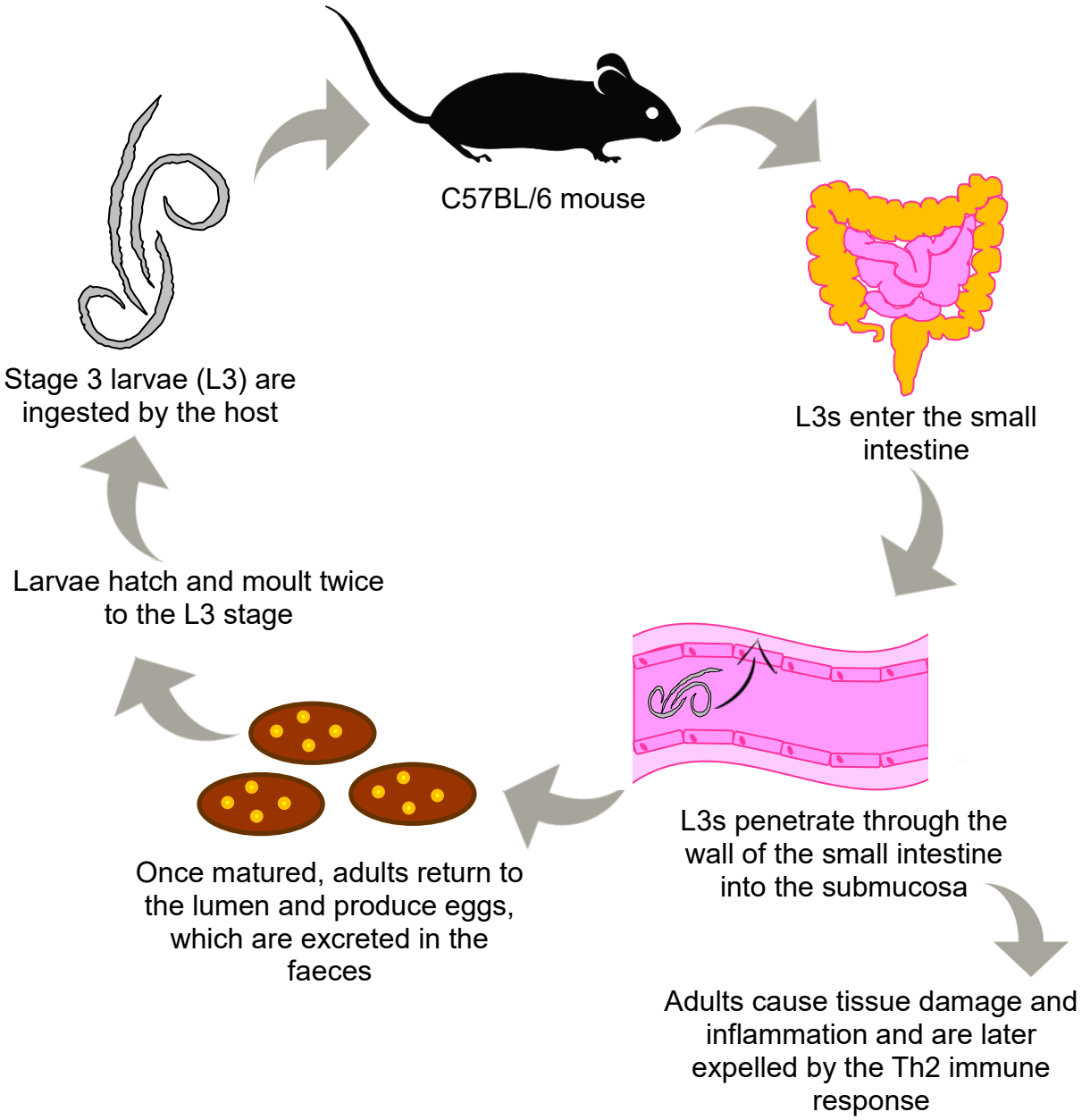

Figure 2.2 The lifecycle of *H. polygyrus.*

The funnel was then filled with Hanks media (appendix 8.1) and the apparatus stored at 37°C for two hours with intermittent agitation. The worms were allowed to settle and then removed and placed in a 50ml falcon tube. The worms were washed six times with Hanks media, steeped in 10% Gentomycin and finally washed a further six times with Hanks media. The worms were then separated into T25 flasks containing *H. polygyrus* media (appendix 8.1). Twice a week, for three weeks, the medium was collected and replaced with fresh *H. polygyrus* media. The medium was then spun down, the supernatant sterile filtered (40µm) and stored at -20°C. A 3000MW filter (EMD Millipore™ PLTK04310), in an Amicon concentrator, was used to concentrate the medium and dialyse the resulting protein, glycoprotein mixture to 1X

Phosphate Buffered Saline (PBS) (appendix 8.4). The protein concentration of the resulting HES was subsequently measured, using a nanodrop, and stored at -80°C.

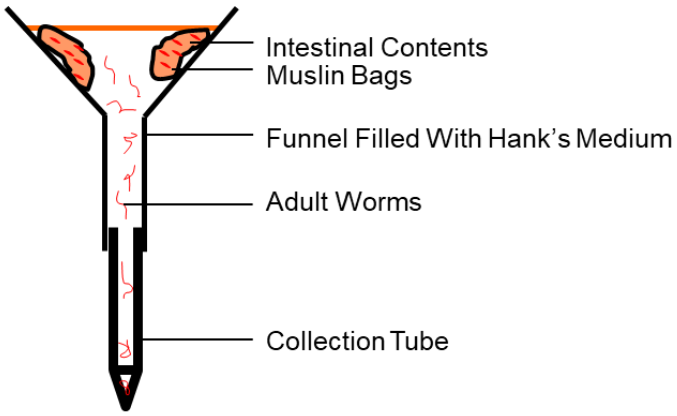

Figure 2.3 *H. polygyrus* adult worm isolation. Muslin bags containing adult worms are secured to a funnel filled with Hank's media. Adult worms exit the muslin bags and settle to the bottom of a collection tube.

At the end of the three weeks the worms were collected and stored at -80°C. When required, the worms were defrosted, uniformly homogenized in PBS, centrifuged, the supernatant collected and sterile filtered (40µm). Once again, it is undeniable that this preparation contains multiple antigens however for simplicity, it will from here on be referred to as *H. polygyrus* antigen. A Bicinchoninic Acid (BCA) assay was used to quantify the protein concentration in the isolated *H. polygyrus* antigen.

A BCA assay (Thermo Scientific Product #23227) is used to quantify the total protein concentration in a sample. The protein concentration is displayed as a change in colour from green to purple in proportion to the protein concentration, which can be measured using a spectrophotometer and compared to a protein standard of known concentration.

2.1.3 Verification of HES Immune-Regulatory Effects

HES is known to expand the mouse and human Foxp3+ regulatory T cell population through the action of the structurally distinct TGF-β mimic contained within it (16, 33). We therefore needed to ascertain whether the HES harvested for use in this study exhibited this immune-regulatory property before being used in *in vitro* and *in vivo* experiments. To this end, the effect that the harvested HES had on the Foxp3+ T cell population and CD4+ T cell proliferation was determined.

The spleen was removed from one female BALB/c mouse and passed through a cell separator (40µm) into Roswell Park Memorial Institute Medium-1640 (RPMI-1640) (appendix 8.2). The cell suspension was subsequently centrifuged for five minutes at 1500rpm (250g). The pellet

was then resuspended in 2ml Red Blood Cell lysis buffer for two minutes, topped up with RPMI and centrifuged for five minutes at 1500rpm. The cells were then resuspended at a density of 10^7cells/ml in 2µM Carboxyfluorescein Succinimidyl Ester (CFSE) (Life Technologies C34554) in PBS and incubated in the dark for 20 minutes at 37°C.

CFSE is a cell permeable fluorescent staining dye which can be used to monitor cell proliferation due to the progressive halving of the fluorescence intensity of the dye following each cell division (150). CFSE is light sensitive and, therefore all subsequent steps were carried out under the appropriate conditions. After 20 minutes, the tube was topped up with RPMI, to wash off excess CFSE and quench any remaining reaction and incubated for five minutes at 37°C before centrifuged for five minutes at 1500rpm. CFSE labelled cells were then plated at a density of $5x10^5$ cells/100µl per well in a 96-well round-bottom plate. The plate was incubated for 72 hours at 37°C in the presence of 1µg anti-CD3 only or anti-CD3 plus 10µg HES (**Figure 2.5A**).

After 72 hours the plate was centrifuged for two minutes at 1500rpm and the pellets resuspended in 200µl MACS buffer (appendix 8.1). A 1:200 dilution of Peridinin Chlorophyll Protein (PerCP)-labelled rat anti-mouse monoclonal CD4 (BD Bioscience, Clone RM4-5) was added to the relevant wells together with 1% rat serum and 1% FcγRII/III to prevent non-specific binding. The plate was then incubated for 20 minutes at 4°C. Wells were topped up with MACs buffer and the plate centrifuged for two minutes at 1500rpm. In order to access intracellular Foxp3, the cells were fixed (eBioscience Ref. 00-5523-00) for a minimum of 45 minutes at 4°C following which the wells were topped up with Perm buffer (supplied in the Foxp3 Staining Buffer Set) and the plate centrifuged for two minutes at 1500rpm. Perm Buffer containing a 1:50 dilution of allophycocyanin (APC)-labelled rat anti-mouse monoclonal Foxp3 (BD Bioscience, Clone FJK-16s) was then added to the relevant wells and the plate incubated for 30 minutes at 4°C. The buffer was then removed, fresh Perm buffer added, and the plate centrifuged for two minutes at 1500rpm. The pellets were then resuspended in MACs buffer in preparation for analysis on the Becton Dickinson (BD) LSR II Flow Cytometer. FlowJo Version 10 was used to analyse the data according to the gating strategy depicted in **Figure 2.4**.

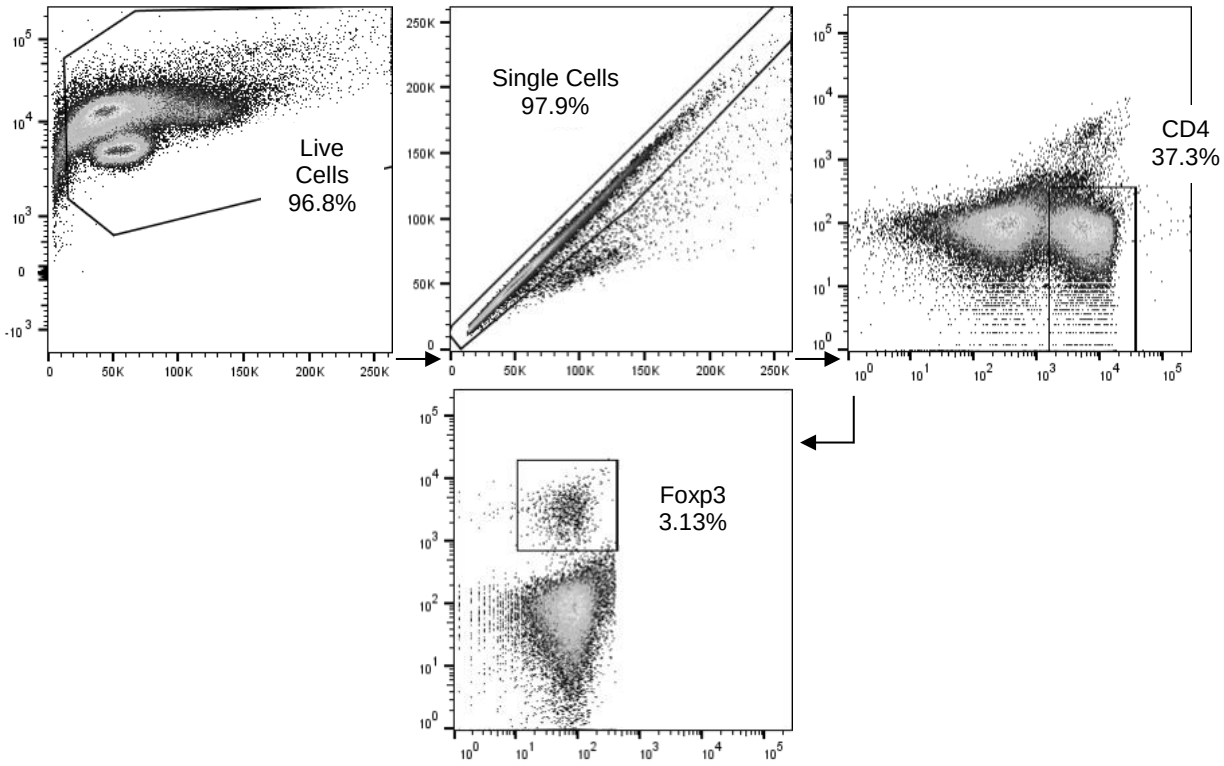

Figure 2.4: Gating strategy applied to obtain the Foxp3+ T cell population. Splenocytes from one female BALB/c mouse were seeded at a density of $5x10^5$ cells per well in a 96-well round-bottom plate and cultured for 72 hours. CD4+ T cells were subsequently labelled and stimulated under different treatment conditions (anti-CD3 or anti-CD3 plus HES). Analysis was performed using FlowJo Version 10.

This revealed that the Foxp3+ T cell population was significantly expanded in the anti-CD3 plus HES stimulated CD4+ T cells compared to that of anti-CD3 only stimulated CD4+ T cells (**Figure 2.5A and Figure 2.5B**). Furthermore, significantly fewer CD4+ T cells underwent two and three cellular divisions when stimulated with anti-CD3 plus HES than that of anti-CD3 only stimulated CD4+ T cells (**Figure 2.5C and Figure 2.5D**).

A

HES Batch	Concentration (µg/ml)	% Foxp3 Positive
1	446	3.2
2	370	2.8
3	197.5	7.4
4	184	2.3
5	159	2.8

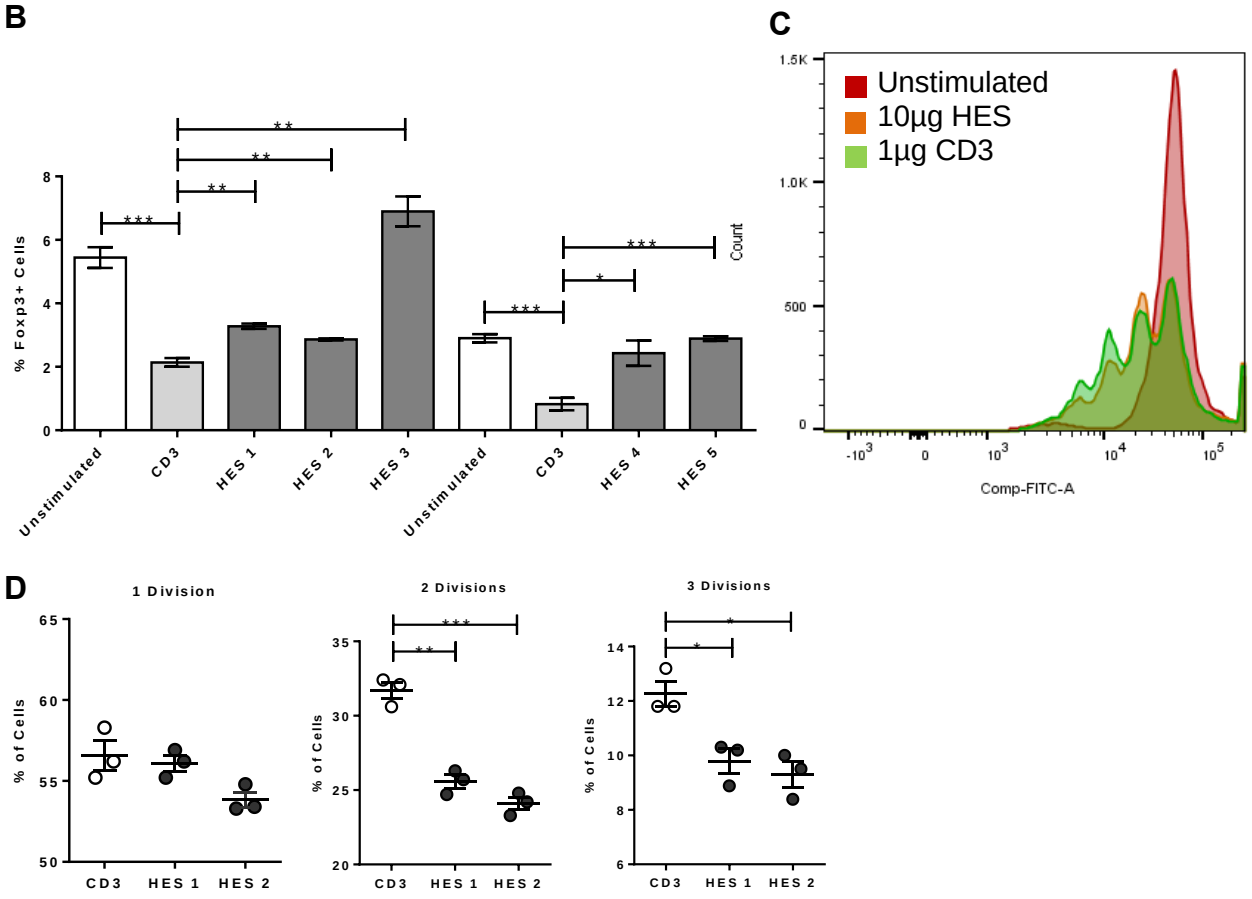

Figure 2.5: HES induces Foxp3+ T cell population expansion and reduces CD4+ T cell proliferation. Cells from the spleen of one female BALB/c mouse were seeded at a density of $5x10^5$ cells per well in a 96-well round-bottom plate, stimulated under different treatment conditions (1µg CD3 or 1µg CD3 and 10µg HES) and cultured for 72 hours. **A.** Summary of the HES batches utilised and the percentage of Foxp3+ T cells induced by each. **B.** Splenocytes were stained appropriately and the Foxp3+ CD4+ T cell population present in each treatment condition were analysed using FlowJo Version 10. **C and D.** CD4+ T cells were stained appropriately, labelled with CFSE and analysed using FlowJo Version 10. Analysis was performed using GraphPad 6.01 and a parametric unpaired t-test was performed *p<0.05 **p<0.01 ***p<0.001 ****p<0.0001. Error bars represent Standard Error of the Mean.

2.2 Limulus Amoebocyte Lysate (LAL) Assay

The LAL assay (Pierce LAL Chromogenic Endotoxin Quantitation Kit, ThermoFisher Scientific 88282) is used to measure the endotoxin concentration (EU/ml) in a given sample. This is achieved by measuring the presence a chromogenic signal, at 405nm, which is generated in the presence of endotoxins and compared to a standard curve created using an *E. coli* endotoxin standard.

This assay was used to determine the endotoxin concentration in all helminth derived antigen preparations to ensure that any significant effects observed in subsequent experiments were due to the antigen and not an endotoxin contamination.

2.3 Cell Line Culture

Cervical cancer cell lines HeLa (HPV18 positive epithelial adenocarcinoma cells), Ca Ski (HPV16 positive epithelial epidermoid carcinoma cells) and C33-A (HPV negative epithelial carcinoma cells) and colorectal cancer cell lines CT26.WT (a murine N-nitroso-N-methylurethane-(NNMU) induced, undifferentiated fibroblast colon carcinoma cell line) and HCT116 (a human epithelial colon carcinoma cell line) were purchased from the American Type Culture Collection (ATCC). HeLa and C33-A cells were maintained in Dulbecco's-Modified Eagle Medium (DMEM) (appendix 8.2), Ca Ski and CT26.WT cells were maintained in RPMI and HCT116 cells were maintained in McCoy's Modified 5a medium (appendix 8.2).

When needed, cells were retrieved from liquid Nitrogen and thawed in a 37°C waterbath. Thawed cells were resuspended in 4ml of the relevant medium and centrifuged for two minutes at 2500rpm. The supernatant was subsequently removed, and the pellet resuspended in 1ml of medium. The cell suspension was then plated into a T75 flask, containing 9ml of medium, and kept at 37°C in an atmosphere of 5% CO_2 and 95% humidity. Once the cells had been passaged at least twice, to ensure stability, they were used in the various experiments. Cells were passaged, and the media replaced every 48-72 hours depending on confluency.

2.4 Mycoplasma Testing

Mycoplasma is a gram-negative bacterium, which lacks a cell wall and is more resistant to common antibiotics. For this reason, cells were regularly mycoplasma tested to ensure that all experimental results were due to the effect of the helminth derived antigens only.

Cells were grown in a 35cm dish in antibiotic-free medium on a sterile coverslip for a minimum of 48 hours. After the incubation period, 1ml of fixative (appendix 8.3) was added to the dish for ten seconds, poured off and repeated. The dish was then rinsed three times with tap water

and once dried stained with 500µl of nucleic acid stain Hoechst No. 33258 (0.5µg/ml) for five seconds. The staining solution was poured off and the dish rinsed three times with tap water. The coverslip was then transferred to a microscope slide containing one drop of mounting fluid (appendix 8.3). Cells were subsequently viewed under a fluorescent microscope using the DAPI filter. The visualization of large nuclei (cell nuclei) surrounded by small nuclei (mycoplasma nuclei) was concluded as positive for mycoplasma.

2.5 *In vitro* Assays

2.5.1 Growth Curve Assay

In order to determine the effect of helminth derived antigen on cancer cell proliferation, the short-term growth of cells was monitored over a 3-day period as previously described (151). The media was removed, and the cells lifted using 2ml of Trypsin- Ethylenediaminetetraacetic acid (EDTA) (appendix 8.4). Cells were resuspended in 4ml of medium for counting and $5x10^4$ cells were seeded per well, in triplicate, in a 24-well plate. *N. brasiliensis* L3 antigen (0.1µg or 1 µg or 10µg), HES (10µg), *H. polygyrus* antigen (10µg) or 1X PBS was added to the required wells and the cells counted 24, 48 and 72 hours post-treatment. To do this, the cells in each well were trypsinised and resuspended in 300µl of medium per well and counted using a haemocytometer.

To ensure that dead cells were excluded from the cells counts of all experiments, Trypan blue (Life Technologies, Ref. 15250-061) was used. Trypan blue is only able to permeate the membrane of dead cells and for this reason; all blue-stained cells were presumed dead and excluded from cell counts.

2.5.2 Scratch Motility Assay

A two-dimensional scratch motility assay was performed, in order to determine the effect of helminth derived antigen on cervical cancer cell migration (152). The media was removed, and the cells lifted using 2ml of Trypsin-EDTA. Cells were resuspended in 4ml of the relevant medium for counting and $5x10^4$ (HeLa), $1x10^5$ (Ca Ski) or $2x10^5$ (C33-A) cells were seeded per well, in triplicate, in a 24-well plate and allowed to reach 100% confluency. The cells were subsequently serum starved in medium containing 0% FBS for 24 hours where after a sterile 2µl pipette tip was used to make a vertical scratch in the cell monolayer of each well. The medium was then removed from each well followed by the addition of 500µl fresh medium and *N. brasiliensis* L3 antigen (0.1µg or 1µg or 10µg), HES (10µg), *H. polygyrus* antigen (10µg) or 1X PBS. Cells were subsequently viewed at zero, four and eight hours post-wound formation (**Figure 2.6**).

Figure 2.6 Two-dimensional scratch motility assay. A vertical scratch is made in the cell monolayer and wound closure monitored over an 8-hour period. Area migrated at T4 = Area at T0 – Area at T4; area migrated at T8 = Area at T0 – Area at T8.

At each time point the total area of the scratch was imaged using ZoomBrowser Ex software with pictures being taken using a non-phase contrast lens at 10X magnification (Canon PowerShot S50). ImageJ Software (National Institute of Health, Bethesda, MD) was used to calculate the area of the scratch and to determine the total area migrated by the cells relative to the wound area at time zero hours.

2.5.3 Transwell Migration Assay

Transwell migration assays are used to determine the migratory response of cells when exposed to different treatments. Serum starved cells are placed on the upper surface of a cell permeable membrane in medium supplemented with a lower percentage of FBS, and medium containing a higher percentage FBS is placed below this. Cells that have migrated from the treatment containing upper chamber, towards the FBS rich medium in the lower chamber, adhere to the lower surface of the cell permeable membrane allowing them to be fixed, stained and quantified appropriately.

An established transwell migration assay was performed in order to further characterise the effect of helminth derived antigen on cancer cell migration (152). This was achieved using 24-well hanging-inserts fitted with an 8µm pore size membrane (Millicell Cell Culture Inserts Category No. MCEP24H48). Cells were cultured to 70% confluency in a 6cm dish and subsequently serum starved for 24 hours in medium supplemented with 0% FBS (HeLa, Ca Ski and C33-A) or 0.2% FBS (CT26.WT and HCT116). Cells were then lifted using 500µl Trypsin-EDTA and resuspended in 4ml of medium supplemented with 1% FBS for counting. 500µl of medium supplemented with 10% FBS was placed into each well followed by the addition of the hanging-insert. A 250µl cell suspension containing $1x10^5$ cells was then seeded, in triplicate, onto the apical surface of each hanging-insert together with *N. brasiliensis* L3 antigen (10µg), HES (10µg), *H. polygyrus* antigen (10µg) or 1X PBS and left to incubate for 24 hours (**Figure 2.7**).

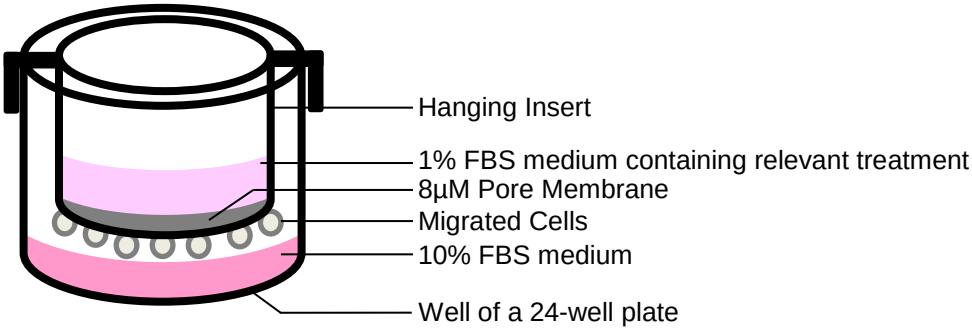

Figure 2.7: Transwell migration assay. Serum starved cells are placed onto the apical surface of a transwell hanging-insert containing medium supplemented with 1% FBS and *N. brasiliensis* L3 antigen (10µg), HES (10µg), *H. polygyrus* antigen (10µg) or 1X PBS. The insert is then placed into a 24-plate well containing medium supplemented with 10% FBS. Migrated cells adhere to the lower surface of the 8µM pore cell permeable membrane and are subsequently fixed using methanol and stained with crystal violet. 50% acetic acid is used to wash off the crystal violet stain and the absorbance of each well's crystal violet wash is read at a wavelength of 595nm.

At the relevant time point the cells on the lower surface of the insert were fixed with 100% methanol for five minutes and stained with crystal violet for five minutes. The crystal violet was then washed off using distilled water and the plate left to dry overnight. 50% acetic acid was used to wash off the crystal violet from the bottom of the insert and the crystal violet washes transferred to corresponding wells of a 96-well plate. The absorbance of each well was then read at a wavelength of 595nm using a Rayto RT-2100C Microplate Reader.

2.5.4 3-(4,5-dimethylthiazol-2-yl)-2,5-diphenyltetrazolium bromide (MTT) Assay

A MTT assay is a colourimetric assay used to measure cell viability. During this assay, yellow MTT is cleaved to purple formazan crystals in the mitochondria of metabolically active cells (**Figure 2.8**) (153).

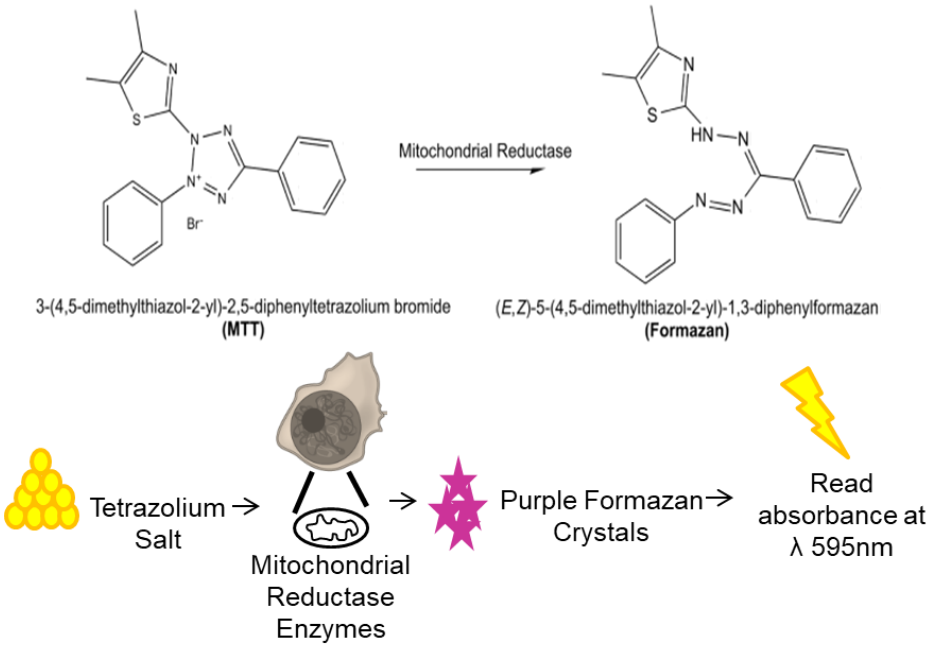

Figure 2.8: MTT reaction. The formation of insoluble formazan crystals from yellow tetrazolium MTT due to active mitochondrial reductase enzymes present in viable cells.

This reduction reaction is only possible in living cells due to their active mitochondrial reductase enzymes. A solubilizing solution, containing acidified isopropanol, is added to dissolve the insoluble purple MTT formazan crystals thus allowing the wavelength of the purple solution to be measured by a spectrophotometer at a wavelength of 595nm. For this reason, the number of viable cells is directly proportional to both the ability of the cells to convert the yellow salt into a purple solution and the spectrophotometric absorbance reading of the purple solution.

To determine colorectal cancer cell viability following treatment with both HES and *H. polygyrus* antigen, a MTT Cell Proliferation Kit (Roche, 11465007001) was used. The media was removed, and the cells lifted using 2ml of Trypsin-EDTA. Cells were resuspended in 4ml of the relevant medium for counting and $8x10^3$ cells were seeded per well, in quadruplicate, in a 96-well plate and HES (10µg), *H. polygyrus* antigen (10µg) or 1X PBS added to each of the required wells for 24 hours. Post-incubation, 10µl of MTT reagent (0.5mg/ml) was added to each well for four hours followed by the addition of 100µl of solubilisation solution. After an overnight incubation, the absorbance reading of each well was read at a wavelength of 595nm. The absorbance of medium only wells was subtracted from the absorbance of sample wells to obtain a final absorbance reading.

2.5.5 Bromodeoxyuridine (BrdU) Incorporation Assay

BrdU is a synthetic nucleoside that is an analogue of the pyrimidine deoxynucleoside thymidine. BrdU is often used in the detection of proliferating cells because it can be incorporated into the newly synthesized DNA of replicating cells as a substitute for thymidine. Antibodies specific for BrdU can then be used to indicate cells that were actively replicating their DNA at the time of BrdU addition (**Figure 2.9**) (154).

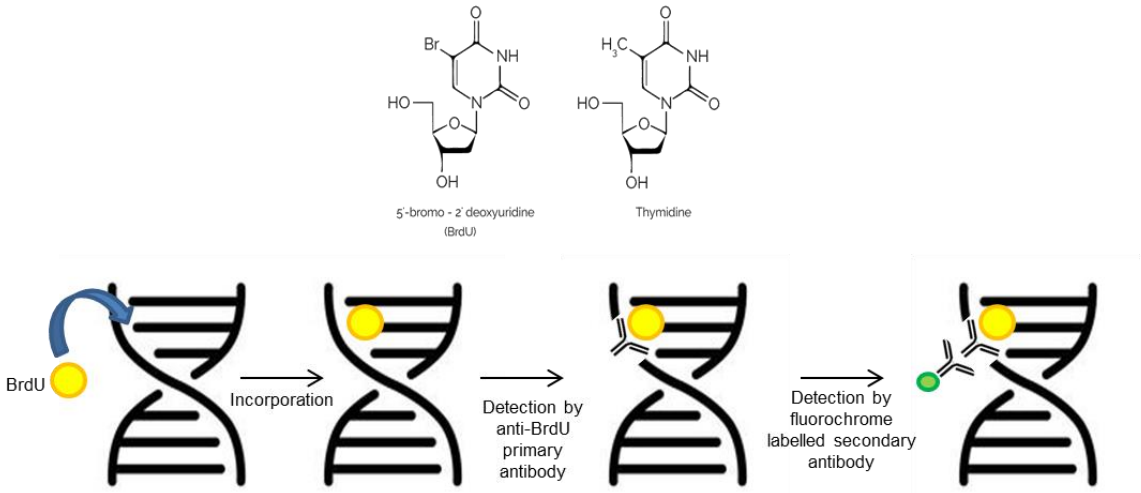

Figure 2.9: BrdU Incorporation Assay. BrdU, a synthetic analogue of thymidine, can be used in the detection of proliferating cells due to its ability to be incorporated into newly synthesized DNA. BrdU specific and fluorochrome labelled antibodies can then be used to indicate cells that were actively replicating their DNA at the time of BrdU addition.

A BrdU incorporation assay was used in order to determine the effect of HES and *H. polygyrus* antigen on CT26.WT proliferation. To this end, $2x10^5$ cells were seeded on a sterile glass coverslip in a 35mm dish, treated with HES (10µg), *H. polygyrus* antigen (10µg) or 1X PBS and allowed to adhere overnight. Cells were then incubated in medium containing 10µm BrdU for eight hours followed by fixation with Carnoy's fixative (appendix 8.4) for 20 minutes at -20°C. For immunostaining, cells were incubated in 2M HCl (appendix 8.4) for one hour at 37°C and then neutralized in 0.1M pH 8.5 borate buffer (appendix 8.4). Cells were washed with PBS/ 0.5% Tween20 (appendix 8.4) and incubated for 30 minutes at 37°C in blocking buffer (5% sheep serum in PBS/ 0.5% Tween20). BrdU was detected with an anti-BrdU mouse monoclonal antibody (6µg, Roche, Germany) for 30 minutes at 37°C, followed by a secondary IgG coupled to Alexa488 (1:1000, Molecular Probes, USA) for 30 minutes at 37°C. Cells were washed with PBS/ 0.5% Tween20, incubated in 1µg DAPI (4',6-diamidino-2-phenylindole) for ten minutes at room temperature, in the dark, and washed with PBS/ 0.5% Tween20. The coverslips were then mounted onto microscope slides, stored in the dark in a humidifying chamber overnight at 4°C and visualized by fluorescence microscopy using an Axiovert Fluorescent microscope (Zeiss, Germany).

2.5.6 Western Blotting

2.5.6.1 Protein Extraction

To determine the effect of helminth derived antigen on the expression of cancer Epithelial-Mesenchymal Transition (EMT) markers and cell cycle regulator proteins, western blotting was performed. The media was removed, and cells lifted using 2ml of Trypsin-EDTA. Cells were resuspended in 4ml of medium for counting and $2x10^5$ (HeLa, CT26.WT and HCT116) or $3.5x10^5$ (C33-A) cells were seeded per well in a 6-well plate and *N. brasiliensis* L3 antigen (10µg or 50µg), HES (10µg), *H. polygyrus* antigen (10µg) or 1X PBS added to each of the required wells. At the relevant time point the protein was harvested from each well. To do this the media from each well was removed, cells lifted using 500µl Trypsin-EDTA, resuspended in 1ml of medium and centrifuged for two minutes at 2500rpm. The supernatant was subsequently removed, and the pellet resuspended in Sodium-Dodecyl-Sulphate Polyacrylamide Gel Electrophoresis (SDS-Page) buffer/boiling blue (appendix 8.5). The harvested protein was placed in a 100°C heating block for 10 minutes and stored at -20°C until required.

2.5.6.2 SDS-PAGE

SDS-PAGE was used to separate the proteins in each sample on 1.5mm 8% resolving gels (15% for p21 only) with a 4% stacking gel (appendix 8.5). Gels were made in a BioRad Mini

PROTEAN© 3 casting apparatus and placed in the BioRad running tank filled with 1X running buffer (appendix 8.5). Equal amounts of sample were loaded into each lane and 5µl of the Thermo Scientific PageRuler™ Prestained Protein Marker (Fermentas, USA) (appendix 8.5) was loaded into its own lane to assist in determining the relative size of the proteins following separation. The running apparatus was connected to the Biorad Powerpack 200 and electrophoresis occurred at 120 Volts, 40 Watts and 0.35 Amperes. The time of the run was dependent on the size of the protein being detected, with smaller proteins requiring less time to separate.

2.5.6.3 Transfer

Following electrophoresis, the separated proteins were transferred onto a nitrocellulose membrane (Amersham, GE Healthcare, Life Sciences, Germany). This was achieved by placing the gel into a transfer cassette containing sponges, Whatman filter paper, the resolving portion of the gel and the nitrocellulose membrane pre-soaked in 1X transfer buffer (appendix 8.5). This set-up was then placed into the transfer unit of the Biorad Mini PROTEAN© 3 transfer tank to ensure that the negatively charged proteins moved from the gel onto the nitrocellulose membrane (**Figure 2.10**).

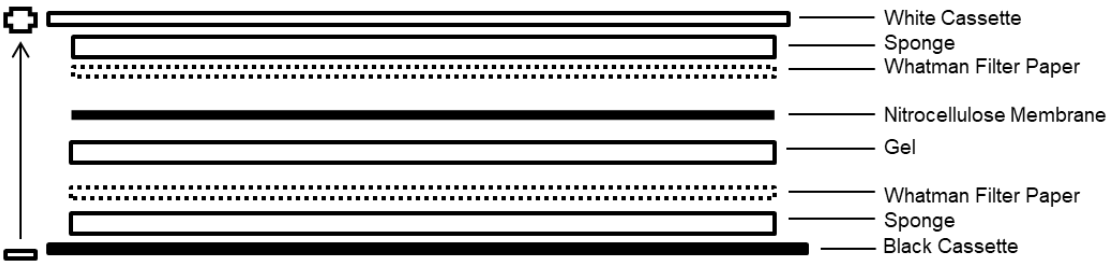

Figure 2.10: Western blot transfer set-up. For the separated proteins to be correctly transferred from the SDS-PAGE gel onto the nitrocellulose membrane the orientation of the above set-up is essential.

To prevent overheating, an ice pack was placed in the tank and the tank was filled with cooled 1X transfer buffer. The transfer apparatus was connected to the Biorad Powerpack 200 and protein transfer took place at 100 Volts, 40 Watts and 0.35 Amperes for two hours.

2.5.6.4 Detection

Following transfer, the nitrocellulose membrane was blocked for one hour at room temperature and then probed with the appropriate primary antibodies overnight at 4^{o}C with continuous shaking. Membranes were washed at 2X five-minute and 2X ten-minute intervals and incubated with the respective secondary antibody: horseradish peroxidase-conjugated anti-rabbit or anti-mouse (1:5000) (BioRad, Hercules, CA, USA) for one hour at room temperature. The membrane was then washed as previously described and visualised by enhanced

chemiluminescence (ECL) by the addition of SuperSignal West Pico Chemiluminescent Substrate (Pierce, Rockford, IL, USA) or WesternBright (Advansta, USA). A 1:1 ratio of detection reagent A and detection reagent B was used per blot (total detection reagent volume = length of blot and breadth of blot x 0.1ml) and left to incubate on the nitrocellulose membrane for five minutes. The membrane was then sealed between two acetate sheets. Once the detection reagents meet the enzyme-conjugated secondary antibody, on the nitrocellulose membrane, light is emitted. This occurs due to the presence of the substrate for horseradish peroxidase in the detection reagents and, therefore oxidation of the substrate by the enzyme leads to the emission of light (**Figure 2.11**).

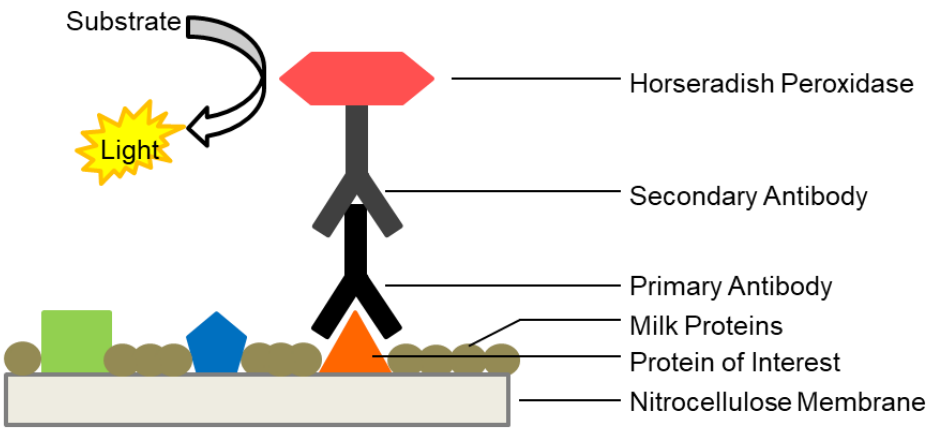

Figure 2.11: Protein detection by enhanced chemiluminescence. The primary antibody, specific to the protein of interest, binds to its target on the nitrocellulose membrane. An enzyme-conjugated secondary enzyme, raised against the animal that the primary antibody was raised in, binds to the primary antibody. The enzyme substrate is added directly onto the nitrocellulose membrane allowing for a chemical reaction to take place. Light is emitted, which is detected by exposure onto an autoradiography film.

Membranes were exposed to autoradiography film and the chemiluminescent signal captured by developing and fixing the blot. ImageJ was used to perform densitometric analysis with the readings normalised to the p38 loading control.

The primary antibodies used were as follows (appendix 8.5):

p38 (38kDa): The nitrocellulose membrane was blocked in 5% fat free milk in 1X PBS/0.1% Tween (PBS/T) and incubated with its' primary antibody (1:5000 rabbit polyclonal anti-p38) (Sigma-Aldrich, USA) in PBS/T only.

p21 (21kDa): The nitrocellulose membrane was blocked and incubated with its' primary antibody (1:200 mouse monoclonal anti-p21) (Santa Cruz, USA) in 5% fat free milk in 1X PBS/0.1% Tween (PBS/T).

p53 (53kDa): The nitrocellulose membrane was blocked and incubated with its' primary antibody (1:100 mouse monoclonal anti-p53) (Santa Cruz, USA) in 5% fat free milk in 1X PBS/0.1% Tween (PBS/T).

Vimentin (57.5kDa): The nitrocellulose membrane was blocked and incubated with its' primary antibody (1:1000 rabbit polyclonal anti-vimentin) (Cell Signaling Technology, USA) in 5% Bovine Serum Albumin (BSA) in TBS/T.

β-catenin (94kDa): The nitrocellulose membrane was blocked and incubated with its' primary antibody (1:500 mouse monoclonal anti-β-catenin) (Thermo Fisher Scientific) in 5% fat free milk in 1X PBS/0.1% Tween (PBS/T).

N-cadherin (140kDa): The nitrocellulose membrane was blocked and incubated with its' primary antibody (1:1000 mouse polyclonal anti-N-cadherin) (Cell Signalling Technology, USA) in 5% fat free milk in 1X TBS/0.1% Tween (TBS/T).

2.5.7 Flow Cytometry on Cell-Surface Vimentin Expression

To determine the effect of *N. brasiliensis* L3 antigen on HeLa cell-surface vimentin expression, the appropriately stained cells were analysed by flow cytometry. The media was removed, and the cells lifted using 2ml of Trypsin-EDTA. Cells were resuspended in 4ml of the DMEM for counting and $1x10^5$ cells were seeded per well, in quadruplicate, in a 24-well plate. *N. brasiliensis* L3 antigen (10µg or 50µg), lipopolysaccharide (LPS) (1µg) or 1X PBS was added to each of the required wells and the cells harvested at 12 hours post-treatment. To do this the cells in each well were lifted using Lidocaine-EDTA (appendix 8.4), to retain surface molecule integrity, and resuspended in 400µl of MACS buffer per well. Samples were centrifuged for five minutes at 1500rpm and 200µl of the supernatant removed. The pellet was then resuspended in the remaining 200µl of MACS buffer and the cell suspension added to individual wells of a 96-well round-bottom plate. The plate was then centrifuged for five minutes at 1500rpm, the supernatant removed, and the pellet resuspended in 20µl of MACS buffer containing a 1:50 dilution of rabbit polyclonal anti-vimentin (Santa Cruz Biotechnology, Clone H84) and R-phycoerythrin (PE)-conjugated donkey anti-rabbit IgG (Jackson ImmunoResearch Laboratories, Inc). The plate was subsequently incubated for 20 minutes at 4°C. Wells were then topped up with MACs buffer and the plate centrifuged for two minutes at 1500rpm. The pellets were resuspended in 200µl of MACs buffer ready for analysis on the BD LSR II Flow Cytometer. FlowJo Version 10 was used to analyse the data according to the gating strategy depicted in **Figure 2.12**.

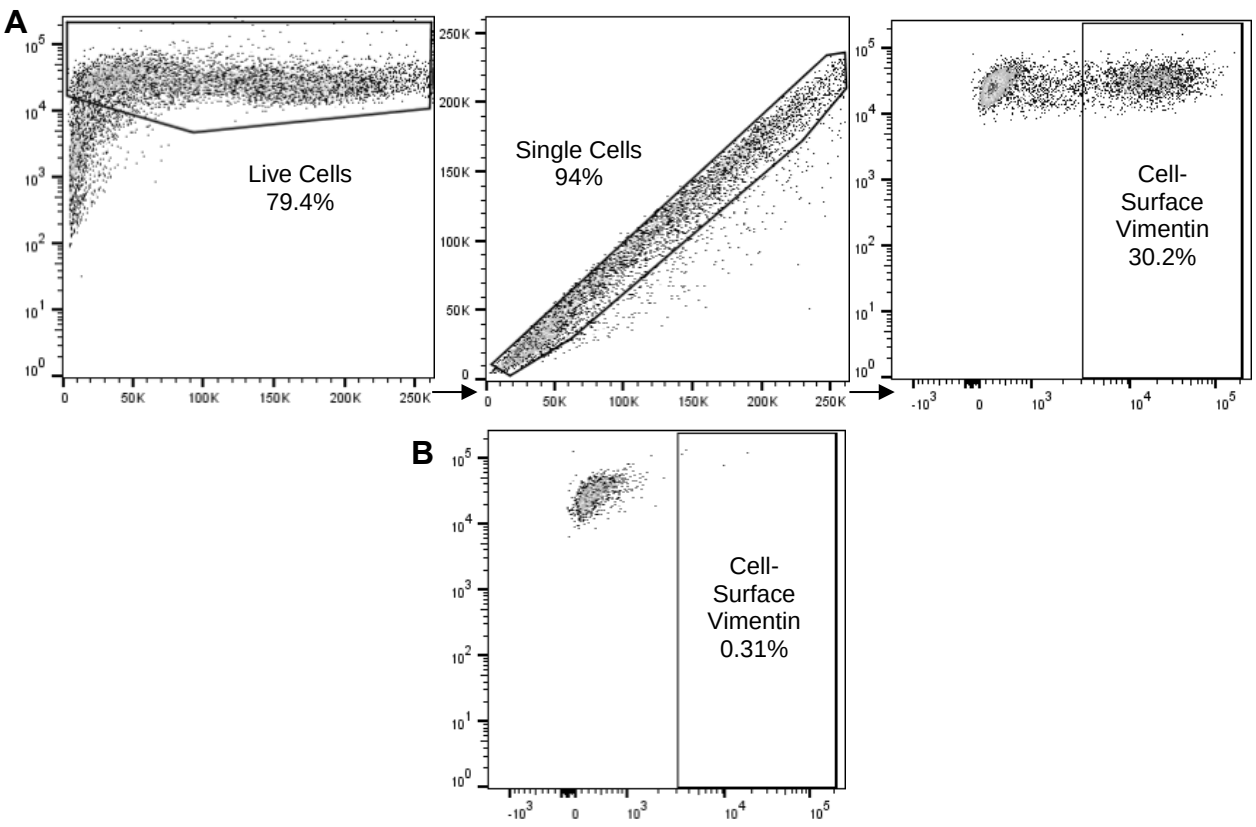

Figure 2.12: Gating strategy applied to obtain the cell-surface vimentin positive population. A. Cells were seeded, in quadruplicate, at a density of $1x10^5$ cells per well in a 24-well plate and treated with 10µg or 50µg *N. brasiliensis* L3 antigen or 1X PBS. Cells were incubated for 12 hours before harvesting in MACS buffer. **B.** Population of cells which have been stained with secondary antibody only. This control was used to determine the positively stained cell-surface vimentin population. Analysis performed using FlowJo Version 10.

2.5.8 HPV16 Pseudovirion Internalisation Assay

In order to determine the effect of *N. brasiliensis* L3 antigen on HPV internalisation in HeLa cells, a HPV pseudovirion internalisation assay was performed whereby cells were exposed to fluorochrome labelled HPV16 pseudovirions and analysed by flow cytometry. HPV16 pseudovirion preparation, labeling, and quality controls were performed as previously described (155).

The media was removed, and the cells lifted using 2ml of Trypsin-EDTA. Cells were resuspended in 4ml of DMEM for counting and $1x10^5$ cells were seeded per well, in quadruplicate, in a 24-well plate. *N. brasiliensis* L3 antigen (10µg or 50µg) or 1X PBS was added to each of the required wells for 12 hours. After this incubation period, 400ng of Alexa488 labelled HPV16 pseudovirions were added to each well (4pg per cell) and incubated for one hour at 4°C, to allow for pseudovirion attachment, and then 30 minutes at 37°C, to allow for pseudovirion internalisation. Cells were then lifted using Trypsin-EDTA, to ensure the removal of any surface-bound pseudovirions and harvested in 200µl of MACS buffer per well

ready for analysis on the BD LSR II Flow Cytometer. FlowJo Version 10 was used to analyse the data according to the gating strategy depicted in **Figure 2.13**.

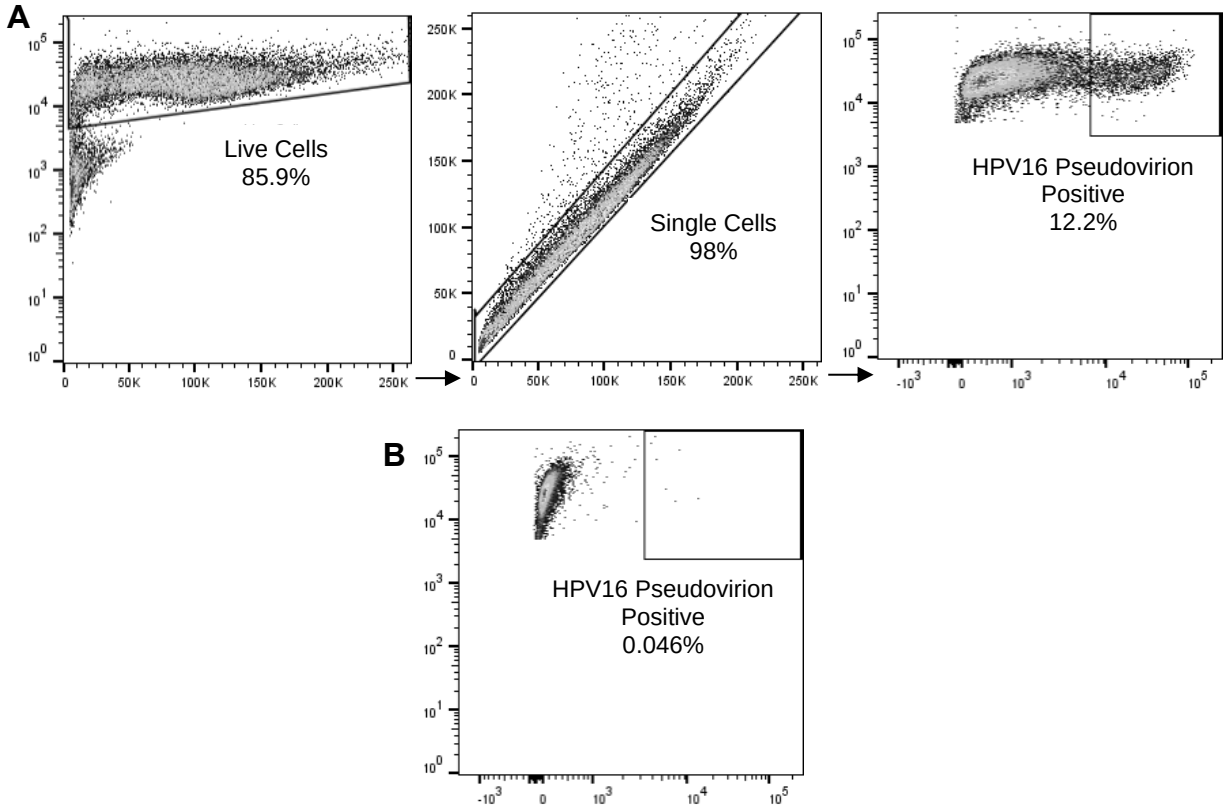

Figure 2.13: Gating strategy applied to obtain the HPV16 pseudovirion positive population. A. Cells were seeded, in quadruplicate, at a density of $1x10^5$ cells per well in a 24-well plate and treated with 10µg or 50µg *N. brasiliensis* L3 antigen or 1X PBS. Cells were incubated for 12 hours before the addition of 400ng of HPV16 pseudovirions per well for 1 hours at 4°C and 30 minutes at 37°C. Cells were subsequently harvested in MACS buffer. **B.** Population of HeLa cells which were not treated with Alexa488 labelled HPV16 pseudovirions. This control was used to generate a gate for HPV16 pseudovirion positive HeLa cells. Analysis performed using FlowJo Version 10.

2.6 *In vivo* Experiments

2.6.1 Mice

Unless stated otherwise, 6-10-week-old female BALB/c mice were used in all experiments. Mice were either bred in house (animal research performed at The University of Cape Town) or purchased from Charles River (animal research performed at Cardiff University).

Section 20 dispensation to carry out animal research at the University of Cape Town was granted by the South African Department of Agriculture Fisheries and Food and by the UCT Health Sciences Animal Ethics Committee (Project number 014/027 and 015/001). All procedures were performed by researchers accredited by the South African Veterinary Council. Permission to perform animal research at Cardiff University was granted by the Home

Office and performed under protocol 5 (Immunotherapy of Primary Tumours), project number 30/3428 (Induction of Anti-tumour Immunity).

2.6.2 Western Blotting on Murine Female Genital Tract (FGT) Tissue

To synchronize the estrous cycles, mice were treated with 2mg Medroxyprogesterone Acetate (Depo Provera®) subcutaneously. A week later, mice were infected subcutaneously with 500 L3 *N. brasiliensis* larvae and killed at day nine post-infection (**Figure 2.14**). The entire FGT was isolated and frozen at -80° C until further analysis.

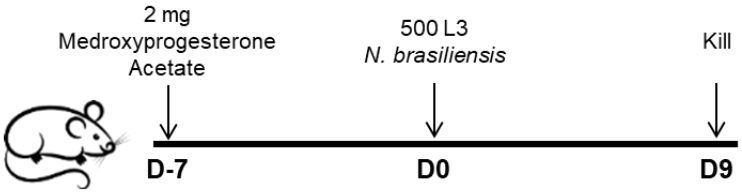

Figure 2.14: Experimental setup followed to determine the effect of *N. brasiliensis* infection on EMT marker expression in the mouse FGT.

Tissue samples were sonicated until uniformly homogenized and centrifuged to remove unwanted debris. The protein concentration of the supernatant was determined using a BCA assay and 20µg of protein per sample was used to run on a SDS-PAGE gel as previously described.

2.6.3 Colorectal Cancer Model

CT26.WT cells were utilized in an *in vivo* model to investigate the effect of HES and *H. polygyrus* antigen on colorectal cancer tumour development and progression. To achieve this, CT26.WT cells were cultured *in vitro* for a maximum of seven days and passaged at least twice before being injected subcutaneously into the left flank of mice. Each mouse received $5x10^5$ cells in a total volume of 100µl of PBS with either HES (10µg), *H. polygyrus* antigen (10µg) or 1X PBS. Tumour width and height were regularly measured using digital calipers, and the tumour volume calculated according to the equation:

$$\text{Volume} = 0.5 * (\text{Height} \times \text{Width}^2).$$

Two weeks later, mice were sacrificed and the tumours, inguinal draining (dLN) and non-draining lymph nodes (ndLN) removed. The lymph nodes were passed through a cell separator (70µm) into RPMI and the cell suspension centrifuged for five minutes at 1500rpm. The pellet was resuspended in 150µl of RPMI and 100µl of this placed into individual wells of a 96-well round-bottom plate. 100µl of 50ng/ml Phorbol Myristate Acetate (PMA) (EMD Millipore) plus 50ng/ml of ionomycin (Sigma-Aldrich, USA) was added to each well and the plate was left to incubate for four hours at 37°C. PMA (a protein kinase C activator) and

ionomycin (a calcium ionophore) are used to stimulate the production of intracellular cytokines by lymphocytes. One hour into the stimulation a 1:1000 dilution of Brefeldin A (Brev A) (Sigma-Aldrich, USA) was added to each well. Brev A inhibits protein transport, in this case the newly produced cytokines, from the endoplasmic reticulum to the Golgi apparatus and, therefore prevents release from the cell allowing the proteins to be stained and analysed appropriately (156).

After stimulation, the plate was centrifuged for three minutes at 1750rpm, the supernatant removed and a 1:10 dilution of live/dead aqua stain (Thermo Fisher Scientific) added to each well. The plate was then incubated for 15 minutes at room temperature. 150µl of FACS buffer (appendix 8.6) was added to each well and the plate centrifuged for three minutes at 1750rpm. 50µl containing a 1:100 dilution of FcγRII/III (eBioscience) was added to each well and the plate placed at 4°C for 15 minutes. 50µl containing a 1:100 dilution of Phycoerythrin Cyanine 7 (PeCy7)-labelled rat anti-mouse monoclonal CD3 (BioLegend, Clone 17A2), Brilliant Violet (BV) 421-labelled rat anti-mouse monoclonal CD8 (BioLegend, Clone 53-6.7) and BV605-labelled rat anti-mouse monoclonal CD4 (BioLegend, Clone GK1.5) was added to each well. The plate was then incubated for 30 minutes at 4°C. Wells were subsequently topped up with FACS buffer and the plate centrifuged for three minutes at 1750rpm. The cells were then fixed (eBioscience Ref. 00-5523-00) overnight at 4°C.

The plate was centrifuged for three minutes at 1750rpm and 100µl of Perm buffer (supplied in the Foxp3 Staining Buffer Set) was added to each well. 50µl containing a 1:100 dilution of FcγRII/III was added to each well and the plate placed at 4°C for 15 minutes. 50µl containing a 1:100 dilution of APC-labelled rat anti-mouse monoclonal Foxp3 (BD Bioscience, Clone FJK-16s) was then added to each well. The plate was then incubated for 30 minutes at 4°C and subsequently centrifuged for three minutes at 1750rpm. The cells were then washed once with Perm buffer and twice with FACS buffer for three minutes at 1750rpm per wash. The pellets were then resuspended in 200µl of FACS buffer in preparation for analysis on the ACEA Novocyte. FlowJo Version 10 was used to analyse the data according to the gating strategy depicted in **Figure 2.15**.

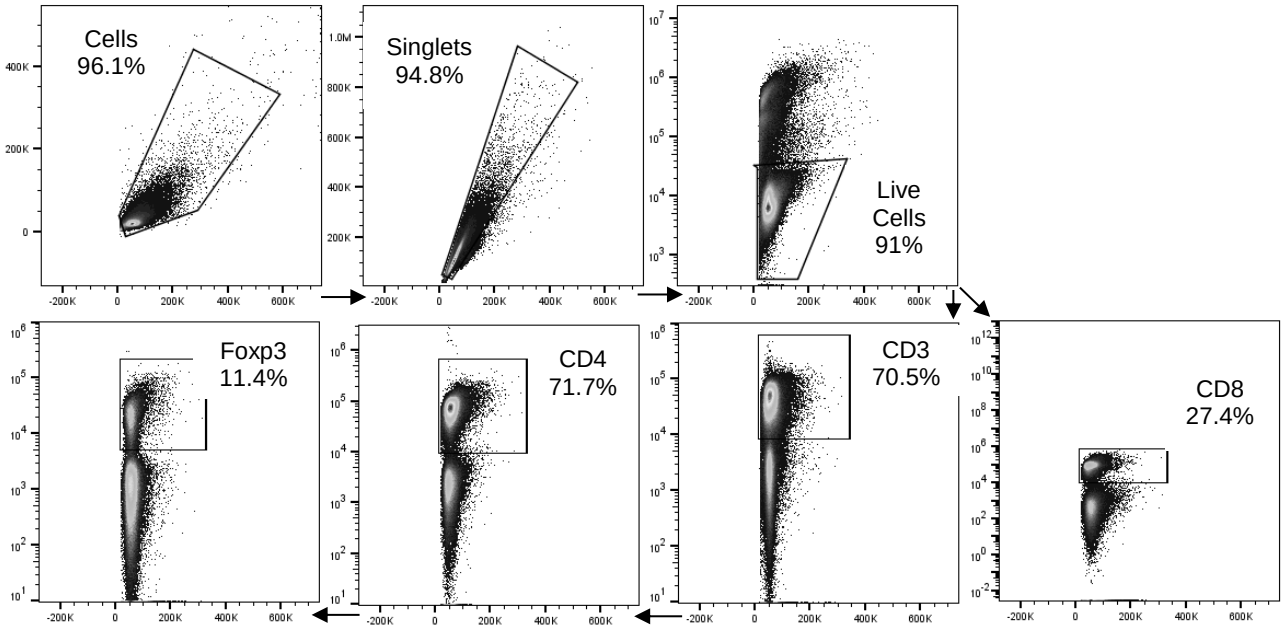

Figure 2.15: Gating strategy applied to cells of the draining (dLN) and non-draining (ndLN) lymph nodes. The dLN and ndLN were removed from CT26.WT tumour bearing mice, the cells seeded in a 96-well round-bottom plate and labelled and fixed appropriately. Analysis was performed using FlowJo Version 10.

The CT26.WT tumours were passed through a cell separator (70µm) into RPMI and the cell suspension centrifuged for five minutes at 1500rpm. The pellet was resuspended in 150µl of RPMI and 100µl of this placed into individual wells of a 96-well round-bottom plate. The plate was then centrifuged for three minutes at 1750rpm, the supernatant removed and a 1:10 dilution of live/dead aqua stain was added to each well. The plate was then incubated for 15 minutes at room temperature. 150µl of FACS buffer was added to each well and the plate centrifuged for three minutes at 1750rpm. 50µl of a 1:100 dilution of FcγRII/III was added to each well and the plate placed at 4°C for 15 minutes. 50µl containing a 1:100 dilution of BV421-labelled rat anti-mouse monoclonal Ly6C (BioLegend, Clone HK1.4), FITC-labelled rat anti-mouse monoclonal Ly6G (BioLegend, Clone 1A8), PerCpCy5.5-labelled rat anti-mouse monoclonal CD11b (BioLegend, Clone M1/70) and BV605-labelled mouse anti-rat monoclonal CD4 (BioLegend, Clone GK1.5) was added to each well. The plate was then incubated for 30 minutes at 4°C. Wells were subsequently topped up with FACS buffer and the plate centrifuged for three minutes at 1750rpm. The cells were then fixed (eBioscience Ref. 00-5523-00) overnight at 4°C.

The plate was centrifuged for three minutes at 1750rpm and 100µl of Perm buffer was added to each well. 50µl containing a 1:100 dilution of FcγRII/III was added to each well and the plate placed at 4°C for 15 minutes. 50µl containing a 1:100 dilution of APC-labelled rat anti-mouse monoclonal Foxp3 (BD Bioscience, Clone FJK-16s) was added to each well. The plate was

then incubated for 30 minutes at 4°C and subsequently centrifuged for three minutes at 1750rpm. The cells were then washed once with Perm buffer and twice with FACS buffer for three minutes at 1750rpm per wash. The pellets were then resuspended in 200µl of FACs buffer in preparation for analysis on the ACEA Novocyte. FlowJo Version 10 was used to analyse the data according to the gating strategy depicted in **Figure 2.16.**

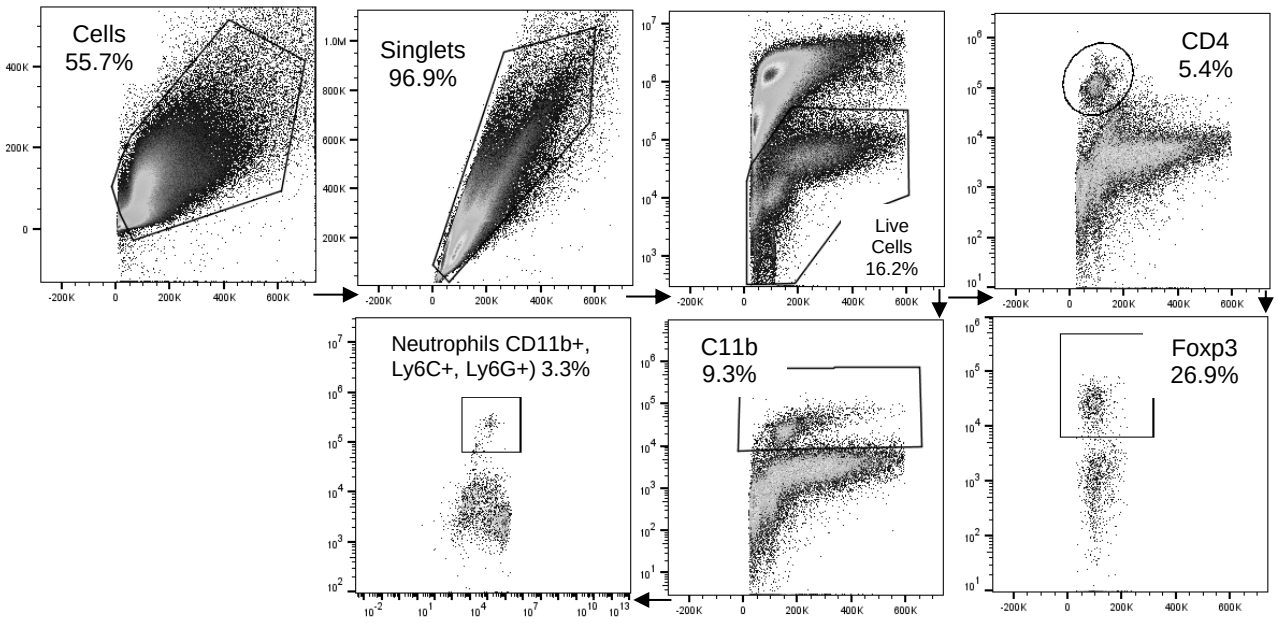

Figure 2.16: Gating strategy applied to CT26.WT tumour cells. CT26.WT tumours were removed from mice, the cells seeded in a 96-well round-bottom plate and labelled and fixed appropriately. Analysis was performed using FlowJo Version 10.

Cell counts were performed on all samples using the ACEA Novocyte. Propidium Iodide (Sigma-Aldrich, USA) was used to exclude dead cells. PI is a fluorescent intercalating agent that is able to cross the membrane of dead cells making it possible to distinguish between viable and dead cells (157).

2.6.4 The Effect of HES on Colitis-Associated Colorectal Cancer (CAC) Development

When introduced in combination, the carcinogen azoxymethane (AOM) and inflammatory agent dextran sulphate sodium (DSS) are able to model the development of CAC *in vivo* (158). Importantly, when placed on DSS and a diet high in linoleic acid mice are at an increased risk of developing colitis and consequently, when used in conjunction with a carcinogen, colorectal cancer development. This is due to nano-lipocomplex formation between DSS and medium-chain-length fatty acids present in the colon which are thought to activate intestinal inflammatory pathways (159). In order to determine whether HES is able to affect the development of CAC, mice were placed on AIN-76A food (a rodent diet high in linoleic acids) for one week and the experimental setup depicted in **Figures 2.17** followed.

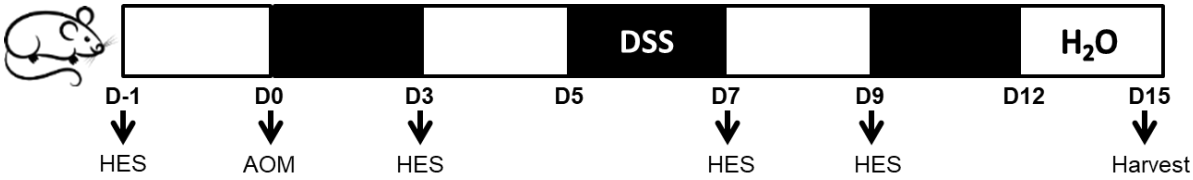

Figure 2.17: Experimental setup followed to determine the effect of HES on the development of colitis-associated colorectal cancer (CAC).

The weight of each mouse was monitored daily and on day 15 the mice were sacrificed, and the colon and spleen harvested. The length of the colon was measured from the end of the cecum to the rectum and a portion placed in 4% paraformaldehyde (appendix 8.6) in preparation for histological processing. The spleen was weighed and stored in MACS buffer for further processing.

Each spleen was passed through a cell separator (40µm) into RPMI and the cell suspension centrifuged for five minutes at 1500rpm. The pellet was then resuspended in 2ml Red Blood Cell lysis buffer for two minutes, topped up with RPMI and centrifuged for five minutes at 1500rpm. $1x10^5$ cells were seeded per well in a 96-well round-bottom plate and a 1:200 dilution of Alexa700-labelled rat anti-mouse monoclonal CD3 (BD Bioscience), PerCpCy5.5-labelled rat anti-mouse monoclonal CD4 (BD Bioscience), BV421-labelled rat anti-mouse monoclonal CD11b (BD Bioscience), PE-labelled rat anti-mouse monoclonal SiglecF (BD Bioscience), APC-labelled rat anti-mouse monoclonal Ly6G (BD Bioscience) and APC-Cy7-labelled rat anti-mouse monoclonal Ly6C/G-Gr1 (BD Bioscience) was added to the relevant wells together with 1% rat serum and 1% FcγRII/III. The plate was then incubated for 30 minutes at 4°C. Wells were then topped up with MACs buffer and the plate centrifuged for two minutes at 1500rpm. The pellets were then resuspended in MACs buffer in preparation for analysis on the BD LSR II Flow Cytometer. FlowJo Version 10 was used to analyse the data according to the gating strategy depicted in **Figure 2.18**.

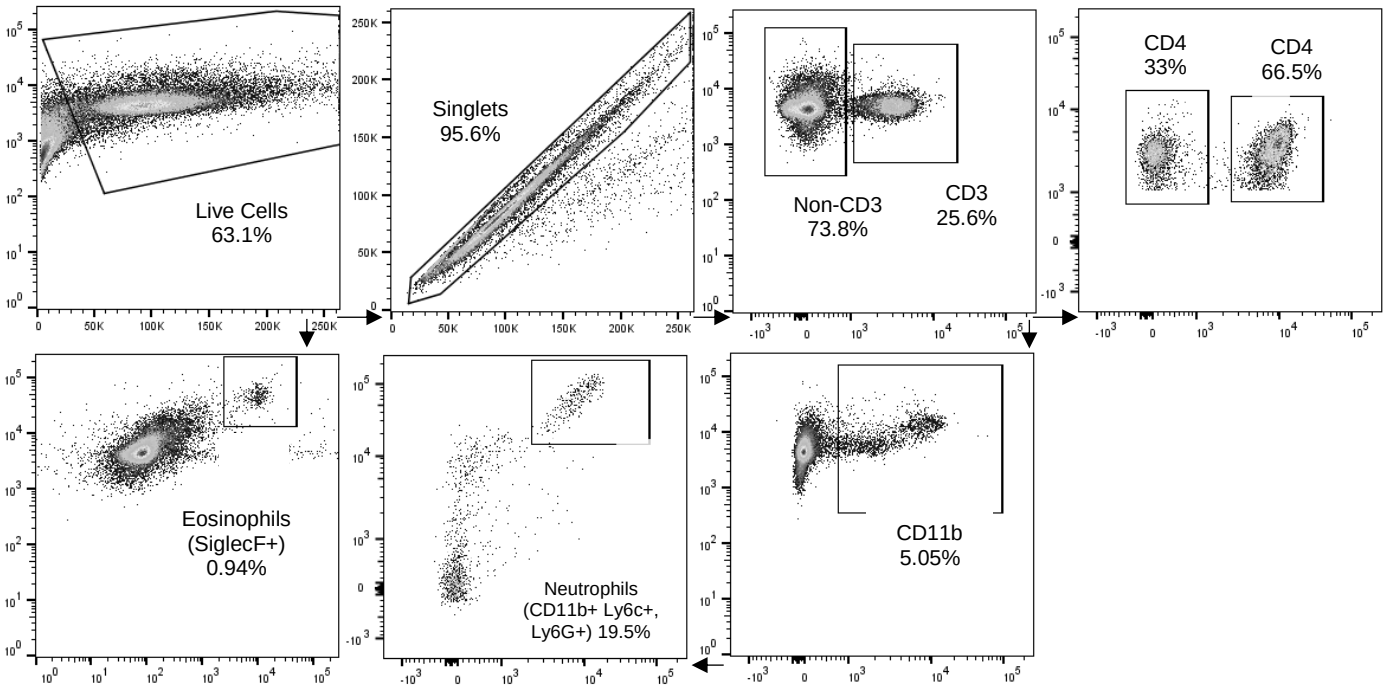

Figure 2.18: Gating strategy applied to splenocytes. Cells from the spleen were seeded at a density of $1x10^6$ cells per well in a 96-well round-bottom plate and labelled and fixed appropriately. Analysis was performed using FlowJo Version 10.

2.6.5 The Effect of the TGF-β Mimic Contained in HES on CAC Development *in vivo*

In order to determine whether the TGF-β mimic contained within HES is able to affect the development of CAC, mice were placed on AIN-76A for one week and the experimental setup depicted in **Figure 2.19** followed.

Figure 2.19: Experimental setup followed to determine the effect of the TGF-β mimic in HES on the development of colitis-associated colorectal cancer (CAC).

SB-431542 (Sigma-Aldrich - S4317) is a small molecule inhibitor of the TGF-β type I receptor (160). By inhibiting this receptor, SB-431542 prevents the phosphorylation of Smad2/3, which is then unable to form a complex with Smad4 and translocate into the nucleus. Ultimately, gene expression induced by TGF-β signaling does not occur (**Figure 2.20**).

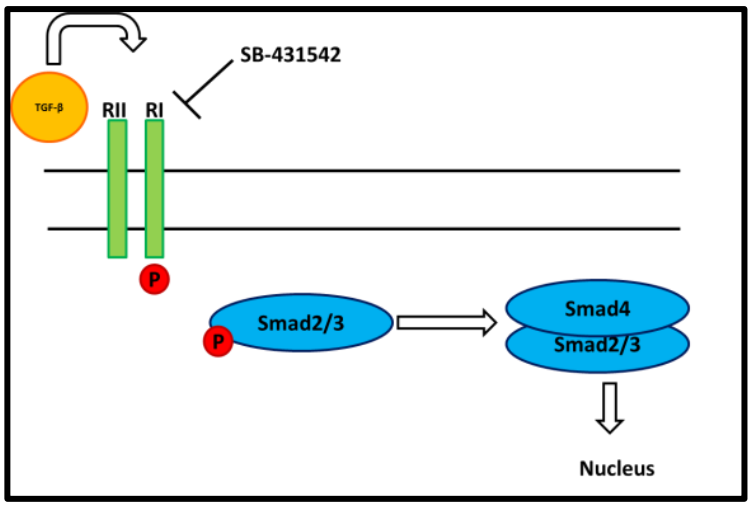

Figure 2.20: SB-431542 method of action. Small molecule inhibitor, SB-431542, inhibits the TGF-β type I receptor. This prevents the phosphorylation of Smad2/3 and complex formation with Smad4, thus inhibiting translocation into the nucleus as well as gene expression.

The weight and distress scores (**Figure 2.21**) of each mouse was monitored daily and on day 15 the mice were sacrificed, and the colon and spleen harvested. The length of the colon was measured from the end of the cecum to the rectum and the spleen was weighed and stored in MACS buffer for further processing. FlowJo Version 10 was used to analyse the data according to the gating strategy depicted in **Figure 2.22**.

Appearance		**Natural behaviour**	
Normal	0	Normal	0
General lack of grooming	1	Minor changes	1
Coat staring. Ocular and nasal discharges	2	Less mobile and alert, isolated	2
Pilo-erection, hunched up	3	Vocalisation, restlessness, very still	3
Clinical sign		**Provoked behaviour**	
Normal colour and movement	0	Normal	0
Slight changes in activity	1	Minor depression or exaggerated response	1
Moderate Changes:weight loss, diarhoea, fecal blood (min)	2	Moderate change in expected behaviour	2
Severe changes:immobility, lameness, extensive fecal blood	3	Reacts violently or very weak	3

*If 3 was scored more than once, an extra point was scored for every 3. Total=16

Figure 2.21: Criteria used to calculate the total distress score for each mouse. Adapted from Professor Awen Gallimore's laboratory at Cardiff University.

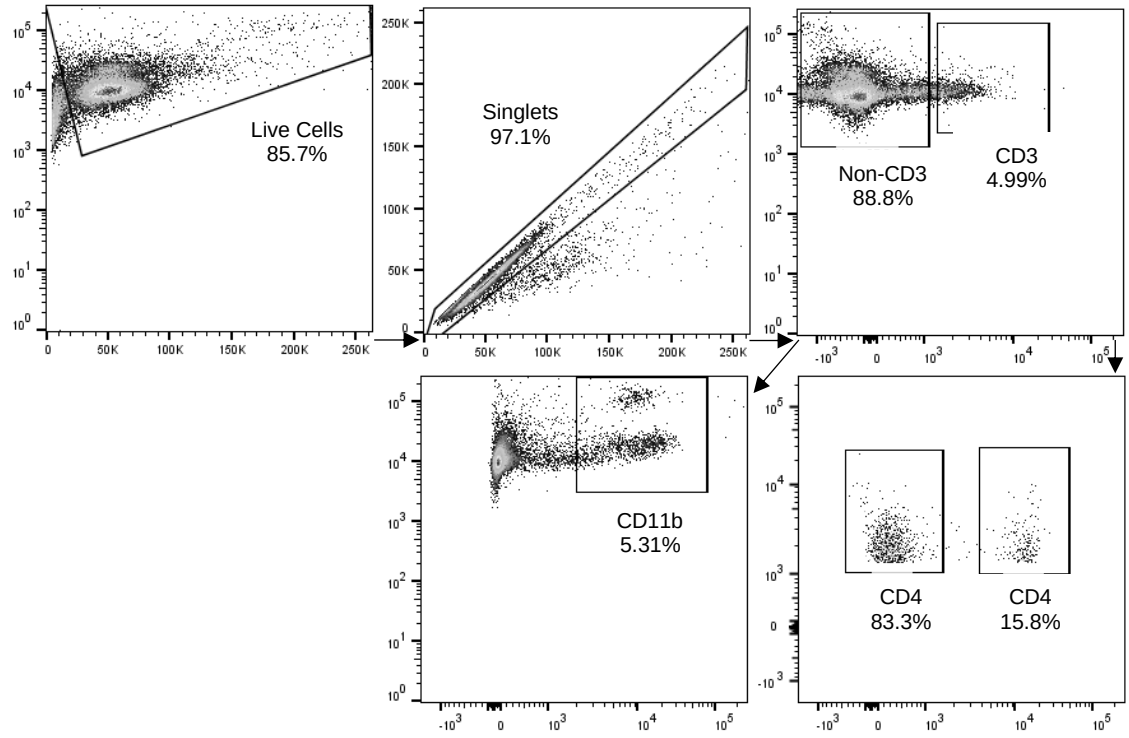

Figure 2.22: Gating strategy applied to splenocytes. Cells from the spleen were seeded at a density of $1x10^6$ cells per well in a 96-well round-bottom plate and labelled and fixed appropriately. Analysis was performed using FlowJo Version 10.

2.7 Statistical Analyses

Data were assessed for normality and equal variance and were log transformed if required using the GraphPad Prism 6.01 software (La Jolla, CA). For comparison between two groups, an unpaired t-test was used; where more than three groups were being tested, a parametric two-way or one-way analysis of variance with multiple comparisons was used. Error bars represent Standard Error of the Mean and *p<0.05, **p<0.01, ***p<0.001 and ****p<0.0001.

3. Results

3.1 Investigating the Effect of Parasite Antigen on Cervical Cancer Behaviour *in vitro*

The impact of exposure to soil-transmitted helminths (STH) on cervical cancer cell growth, and migration is unknown. To this end, *in vitro* assays were performed investigating the effect of different parasite antigens on cervical cancer behaviour.

3.1.1 *Nippostrongylus brasiliensis* L3 Antigen Does Not Affect HeLa Cell Proliferation

The Human Papillomavirus type 18 (HPV18) positive cervical cancer cell line, HeLa, was exposed to a titration of *N. brasiliensis* L3 antigen concentrations and the cell proliferation monitored by counting cells over a 3-day period using a haemocytometer. When compared to untreated cells, *N. brasiliensis* L3 antigen did not have a significant effect on HeLa cell proliferation at any of the time points or concentrations tested (**Figure 3.1**).

3.1.2 *N. brasiliensis* L3 Antigen Significantly Reduces HeLa Cell Migration and Expression of EMT Markers

The possibility was considered that while *N. brasiliensis* L3 antigen did not affect HeLa cell proliferation, it may influence cell migration. To address this, HeLa cells were treated with *N. brasiliensis* L3 antigen and two-dimensional scratch motility and transwell migration assays were performed.

Results from both assays indicated that *N. brasiliensis* L3 antigen decreased HeLa cell migration. Indeed, in the two-dimensional scratch motility assay, 10µg of *N. brasiliensis* L3 antigen significantly decreased HeLa cell migration at 8 hours post-wound formation (**Figure 3.2A and Figure 3.2B**). Similarly, the transwell migration assay revealed a 1.36-fold decrease in the migration of HeLa cells treated with 10µg of *N. brasiliensis* L3 antigen compared to that of untreated cells (**Figure 3.2C**).

To determine whether this effect was hookworm specific, HeLa cells were exposed to antigen derived from the adult stage of the solely gastrointestinal nematode *H. polygyrus* or its excretory-secretory product (HES). Notably, no significant effect on the migration of *H. polygyrus* antigen or HES treated HeLa cells was observed (**Figure 3.2D**), suggesting that the inhibitory effect of *N. brasiliensis* L3 antigen on HeLa cell migration is hookworm dependent.

It was speculated that *N. brasiliensis* L3 antigen may be inhibiting HeLa cell migration by repressing Epithelial-Mesenchymal Transition (EMT) markers. To investigate this, levels of vimentin and N-cadherin were determined by western blotting using protein from HeLa cells

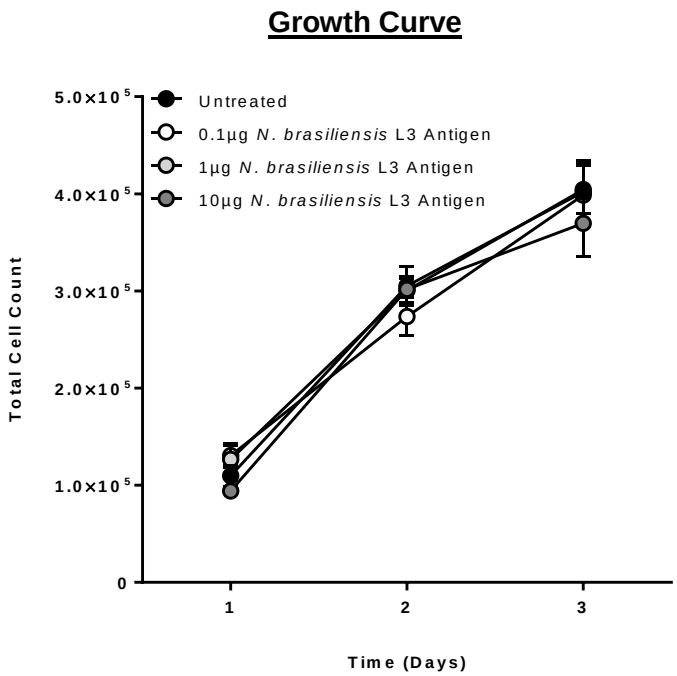

Figure 3.1: *N. brasiliensis* L3 antigen does not affect HeLa cell proliferation. Cells were seeded in triplicate at a density of $5x10^4$ cells per well in a 24-well plate and treated with 0.1µg, 1µg or 10µg *N. brasiliensis* L3 antigen or 1X PBS. Growth curve analyses were performed over a 3-day period by harvesting trypsinised cells and counting the cells using a haemocytometer. This figure shows pooled data from two independent experiments each performed in triplicate. The data were analysed using GraphPad Prism 6.01 and a parametric unpaired t-test was performed. Error bars represent Standard Error of the Mean.

treated with or without *N. brasiliensis* L3 antigen. p38 was used throughout this study as a loading control in western blot analyses because although its activity is modulated by phosphorylation, total levels of this protein remain unchanged in response to stimuli (161). The results revealed that the observed reduction in HeLa cell migration was indeed associated with a decrease in the expression of the EMT markers vimentin and N-cadherin (**Figure 3.3**).

3.1.3 *N. brasiliensis* L3 Antigen Significantly Reduces Ca Ski Cell Migration

To investigate whether *N. brasiliensis* L3 antigen could also inhibit the migratory ability of other cervical cancer cells i.e. that the effect seen was not specific to HeLa cells, the above experimental conditions and migration assays were repeated for the Human Papillomavirus type 16 (HPV16) positive cervical cancer cell line Ca Ski. Indeed, results from the two-dimensional scratch motility assay revealed that 10µg of *N. brasiliensis* L3 antigen significantly decreased Ca Ski cell migration at 4 and 8 hours post-wound formation (**Figure 3.4A and Figure 3.4B**). Furthermore, albeit not significant, when treated with 10µg of *N. brasiliensis* L3 antigen, Ca Ski cell migration was also reduced in the transwell migration assay (**Figure 3.4C**). The impact of *N. brasiliensis* L3 antigen on the EMT markers vimentin and N-cadherin in Ca Ski cells was also explored by western blotting as described for the HeLa cells.

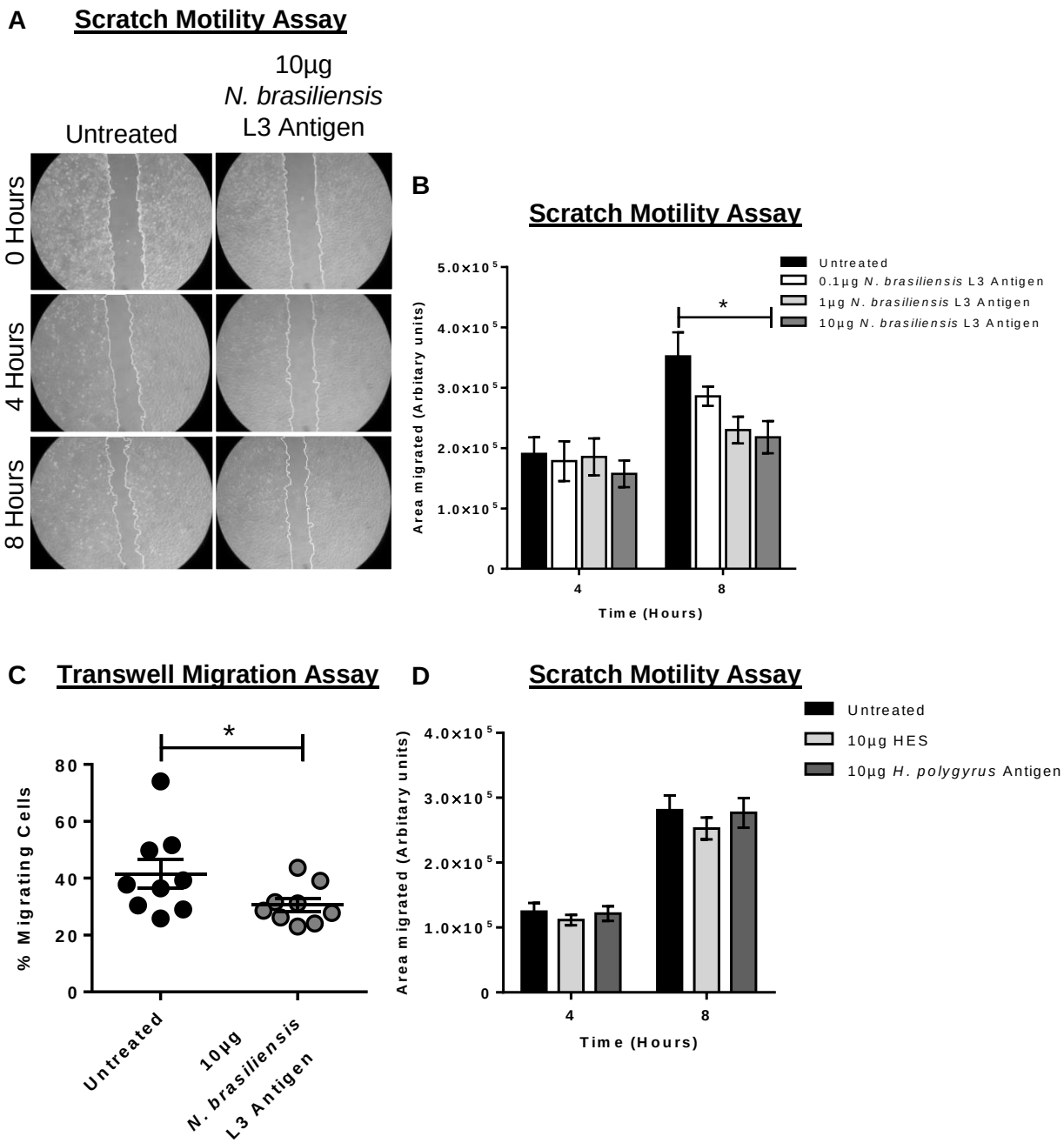

Figure 3.2: *N. brasiliensis* L3 antigen decreases HeLa cell migration. A and B. Migration was measured using a two-dimensional scratch motility assay. $5x10^4$ cells were seeded per well in a 24-well plate and allowed to reach confluency. Cells were treated with 0.1µg, 1µg or 10µg *N. brasiliensis* L3 antigen or 1X PBS and a sterile 2µl pipette tip was used to form a linear wound in the cell monolayer. Cells were imaged at 0, 4 and 8 hours post-wound formation with the total area migrated calculated relative to wound area at time 0 hours. **C.** Serum starved cells were seeded at a density of $1x10^5$ cells per well into a 24-well transwell hanging-insert containing DMEM supplemented with 1% FBS and 10µg *N. brasiliensis* L3 antigen or 1X PBS. Each insert was then placed individually into a well containing DMEM supplemented with 10% FBS. Migrated cells, which had adhered to the lower surface of the 8µm membrane, were fixed with methanol and stained with crystal violet. 50% acetic acid was used to wash off the crystal violet stain and the absorbance of each well was read at a wavelength of 595nm. **D** Migration was measured using a two-dimensional *in vitro* scratch motility assay as described for **A and B**. using 10µg HES or 10µg *H. polygyrus* antigen. All the panels in this figure represent pooled data from three independent experiments each performed in triplicate. The data were analysed using GraphPad Prism 6.01 and a parametric unpaired t-test was performed. **C.** Pooled data was log transformed before performing a parametric unpaired t-test. *p<0.05 **p<0.01 ***p<0.001 ****p<0.0001. Error bars represent Standard Error of the Mean.

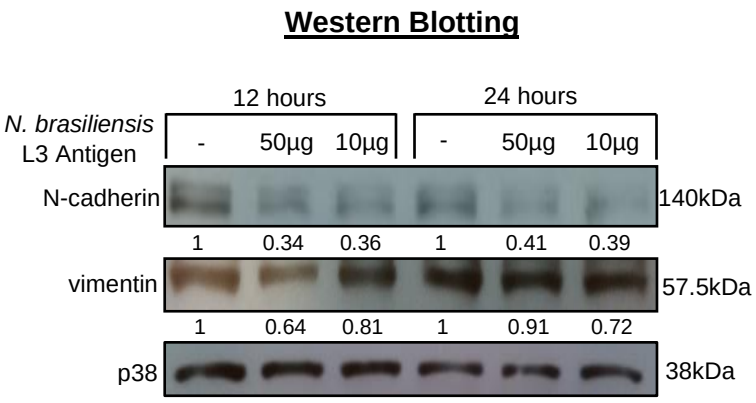

Figure 3.3: *N. brasiliensis* L3 antigen decreases levels of EMT marker expression in HeLa cells. Cells were seeded at a density of $2x10^5$ cells per well in a 6-well plate and treated with 10µg or 50µg *N. brasiliensis* L3 antigen or 1X PBS. Cells were incubated for 12 or 24 hours before harvesting the cells and extracting total protein. Western blotting was performed with antibodies specific for vimentin and N-cadherin with p38 used as the loading control. Densitometry readings were obtained using ImageJ to determine the changes in protein expression of vimentin and N-cadherin normalised to p38 and expressed as a fold-change relative to control wells. This figure is representative of three independent experiments.

However, despite numerous attempts the results were inconsistent and are, therefore not included in the thesis. Possible reasons for this are commented on in the Discussion.

3.1.4 *N. brasiliensis* L3 Antigen Significantly Reduces C33-A Cell Migration and Expression of EMT Markers

The HeLa and Ca Ski cervical cancer cell lines are HPV positive and it was, therefore of interest to determine whether the HPV status impacts the effects of *N. brasiliensis* L3 antigen on cervical cancer cell migration. To address this, C33-A HPV negative cervical cancer cells were exposed to the *N. brasiliensis* L3 antigen and their migration was measured by the two-dimensional scratch motility and transwell migration assays. Indeed, the results from both assays show that the migration of C33-A cells was significantly inhibited following *N. brasiliensis* L3 antigen treatment (**Figure 3.5A - 3.5C)**. Interestingly, C33-A cells appear to be more sensitive to *N. brasiliensis* L3 antigen as even the lower concentrations of antigen used in the two-dimensional scratch motility assay significantly reduced cell migration at 4 and 8 hours post wound-formation (**Figure 3.5B**).

Furthermore, as observed in the HeLa cells, both 10µg and 50µg *N. brasiliensis* L3 antigen reduced the expression of vimentin and N-cadherin in C33-A cells (**Figure 3.6**). Together these results show that *N. brasiliensis* L3 antigen reduces cervical cancer cell migration independent of HPV status by targeting EMT makers.

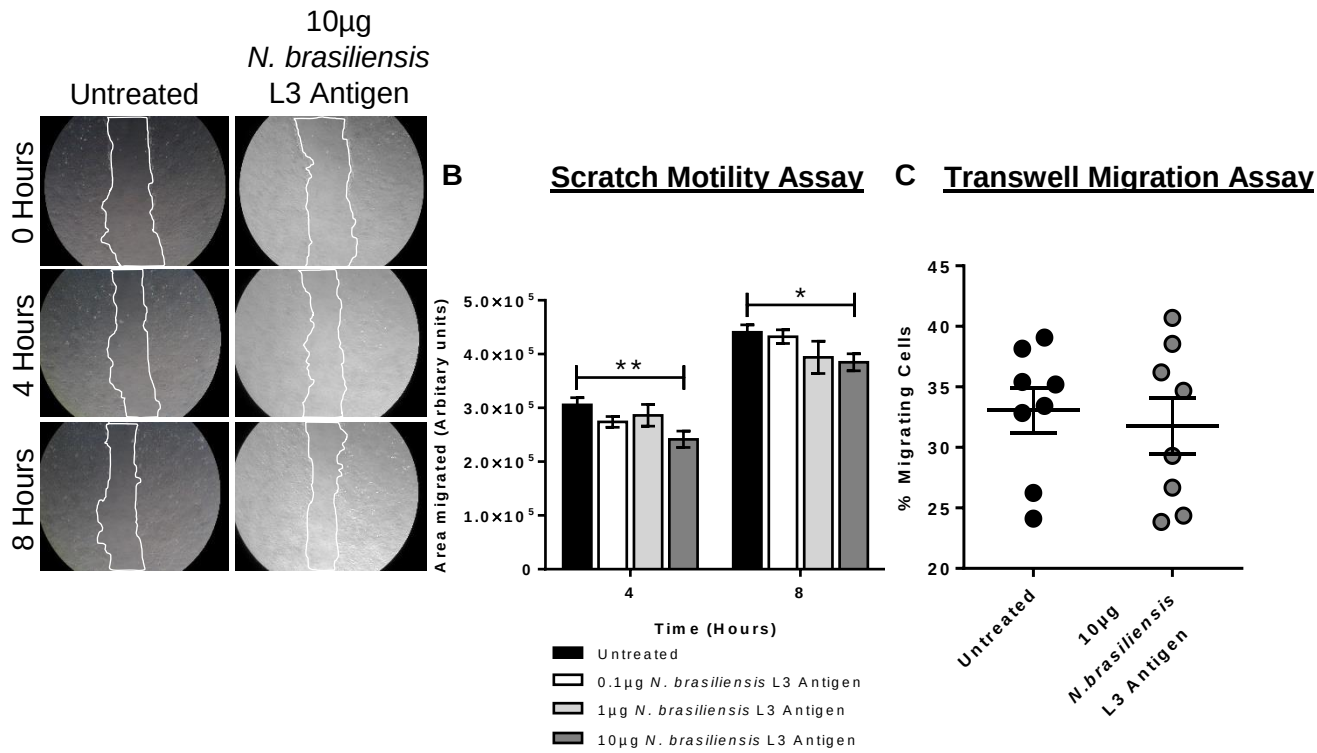

Figure 3.4: *N. brasiliensis* L3 antigen decreases Ca Ski cell migration. A and B. Migration was measured using a two-dimensional scratch motility assay. 1x10^5 cells were seeded per well in a 24-well plate and allowed to reach confluency. Cells were treated with 0.1µg, 1µg or 10µg *N. brasiliensis* L3 antigen or 1X PBS and a sterile 2µl pipette tip was used to form a linear wound in the cell monolayer. Cells were imaged at 0, 4 and 8 hours post-wound formation with the total area migrated calculated relative to wound area at time 0 hours. **C.** Serum starved cells were seeded at a density of 1x10^5 cells per well into a 24-well transwell hanging-insert containing RPMI supplemented with 1% FBS and 10µg *N. brasiliensis* L3 antigen or 1X PBS. Each insert was then placed individually into a well containing RPMI supplemented with 10% FBS. Migrated cells, which had adhered to the lower surface of the 8µm membrane, were fixed with methanol and stained with crystal violet. 50% acetic acid was used to wash off the crystal violet stain and the absorbance of each well was read at a wavelength of 595nm. All the panels in this figure represent pooled data from three independent experiments each performed in triplicate. The data were analysed using GraphPad Prism 6.01 and a parametric unpaired t-test was performed *p<0.05 **p<0.01 ***p<0.001 ****p<0.0001. Error bars represent Standard Error of the Mean.

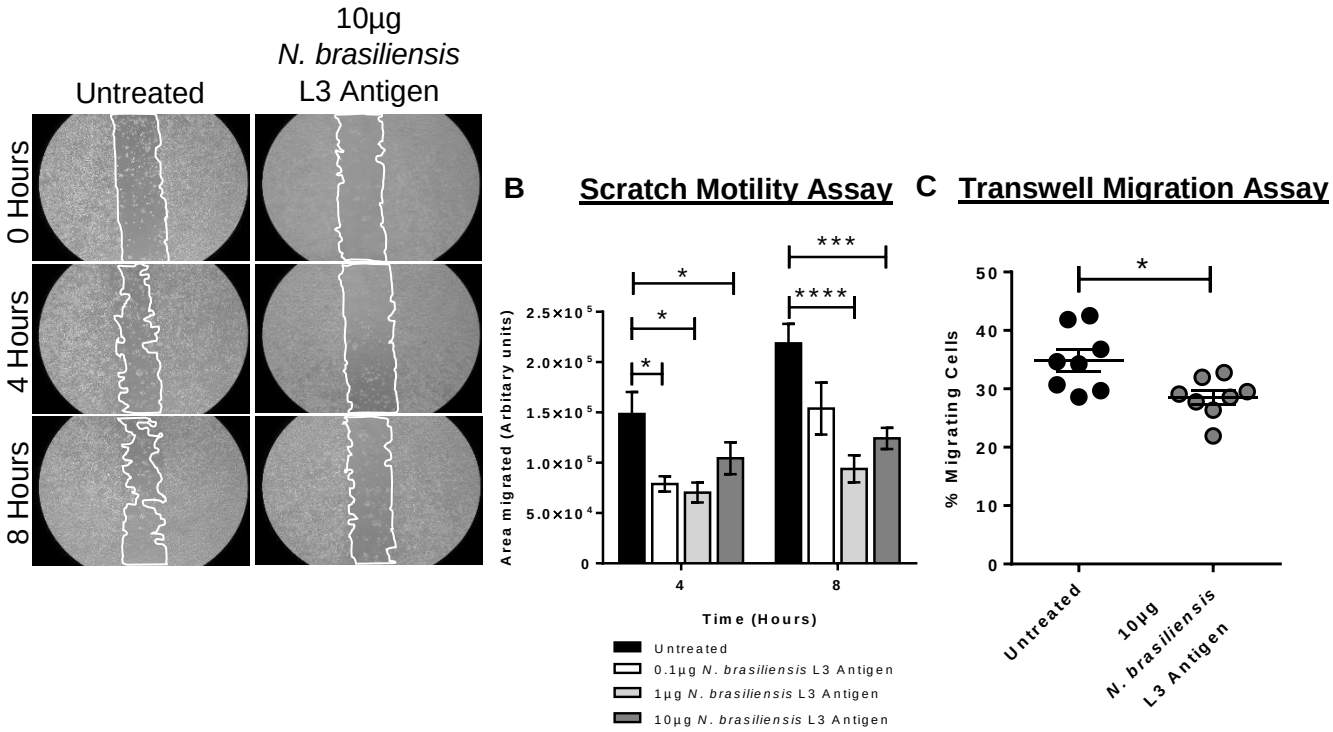

Figure 3.5: *N. brasiliensis* L3 antigen decreases C33-A cell migration. A and B. Migration was measured using a two-dimensional scratch motility assay. Cells were seeded at a density of $2x10^5$ cells per well in a 24-well plate and allowed to reach confluency. Cells were treated with 0.1µg, 1µg or 10µg *N. brasiliensis* L3 antigen or 1X PBS and a sterile 2µl pipette tip was used to form a linear wound in the cell monolayer. Cells were imaged at 4 and 8 hours post-wound formation with the total area migrated calculated relative to wound area at time 0 hours. **C.** Serum starved cells were seeded at a density of $1x10^5$ cells per well into a 24-well transwell hanging-insert containing medium supplemented with 1% FBS and 10µg *N. brasiliensis* L3 antigen or 1X PBS. Each insert was then placed individually into a well containing medium supplemented with 10% FBS. Migrated cells, which had adhered to the lower surface of the 8µm membrane, were fixed with methanol and stained with crystal violet. 50% acetic acid was used to wash off the crystal violet stain and the absorbance of each well was read at a wavelength of 595nm. All the panels in this figure represent pooled data from three independent experiments each performed in triplicate. The data were analysed using GraphPad Prism 6.01 and a parametric unpaired t-test was performed *p<0.05 **p<0.01 ***p<0.001 ****p<0.0001. Error bars represent Standard Error of the Mean.

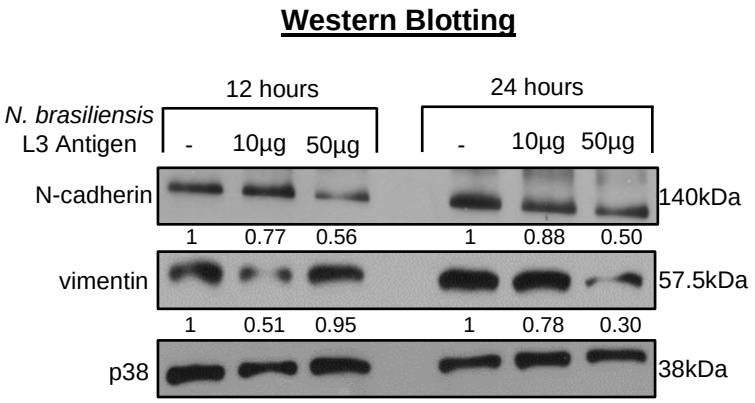

Figure 3.6: *N. brasiliensis* L3 antigen decreases levels of EMT marker expression in C33-A cells. Cells were seeded at a density of $2x10^5$ cells per well in a 6-well plate and treated with 10µg or 50µg *N. brasiliensis* L3 antigen or 1X PBS. Cells were incubated for 12 or 24 hours before harvesting the cells and extracting total protein. Western blotting was performed with antibodies specific for vimentin and N-cadherin with p38 used as the loading control. Densitometry readings were obtained using ImageJ to determine the changes in protein expression of vimentin and N-cadherin normalised to p38 and expressed as a fold-change relative to control wells. This figure is representative of two independent experiments.

3.1.5 *N. brasiliensis* Infection Reduces the Expression of EMT Makers in the Mouse Female Genital Tract (FGT)

The observations that *N. brasiliensis* L3 antigen reduces the expression of vimentin and N-cadherin in both HPV positive and HPV negative cervical cancer cells begged the question whether live infection with *N. brasiliensis* would similarly affect these markers in non-cancerous cervical tissue. Briefly to address this, mice were infected subcutaneously with 500 L3 *N. brasiliensis* larvae and a week later the FGTs of infected and naïve mice were harvested and total protein extracted from them were subjected to western blotting with antibodies to vimentin and N-cadherin. The results revealed that, compared to the naïve mice, the FGTs of mice infected with *N. brasiliensis* had decreased expression of vimentin and N-cadherin (**Figure 3.7A**). Indeed, the densitometric analyses of the western blots show that the average expression of vimentin (**Figure 3.7B**) and N-cadherin (**Figure 3.7C**) in infected mice were 0.62 and 0.55 compared to 1.29 and 0.73 in naïve mice respectively.

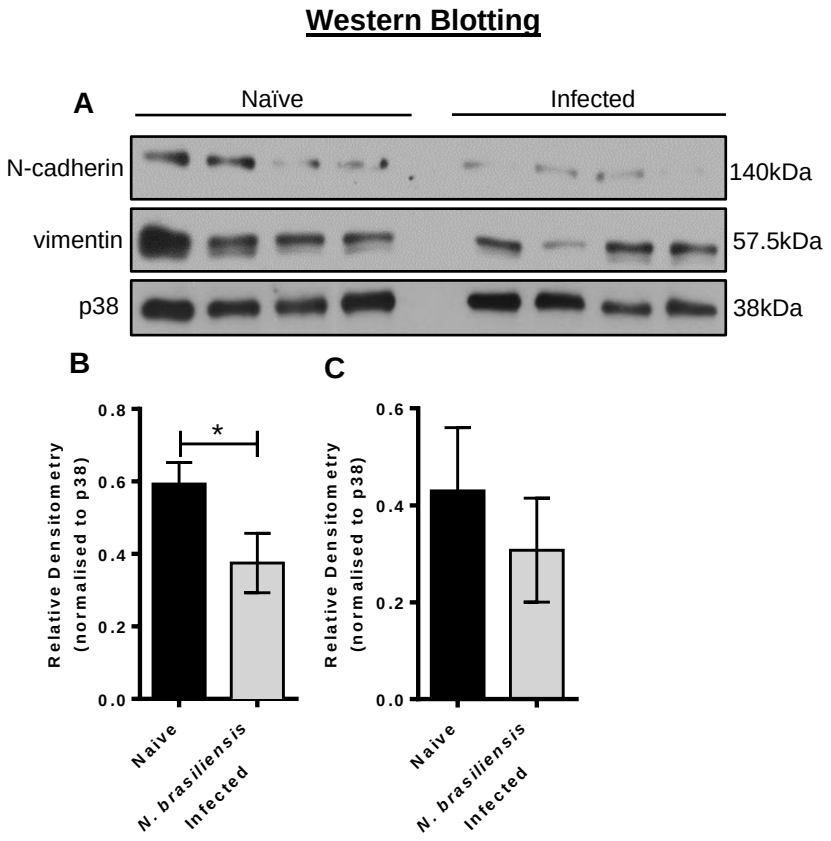

Figure 3.7: *N. brasiliensis* infection leads to reduced EMT marker expression in mouse female genital tracts (FGTs). A. FGTs were removed from four naïve and four *N. brasiliensis* infected mice, homogenised and total protein extracted and quantified. 20µg of protein was loaded onto an SDS-PAGE gel and western blotting was performed with antibodies specific for vimentin and N-cadherin with p38 used as the loading control. This figure is representative of two independent experiments. Densitometry readings were obtained using ImageJ to determine the changes in protein expression of **B.** vimentin and **C.** N-cadherin normalised to p38. This figure shows pooled data from two independent experiments. The data were analysed using GraphPad Prism 6.01 and a parametric unpaired t-test was performed *p<0.05 **p<0.01 ***p<0.001 ****p<0.0001. Error bars represent Standard Error of the Mean.

3.1.6 Cell-Surface Vimentin Expression and HPV16 Pseudovirion Internalisation is Diminished in *N. brasiliensis* L3 Antigen Treated HeLa Cells

Gastrointestinal helminths have been implicated in increasing the susceptibility of cervical tissue to the cancer-causing virus HPV (162). Interestingly, cell-surface vimentin expression has been shown to act as a restriction factor on HeLa cells for HPV16 pseudovirions (163). Due to the decrease in total vimentin expression observed following exposure of HeLa cells to *N. brasiliensis* L3 antigen, the possibility was considered that the expression of cell-surface vimentin would be similarly reduced and lead to increased susceptibility to pseudovirion internalisation. To investigate this, HeLa cells were exposed to *N. brasiliensis* L3 antigen and cell-surface vimentin expression analysed by flow cytometry. The results showed that 50µg of *N. brasiliensis* L3 antigen also significantly reduced the expression of cell-surface vimentin (**Figure 3.8**).

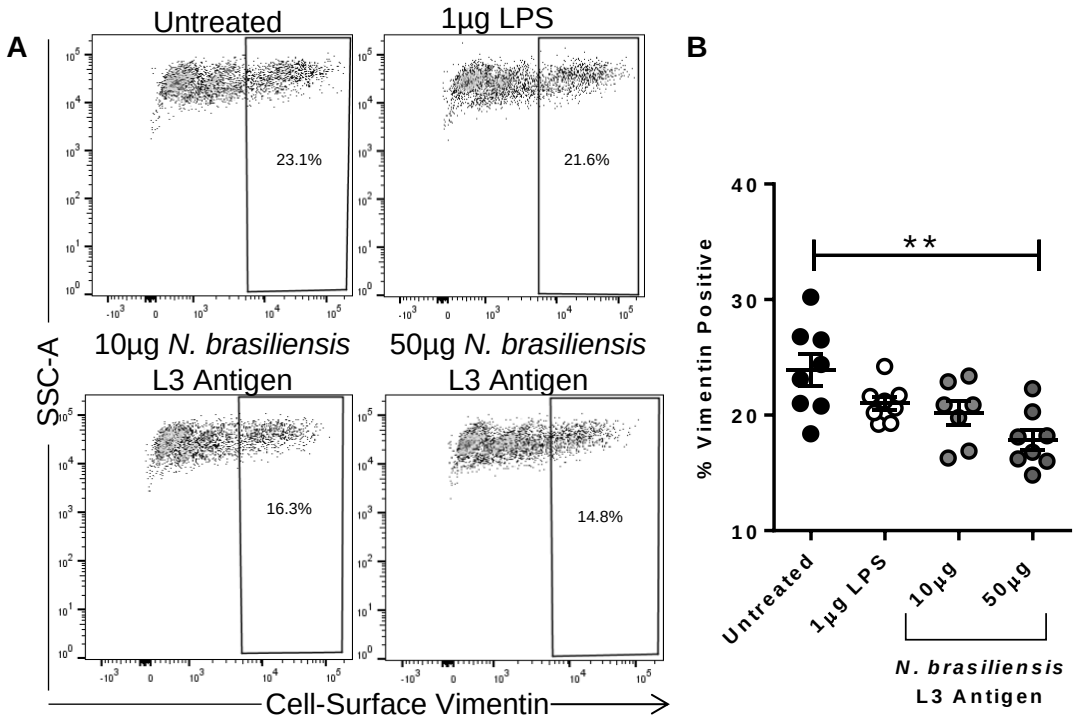

Figure 3.8: *N. brasiliensis* L3 antigen decreases HeLa cell-surface vimentin expression. Cells were seeded at a density of $1x10^5$ per well in a 24-well plate and treated with 10µg or 50µg *N. brasiliensis* L3 antigen, 1X PBS or 1µg LPS. **A.** Cells were incubated for 12 hours with *N. brasiliensis* L3 antigen, harvested in MACS buffer and analysed by flow cytometry. **B.** Graph shows pooled data from two independent experiments each performed in quadruplicate. The data were analysed using FlowJo Version 10 and GraphPad Prism 6.01 and a parametric unpaired t-test was performed *p<0.05 **p<0.01 ***p<0.001 ****p<0.0001. Error bars represent Standard Error of the Mean.

To exclude the possibility that the *N. brasiliensis* L3 antigen used in the above experiments was contaminated with Lipopolysaccharide (LPS), which could have occurred during the harvesting process, and that the LPS was responsible for the effects seen, the *Limulus* Amoebocyte Lysate (LAL) assay was performed. The results showed that the *N. brasiliensis* L3 antigen contained low levels of endotoxin (2.80EU/ml) which is used as a proxy for LPS in this assay. However, when analysed by flow cytometry, the endotoxin (from 1µg of LPS) had no significant impact on cell-surface vimentin expression (**Figure 3.8**). Together this data confirm that the effect observed for *N. brasiliensis* L3 antigen on HeLa cell-surface vimentin was not due to contaminating LPS.

The next experiment sought to determine whether the *N. brasiliensis* L3 antigen induced decrease in cell-surface vimentin expression correlated with an increase in pseudovirion internalisation. To this end, *N. brasiliensis* L3 antigen treated HeLa cells were incubated with fluorochrome-labelled HPV16 pseudovirions and the degree of internalisation of these

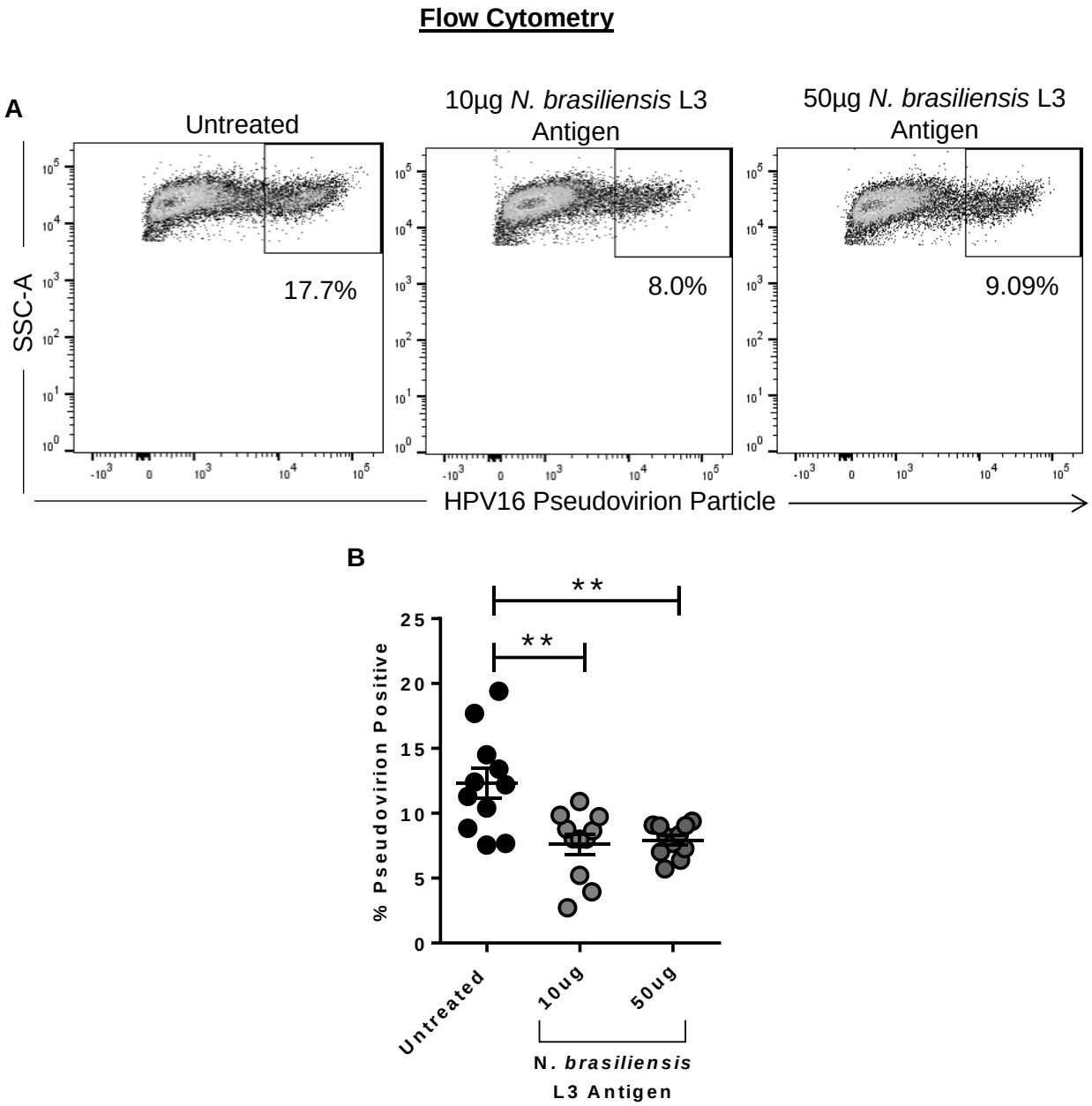

Figure 3.9: *N. brasiliensis* L3 antigen decreases HPV16 pseudovirion internalisation by HeLa cells. Cells were seeded at a density of 1x10^5 cells per well in a 24-well plate and treated with 10µg or 50µg *N. brasiliensis* L3 antigen or 1X PBS. Cells were incubated for 12 hours with *N. brasiliensis* L3 antigen before the addition of 400ng of HPV16 pseudovirions per well for 1 hour at 4°C and then 30 minutes at 37°C. **A.** Flow cytometry analyses of cells subsequently harvested in MACS buffer. **B.** Graph shows pooled data from two independent experiments each performed in quadruplicate. The data were analysed using FlowJo Version 10 and GraphPad Prism 6.01 and a parametric unpaired t-test was performed *p<0.05 **p<0.01 ***p<0.001 ****p<0.0001. Error bars represent Standard Error of the Mean.

pseudovirions was determined by flow cytometry (**Figure 3.9**). Surprisingly, HPV16 pseudovirion internalisation was significantly diminished in *N. brasiliensis* L3 antigen treated HeLa cells suggesting that the decrease in cell-surface vimentin expression did not significantly impact the degree of pseudovirion internalisation.

In summary, the results shown in section 3.1 provide compelling evidence that *N. brasiliensis* inhibits cervical cancer cell migration and HPV16 pseudovirion uptake, which is associated with a decrease in expression of EMT markers.

3.2 Investigating the Effect of *Heligmosomoides polygyrus* Derived Antigens on Colorectal Cancer Behaviour *in vitro*

The aim of this section was to determine the effect of antigens derived from the gastrointestinal nematode *H. polygyrus* on colorectal cancer cell behaviour using several *in vitro* assays.

3.2.1 *H. polygyrus* Derived Antigens Significantly Decrease Colorectal Cancer Cell Proliferation with an Associated Increase in Expression of Cell Cycle Regulators

To determine the effect of *H. polygyrus* derived antigens on colorectal cancer cells, CT26.WT cells were exposed to 10µg HES or 10µg *H. polygyrus* antigen and cell proliferation was monitored by counting cells over a 3-day period using a haemocytometer. **Figure 3.10A** shows that both *H. polygyrus* derived antigens significantly decreased cell proliferation at 3 days post-treatment.

As in section 3.1, the LAL assay was performed to exclude the possibility that *H. polygyrus* derived antigens were contaminated with LPS. The results showed that HES and *H. polygyrus* antigen contained low endotoxin levels of 0.7EU/ml and 2.8EU/ml respectively.

It was speculated that *H. polygyrus* derived antigens may be supressing CT26.WT cell proliferation by activating cell cycle regulator proteins. To investigate this, protein levels of the tumour suppressor p53 and its downstream target gene p21 were determined by western blotting using protein from CT26.WT cells treated as described above. The results showed that, compared to the untreated control cells, the expression of p53 and p21 were considerably higher following treatment with these antigens (**Figure 3.10B**).

To determine whether this effect was *H. polygyrus* specific, CT26.WT cells were exposed to SEA, egg antigen from *Schistosoma mansoni,* a blood fluke associated with colorectal cancer development (164, 165). Surprisingly, SEA had no effect on CT26.WT cell proliferation (**Figure 3.10C**), suggesting that the inhibitory effect of *H. polygyrus* derived antigens on CT26.WT cell proliferation is specific to this nematode.

To validate the findings that *H. polygyrus* derived antigens inhibit CT26.WT cell proliferation the cells were treated as described earlier and the Methylthiazol Tetrazolium (MTT) and Bromodeoxyuridine (BrdU) incorporation assays were performed.

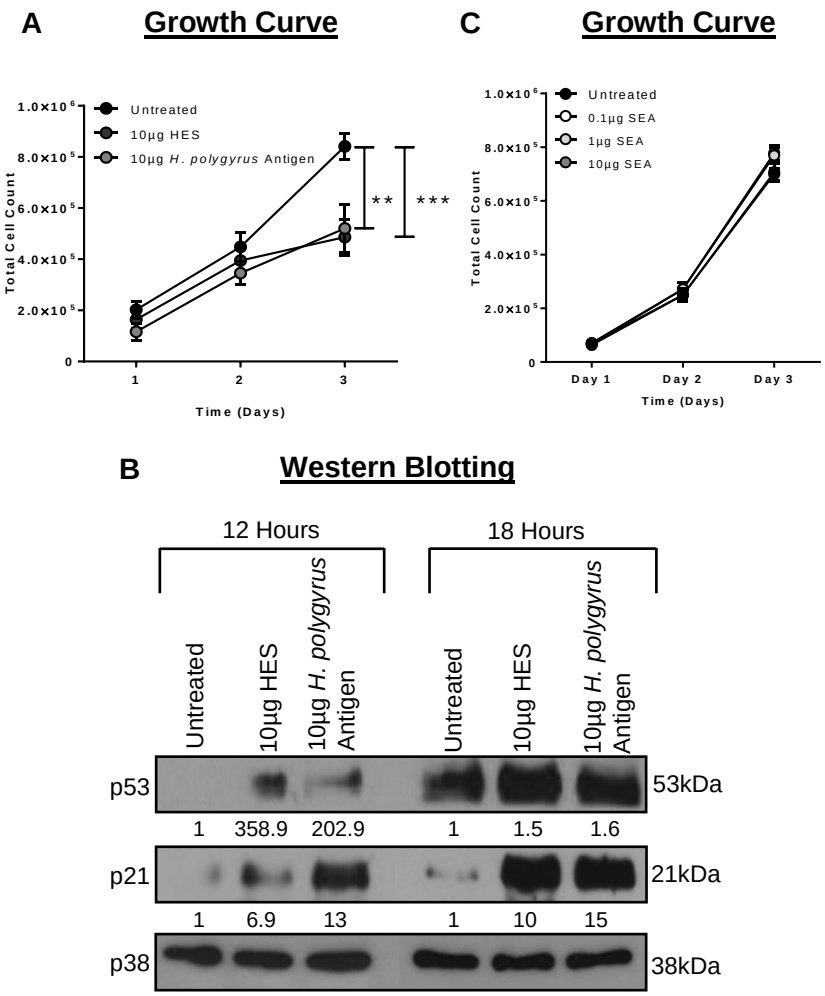

Figure 3.10: *H. polygyrus* derived antigens decrease CT26.WT cell proliferation and increase cell cycle regulator protein expression. A. 5x10^4 cells were seeded per well in a 24-well plate and treated with 10µg HES, 10µg *H. polygyrus* antigen or 1X PBS. Growth curve analyses were performed over a 3-day period by harvesting trypsinised cells and counting the cells using a haemocytometer. **B.** 2x10^5 cells were seeded per well in a 6-well plate and treated with 10µg HES, 10µg *H. polygyrus* antigen or 1X PBS for 12 or 18 hours before harvesting the cells and extracting the total protein. Western blotting was performed with antibodies specific for p53 and p21 with p38 used as the loading control. This result is representative of three independent experiments. Densitometry readings were obtained using ImageJ to determine the changes in protein expression of p53 and p21 normalised to p38 and expressed as a fold-change relative to control wells. **C.** 5x10^4 cells were seeded per well in a 24-well plate and treated with 0.1µg, 1µg or 10µg SEA or 1X PBS. Growth curve analyses were performed over a 3-day period by harvesting trypsinised cells and counting the cells using a haemocytometer. This figure shows pooled data from four (**A**) and two (**C**) independent experiments each performed in triplicate. The data were analysed using GraphPad Prism 6.01 and a parametric unpaired t-test was performed *p<0.05 **p<0.01 ***p<0.001 ****p<0.0001. Error bars represent Standard Error of the Mean.

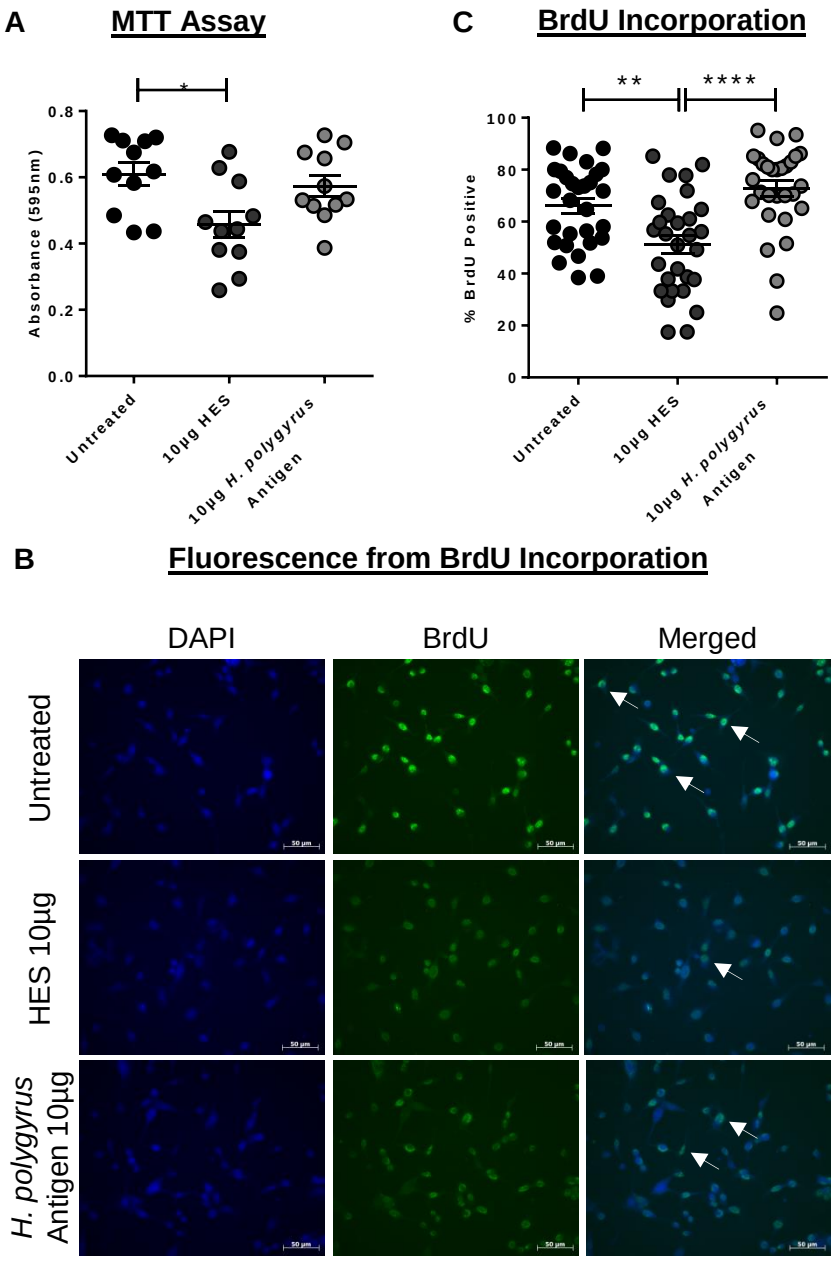

Figure 3.11: HES, but not *H. polygyrus* antigen, decreases CT26.WT cell viability and BrdU incorporation. A. 4x10^3 cells were seeded per well in a 96-well plate and treated with 10µg HES, 10µg *H. polygyrus* antigen or 1X PBS for 48 hours. MTT was added to each well for 4 hours followed by the addition of the solubilizer and 24 hours later the absorbance of each well was read at a wavelength of 595nm. **B.** 2x10^5 cells were seeded in a 35mm dish and treated with 10µg HES, 10µg *H. polygyrus* antigen or 1X PBS. 8 hours before immuno-processing 10µM BrdU was added to each dish and the relevant cells co-stained with DAPI. An Axiovert Fluorescent microscope (Zeiss, Germany) was used to visualise and image 15 fields of view per treatment condition. **C.** To quantify the images, the presence of a green nuclear stain, compared to a blue DAPI only nuclear stain, was concluded to be BrdU positive (white arrows). This figure shows pooled data from three (**A**) and two (**B and C**) independent experiments each performed in triplicate. The data were analysed using GraphPad Prism 6.01 and a parametric unpaired t-test was performed *p<0.05 **p<0.01 ***p<0.001 ****p<0.0001. Error bars represent Standard Error of the Mean.

Results from the MTT assay (**Figure 3.11A**) and BrdU incorporation (**Figure 3.11B and Figure 3.11C**) assays showed that HES treatment indeed resulted in a significant reduction in CT26.WT cell viability/proliferation. However, no significant effect was observed for *H. polygyrus* antigen treatment.

The CT26.WT cell line is a murine colorectal cancer cell line and it was therefore, of interest to determine whether the *H. polygyrus* derived antigens would similarly inhibit the proliferation of a human colorectal cancer cell line, HCT116. As observed in CT26.WT cells, growth curve analyses showed that the proliferation of HCT116 cells was significantly decreased following treatment with both HES and *H. polygyrus* antigen (**Figure 3.12A**). Furthermore, the expression of p53 and p21 was notably elevated in treated compared to untreated cells (**Figure 3.12B**). Consistent with the MTT results obtained for the murine CT26.WT colorectal cancer cells, HES caused a trend towards lowered cell viability of the human HCT116 cells (**Figure 3.12C**). In contrast to the MTT assay results obtained for the CT26.WT cells, however, *H. polygyrus* antigen significantly decreased human HCT116 cell viability (**Figure 3.12C**).

3.2.2 *H. polygyrus* Derived Antigens Significantly Alter Colorectal Cancer Cell Migration

Having established that antigen derived from *H. polygyrus* significantly decreased both CT26.WT and HCT116 cell proliferation, whether these antigens would alter cell migration was of interest. To this end, CT26.WT and HCT116 cells were exposed to HES and *H. polygyrus* antigen and their migratory ability measured using the transwell migration assay. Interestingly, the results obtained showed that while HES and *H. polygyrus* antigen significantly increased CT26.WT cell migration (**Figure 3.13A**), they significantly reduced the migration of HCT116 cells (**Figure 3.13B**). These results indicated that HES and *H. polygyrus* antigen impacted the migratory ability of mouse and human colorectal cancer cells differently.

In an attempt to explain the molecular mechanism by which HES and *H. polygyrus* antigen affected colorectal cancer cell migration, the levels of β-catenin were determined using western blotting. The rationale for this was that β-catenin levels have been positively associated with colitis-associated colorectal cancer (CAC) tumourigenesis and, in particular, migration (100, 166-169). β-catenin levels increased in the mouse CT26.WT cells treated with *H. polygyrus* derived antigens which correlated well with their pro-migratory effect on these cells (**Figure 3.13C**). On the other hand, *H. polygyrus* derived antigens decreased β-catenin levels in human HCT116 cells which was consistent with their inhibitory effect on the migration of these cells (**Figure 3.13D**). It is important to note that this experiment was only

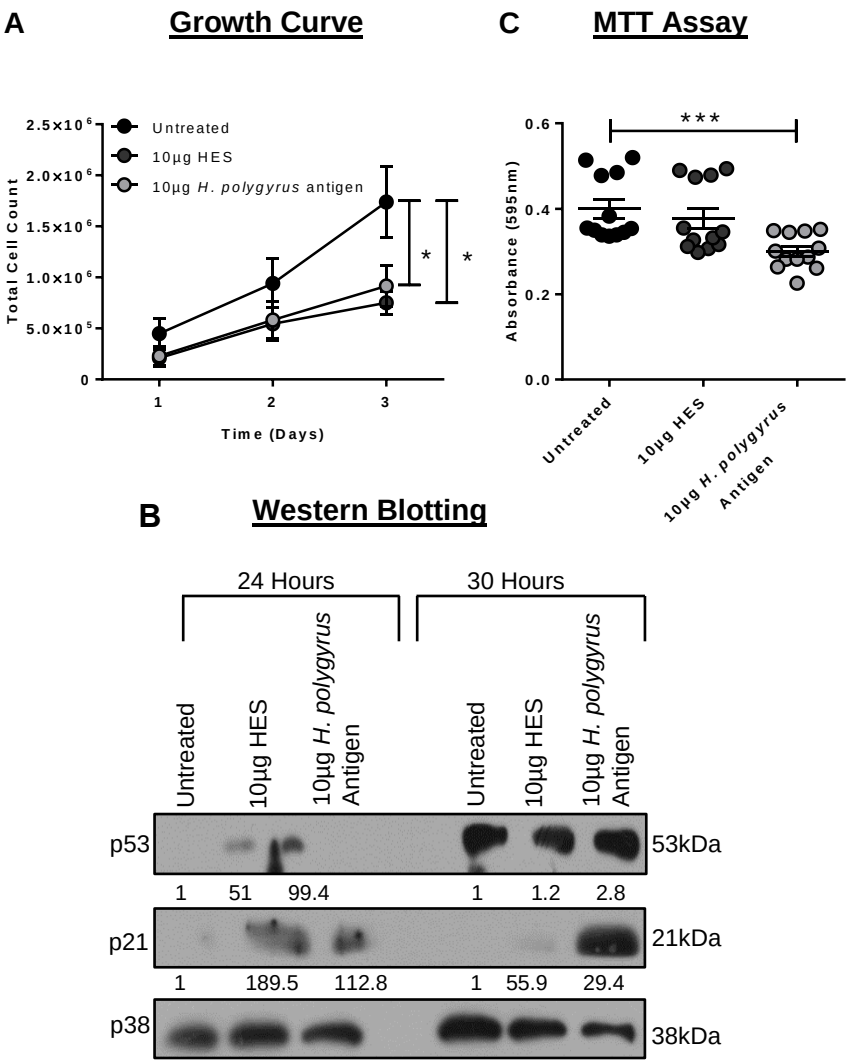

Figure 3.12: *H. polygyrus* derived antigens decrease HCT116 cell proliferation and increase cell cycle regulator protein expression. A. 5x10^4 cells were seeded per well in a 24-well plate and treated with 10µg HES, 10µg *H. polygyrus* antigen or 1X PBS. Growth curve analyses were performed over a 3-day period by harvesting trypsinised cells and counting the cells using a haemocytometer. **B.** 2x10^5 cells were seeded per well in a 6-well plate and treated with 10µg HES, 10µg *H. polygyrus* antigen or 1X PBS. Cells were incubated for 24 or 30 hours before harvesting the cells and extracting the total protein. Western blotting was performed with antibodies specific for p53 and p21 with p38 used as the loading control. This result is representative of two independent experiments. Densitometry readings were obtained using ImageJ to determine the changes in protein expression of p53 and p21 normalised to p38 and expressed as a fold-change relative to control wells. **C.** 4x10^3 cells were seeded per well in a 96-well plate and treated with 10µg HES, 10µg *H. polygyrus* antigen or 1X PBS for 48 hours. MTT was added to each well for 4 hours followed by the addition of the solubilizer and 24 hours later the absorbance of each well was read at a wavelength of 595nm. **A and C.** Show pooled data from three independent experiments each performed in triplicate. The data were analysed using GraphPad Prism 6.01 and t-test was performed *p<0.05 **p<0.01 ***p<0.001 ****p<0.0001. Error bars represent Standard Error of the Mean.

performed once and that it would need to be repeated before any conclusive deductions are made.

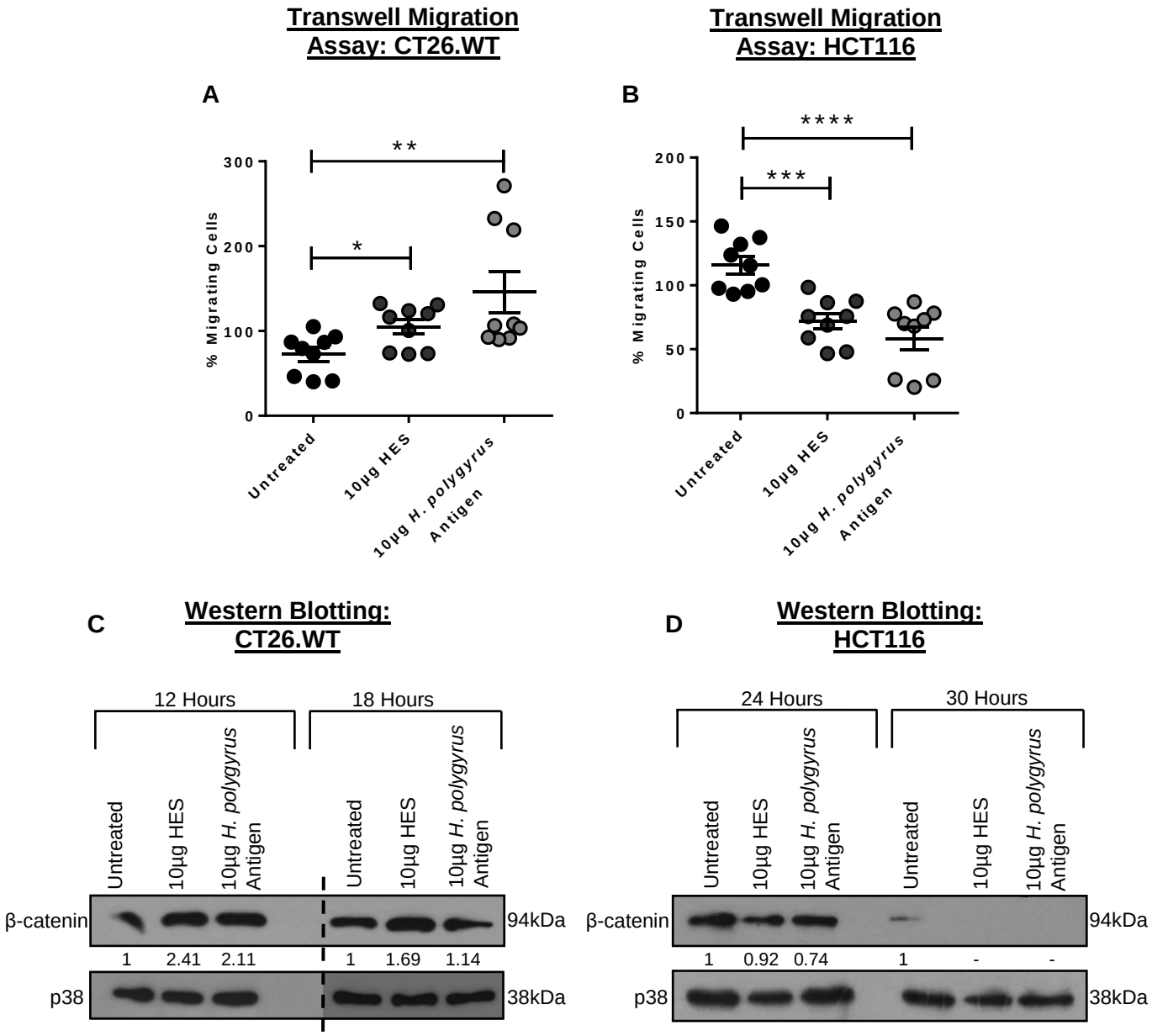

Figure 3.13: *H. polygyrus* antigens alter colorectal cancer cell migration in a species-specific manner. Serum starved CT26.WT (**A**) and HCT116 (**B**) cells were seeded at a density of $1x10^5$ cells per well of a 24-well transwell hanging-insert containing the relevant medium supplemented with 1% FBS and 10µg HES, 10µg *H. polygyrus* antigen or 1X PBS. Each insert was then placed individually into a well containing medium supplemented with 10% FBS. Migrated cells which had adhered to the lower surface of the 8µm membrane were fixed with methanol and stained with crystal violet. 50% acetic acid was used to wash off the crystal violet stain and the absorbance of each well was read at a wavelength of 595nm. **C and D.** Cells were seeded at a density of $2x10^5$ cells per well in a 6-well plate and treated with 10µg HES or 10µg *H. polygyrus* antigen or 1X PBS. Cells were incubated for 12 or 18 hours (**C**) or 24 or 30 hours (**D**) before harvesting the cells and extracting the total protein. Western blotting was performed with antibodies specific for β-catenin with p38 used as the loading control. Densitometry readings were obtained using ImageJ to determine the changes in protein expression of β-catenin normalised to p38 and expressed as a fold-change relative to control wells. Broken lines in western blots shown in this figure indicate where lanes not relevant were removed. **A and B.** represent pooled data from three independent experiments each performed in triplicate. The data were analysed using GraphPad Prism 6.01 and a t-test was performed *p<0.05 **p<0.01 ***p<0.001 ****p<0.0001. Error bars represent Standard Error of the Mean.

3.2.3 HES Significantly Increases Mouse CT26.WT Colorectal Cancer Tumour Growth

The *H. polygyrus* derived antigens significantly reduced the proliferation of CT26.WT cells *in vitro* which suggested that they may have some therapeutic benefits for colorectal cancer. Therefore, their effect on the tumour forming ability of these cells *in vivo* was determined. Briefly, CT26.WT cells treated with either HES or *H. polygyrus* antigen were injected subcutaneously into the flanks of BALB/c mice and the tumours measured every second day over a period of 14 days. While the results show that there was an increase in tumour growth for all treatments tested, tumours derived from HES treated CT26.WT cells displayed drastically accelerated growth (**Figure 3.14A**) and were significantly larger upon resection (**Figure 3.14B**). There was, therefore a discrepancy between the proliferative ability of CT26.WT cells exposed to *H. polygyrus* derived antigens *in vitro* and *in vivo*.

To further investigate the tumour promoting activity of HES on mouse colorectal cancer cells *in vivo*, the inguinal draining lymph nodes (dLN) and non-draining lymph nodes (ndLN) were removed from the tumour bearing mice described above and the immune cell populations present in these structures were explored by flow cytometry. Although there were no differences in the proportion of CD4+ T cells present in the dLN or ndLN between treatment groups (**Figure 3.15A and Figure 3.15E**), the dLNs from mice bearing tumours derived from HES treated CT26.WT cells contained significantly higher total CD4+ T cell numbers (**Figure 3.15B**). A similar trend was observed for CD8+ T cells (**Figures 3.15C. 3.15D and 3.15F**).

HES is well documented to expand the regulatory Foxp3+ T cell population, responsible for suppressing the immune response, in mice and humans (16, 33). It was, therefore important to determine whether this immune-regulatory T cell population was expanded in the dLN of mice bearing tumours derived from HES treated CT26.WT cells. Flow cytometric analysis showed that indeed, mice bearing these tumours had significantly higher proportions and numbers of Foxp3+ T cells present in the dLN (**Figure 3.16**). Foxp3+ T cells have been implicated in dampening anti-tumour immunity, therefore it is possible that the accumulation of Foxp3+ T cells in the dLN could have contributed towards the increased growth of tumours derived from HES treated CT26.WT cells (170-172).

To determine whether the immune response observed above in the lymph nodes of mice was also relevant to the tumours themselves, the experiments described above were repeated for the tumours.

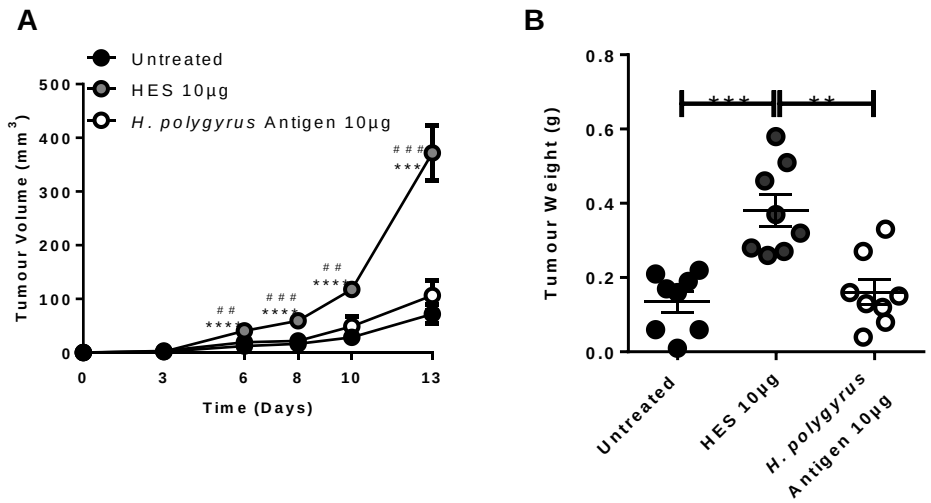

Figure 3.14: HES significantly accelerates CT26.WT tumour growth. 8-week-old BALB/c mice were injected subcutaneously with $5x10^5$ CT26.WT cells treated with either 10µg HES, 10µg *H. polygyrus* antigen or 1X PBS. **A.** Tumour height and width were measured using callipers and the tumour volume calculated using the equation $V=0.5(HxW^2)$. * Untreated vs. HES, # HES vs. *H. polygyrus* antigen. **B.** Mice were sacrificed 14 days later, and the tumours resected and weighed. The data were analysed using GraphPad Prism 6.01 and an unpaired t-test was performed *p<0.05 **p<0.01 ***p<0.001 ****p<0.0001. Error bars represent Standard Error of the Mean.

Mice bearing tumours derived from HES treated CT26.WT cells had lower proportions and total CD4+ T cell numbers within the tumour, while the opposite was observed for tumours derived from *H. polygyrus* antigen treated CT26.WT cells (**Figures 3.17A, 3.17B and 3.17E**). Furthermore, although no differences were observed in the proportion of Foxp3+ T cells present in the tumours between treatment groups (**Figure 3.17C and Figure 3.17F**), tumours derived from HES treated CT26.WT cells had a significantly higher number of Foxp3+ T cells (**Figure 3.17D**). This further implicates HES as an accelerant of CT26.WT tumour growth due to Foxp3+ Treg population expansion.

Additionally, tumours derived from treated CT26.WT cells had lower proportions of CD11b+ cells (**Figure 3.18A and Figure 318C**) but a trend towards a higher number of total CD11b+ cells (**Figure 3.18B**). Notably, these tumours also had higher proportions of neutrophils (**Figure 3.19A and Figure 3.19C**) and a significantly higher total number of neutrophils (**Figure 3.19B**).

Section 3.2 reveals that *H. polygyrus* derived antigens can alter colorectal cancer cell migration and proliferation which is associated with changes in cell cycle regulator protein expression. Furthermore, these antigens have a notable impact on colorectal cancer tumour growth which correlated with altered immune cell accumulation within the lymph nodes and tumour.

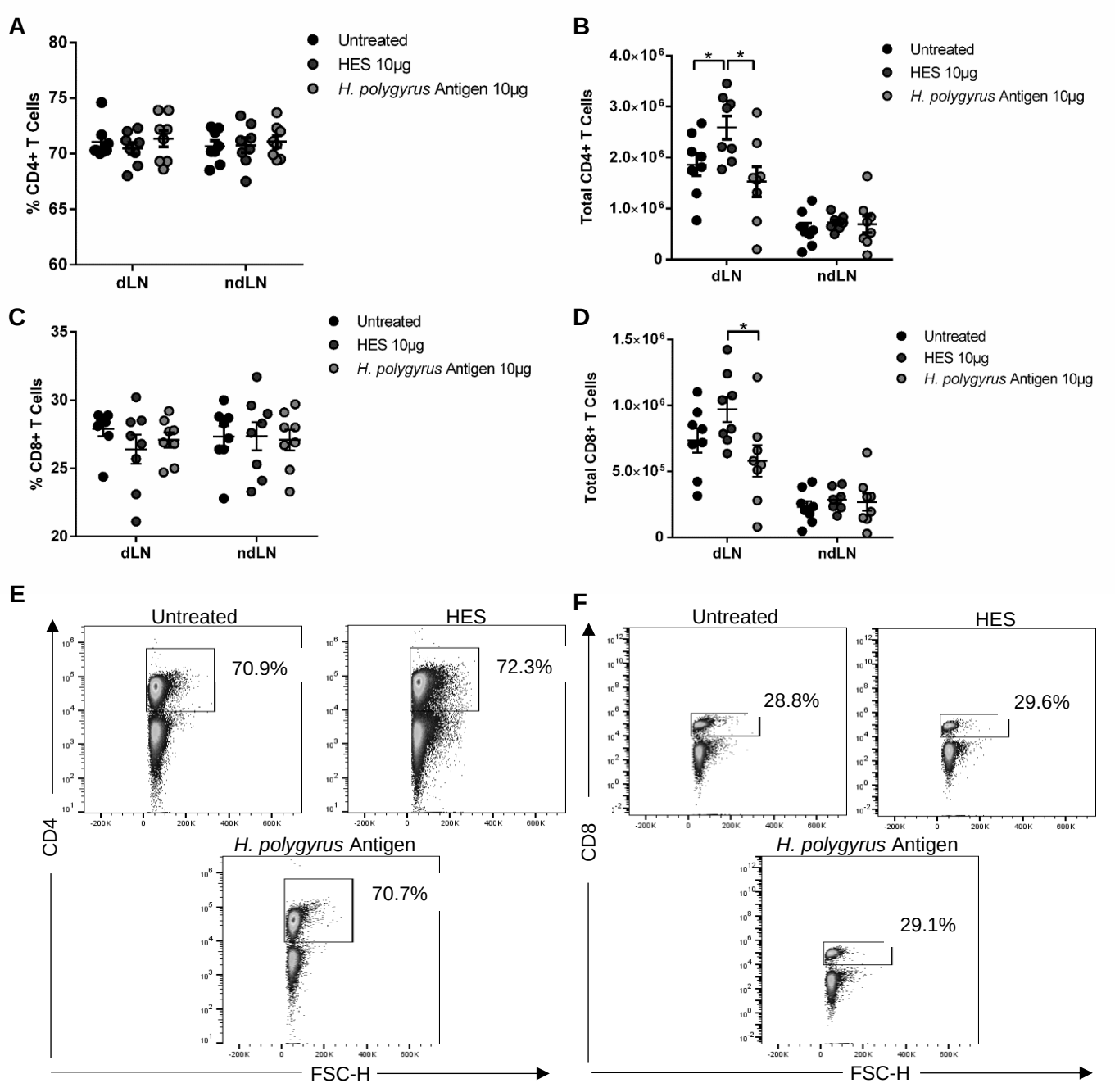

Figure 3.15: HES elevates total CD4+ and CD8+ T cell numbers in the draining lymph node (dLN) of mice bearing tumours derived from HES treated CT26.WT cells. 8-week-old BALB/c mice were injected subcutaneously with $5x10^5$ CT26.WT cells treated with either 10µg HES, 10µg *H. polygyrus* antigen or 1X PBS. Mice were sacrificed 14 days later and the draining lymph nodes (dLN) and non-draining lymph nodes (ndLN) removed. Cells were stained as described in the Materials and Methods section of this thesis and analysed by flow cytometry on the ACEA Novocyte. **A.** Percentage and **B.** Total CD4+ T cells. **C.** Percentage and **D.** Total CD8+ T cells. Representative dot plots showing the **E.** CD4+ and **F.** CD8+ T cell populations in the dLN for each treatment analysed using FlowJo Version 10. Analysis was performed using GraphPad Prism 6.01 and a parametric unpaired t-test was performed *p<0.05 **p<0.01 ***p<0.001 ****p<0.0001. Error bars represent Standard Error of the Mean.

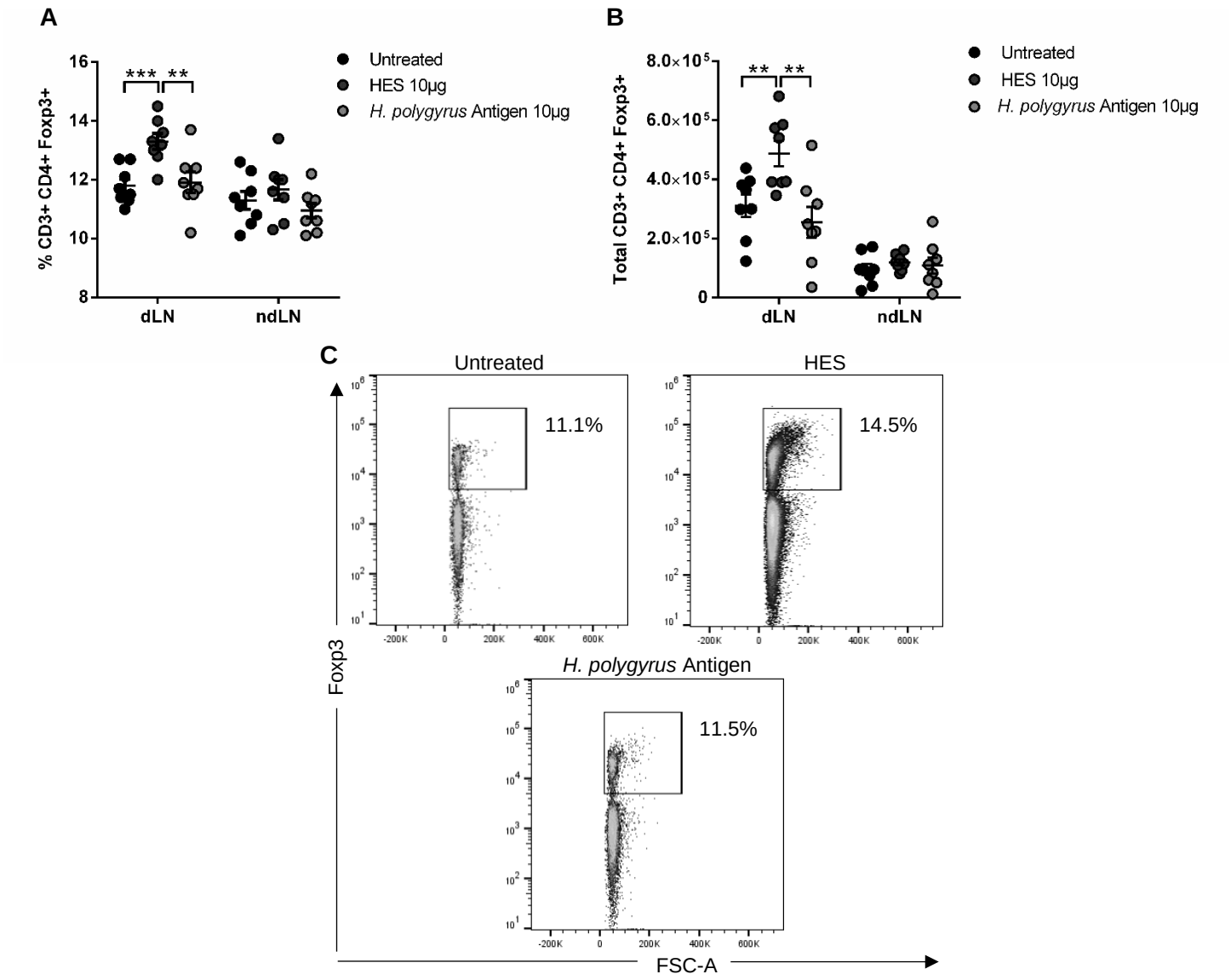

Figure 3.16: HES significantly increases the proportion and number of regulatory Foxp3+ T cells in the draining lymph node (dLN) of tumours derived from treated CT26.WT cells. 8-week-old BALB/c mice were injected subcutaneously with 5x10^5 CT26.WT cells treated with either 10µg HES, 10µg *H. polygyrus* antigen or 1X PBS. Mice were sacrificed 14 days later and the draining lymph nodes (dLN) and non-draining lymph nodes (ndLN) removed. Cells were stained as described in the Materials and Methods section of this thesis and analysed by flow cytometry on the ACEA Novocyte. **A.** Percentage and **B.** Total CD3+ CD4+ Foxp3+ T cells. Representative dot plots showing the **C.** Foxp3+ population in the dLN for each treatment analysed using FlowJo Version 10. Analysis was performed using GraphPad Prism 6.01 and a parametric unpaired t-test was performed *p<0.05 **p<0.01 ***p<0.001 ****p<0.0001. Error bars represent Standard Error of the Mean.

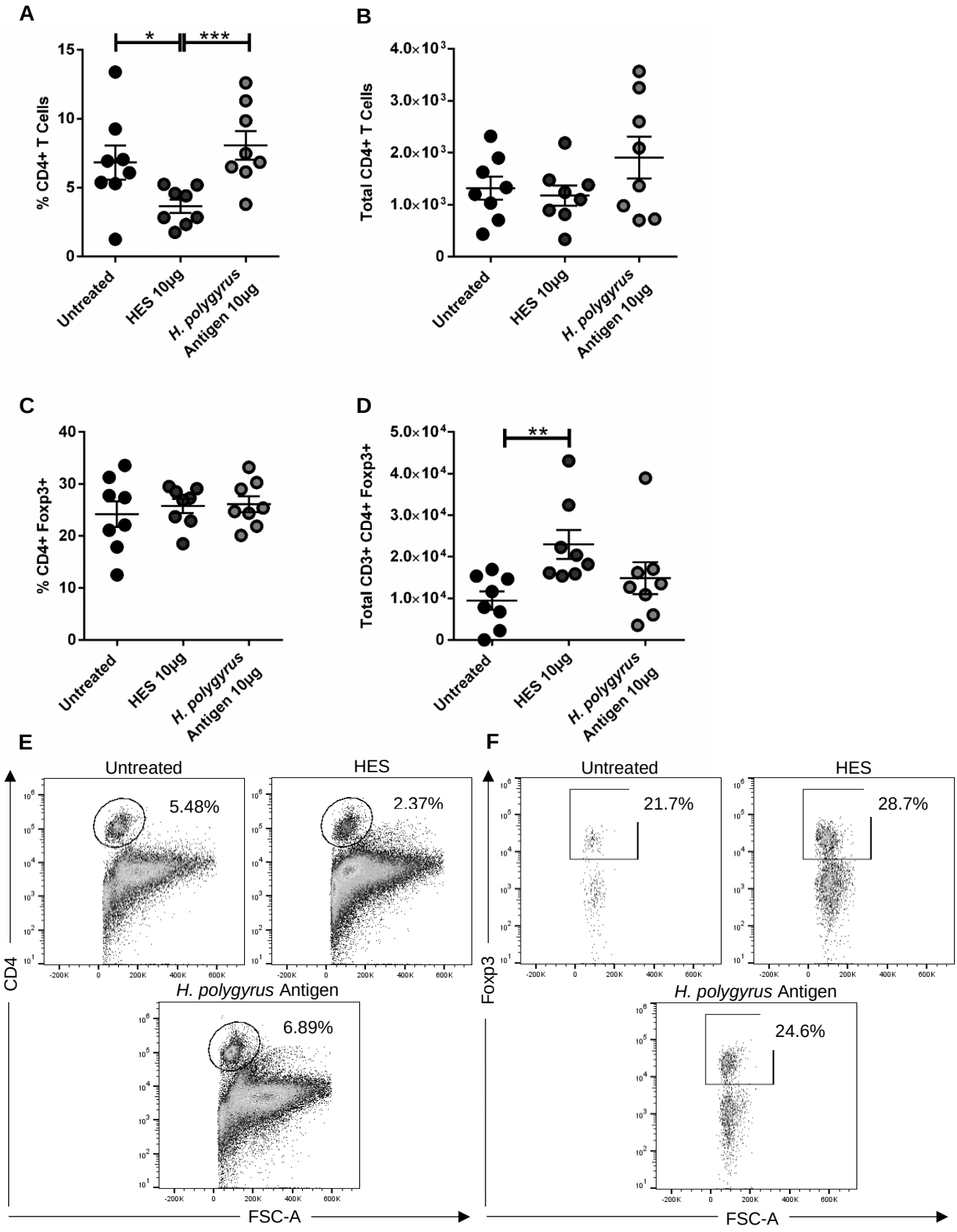

Figure 3.17: HES significantly increases the number of regulatory Foxp3+ T cells in CT26.WT tumours. 8-week-old BALB/c mice were injected subcutaneously with $5x10^5$ CT26.WT cells treated with either 10µg HES, 10µg *H. polygyrus* antigen or 1X PBS. Mice were sacrificed 14 days later, and the tumours removed, stained as described in the Materials and Methods section of this thesis and analysed flow cytometry on the ACEA Novocyte. **A.** Percentage and **B.** Total CD4+ T cells. **C.** Percentage and **D.** Total CD3+ CD4+ Foxp3+ T cells. Representative dot plots showing the **E.** CD3+ CD4+ and **F.** CD3+ CD4+ Foxp3+ populations for each treatment analysed using FlowJo Version 10. Analysis was performed using GraphPad Prism 6.01 and a parametric unpaired t-test was performed *p<0.05 **p<0.01 ***p<0.001 ****p<0.0001. Error bars represent Standard Error of the Mean.

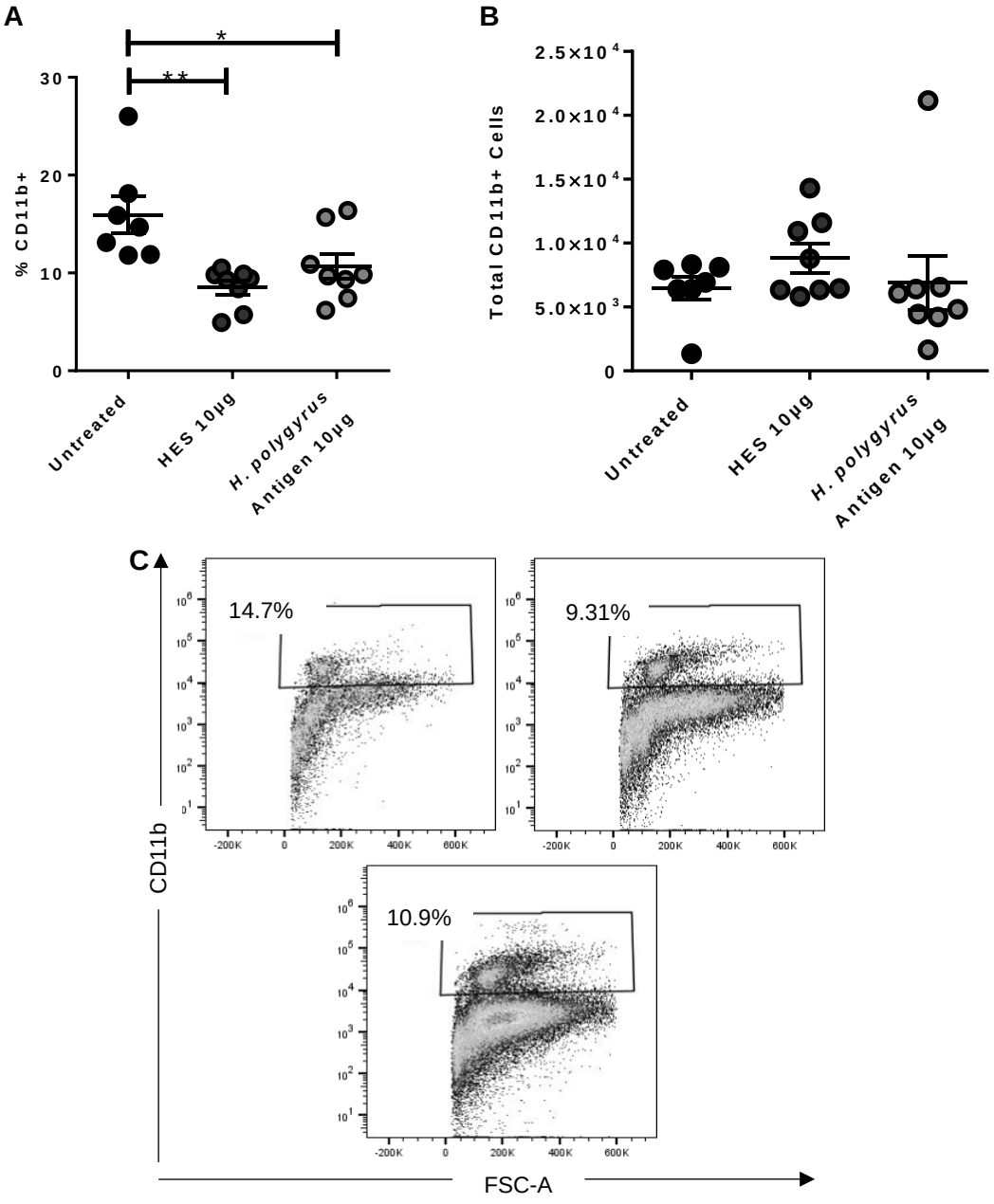

Figure 3.18: HES significantly decreases the proportion of CD11b+ cells in the tumour. 8-week-old BALB/c mice were injected subcutaneously with 5x10^5 CT26.WT cells treated with either 10µg HES, 10µg *H. polygyrus* antigen or 1X PBS. Mice were sacrificed 14 days later, and the tumours removed, stained as described in the Materials and Methods section of this thesis and analysed flow cytometry on the ACEA Novocyte. **A.** Percentage and **B.** Total CD11b+ cells. Representative dot plots showing the **C.** CD11b+ population for each treatment analysed using FlowJo Version 10. Analysis was performed using GraphPad Prism 6.01 and a parametric unpaired t-test was performed *p<0.05 **p<0.01 ***p<0.001 ****p<0.0001. Error bars represent Standard Error of the Mean.

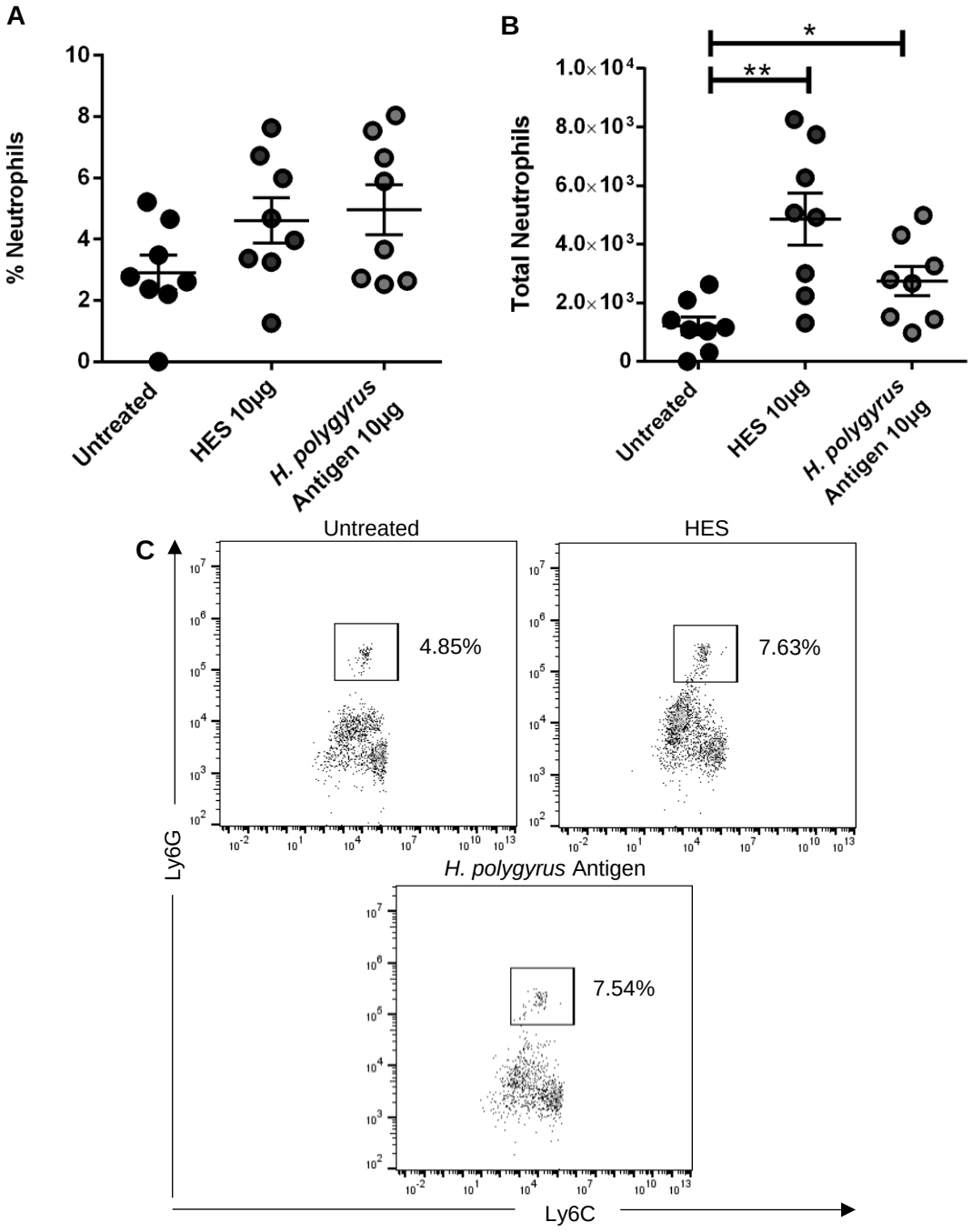

Figure 3.19: *H. polygyrus* derived antigens significantly increase the number neutrophils in CT26.WT tumours. 8-week-old BALB/c mice were injected subcutaneously with 5x10^5 CT26.WT cells treated with either 10µg HES, 10µg *H. polygyrus* antigen or 1X PBS. Mice were sacrificed 14 days later, and the tumours removed, stained as described in the Materials and Methods section of this thesis and analysed flow cytometry on the ACEA Novocyte. **A.** Percentage and **B.** Total neutrophils. Representative dot plots showing the **C.** Neutrophil population for each treatment analysed using FlowJo Version 10. Analysis was performed using GraphPad Prism 6.01 and a parametric unpaired t-test was performed *p<0.05 **p<0.01 ***p<0.001 ****p<0.0001. Error bars represent Standard Error of the Mean.

3.3 Investigating the Role of HES in a Murine Model of Colitis-Associated Colorectal Cancer (CAC)

Having determined that HES had significant effects on *in vitro* colorectal cancer cell behaviour and *in vivo* colorectal cancer tumour growth, whether it would alter the development of colorectal cancer was uncertain. To investigate this, a murine model of CAC was utilised. It is important to note that infection with *H. polygyrus* in the early stages of CAC has been shown to exacerbate tumour development, however whether HES is able to effect CAC has yet to be determined (103).

3.3.1 HES Treatment Worsens Pathology in a Murine Model of CAC

To explore whether HES can affect the development of CAC, mice were injected intraperitoneally with the carcinogen azoxymethane (AOM) and exposed to an inflammatory agent Dextran Sulphate Sodium (DSS) in their drinking water for one week. Over the course of 15 days, mice were injected peritoneally with either HES or a PBS control and the weight, distress scores, colon lengths and weight and total cell count of the spleen determined.

The results showed that mice treated with HES/AOM/DSS had a worse pathology compared to that of naïve or AOM/DSS treated mice. This was evident by increased weight loss (**Figure 3.20A**) and shortened colons (**Figure 3.20B**). No significant difference was seen between spleen weights (**Figure 3.22C**) and spleen total cell counts (**Figure 3.20D**) for the various conditions tested. However, compared to naïve mice the HES/AOM/DSS treated and AOM/DSS groups of mice, had a trend towards larger spleens with higher spleen total cell counts (**Figure 3.20C and Figure 3.20D**).

To determine whether HES/AOM/DSS altered the structure and integrity of the colon, 5µm thick colon sections were stained with Haematoxylin and Eosin (H&E) and Periodic Acid-Schiff (PAS). While Haematoxylin binds negatively charged substances such as DNA and stains nuclei dark blue, Eosin binds positively charged substances such as certain amino acids and stains the cytoplasm pink/red. PAS on the other hand is a specialised stain that binds and stains polysaccharides and mucosubstances such as mucins produced by goblet cells. Colon sections isolated from HES/AOM/DSS and AOM/DSS treated mice exhibited reduced goblet cells (light PAS staining), large submucosal spaces (black arrows), which is illustrative of oedema, lymphocyte infiltration (yellow arrows) and advanced epithelial injury (white arrows) (**Figure 3.21A**). Although no significant differences were observed between HES/AOM/DSS and AOM/DSS treatment groups, HES/AOM/DSS mice did tend to have higher pathology scores (**Figure 3.21B and Figure 3.21C**).

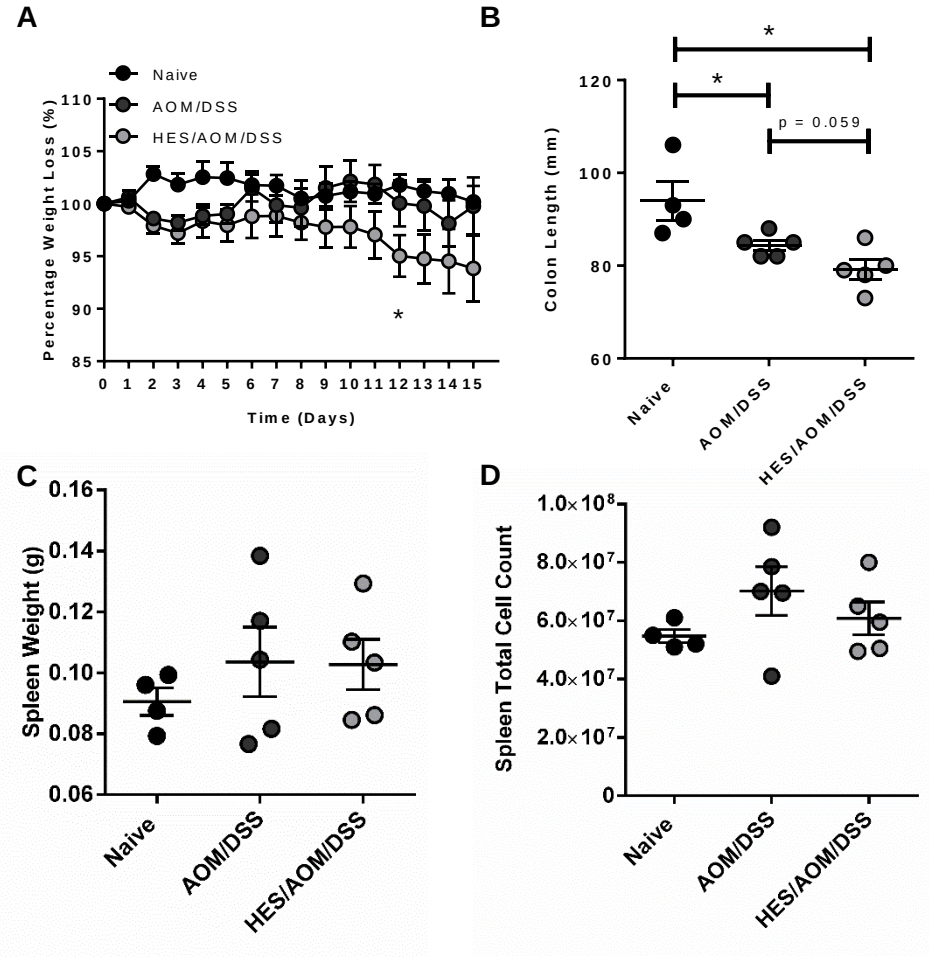

Figure 3.20: HES worsens pathology in a murine model of colitis-associated colorectal cancer (CAC). A. Percentage weight loss over 15 days. * HES/AOM/DSS compared to Naïve. **B.** Colon length (mm) measured from the end of the cecum to the rectum. **C.** Spleen weight (g) and **D.** Spleen total cell count. The data were analysed using GraphPad Prism 6.01 and a parametric unpaired t-test was performed *p<0.05 **p<0.01 ***p<0.001 ****p<0.0001. Error bars represent Standard Error of the Mean.

To determine the impact of the HES/AOM/DSS and AOM/DSS treatments on the immune cell populations, the spleens of the naive and treated mice were removed and analysed by flow cytometry. The results showed that spleens from the HES/AOM/DSS treated mice had a significantly larger proportion of CD11b+ cells compared to that of naïve mice and a trend towards higher than that of AOM/DSS treated mice (**Figure 3.22A and Figure 3.22C**). Both the groups of HES/AOM/DSS and AOM/DSS treated mice had higher numbers of total CD11b+ cells present in the spleen compared to naïve mice, however this was only significant for AOM/DSS treated mice (**Figure 3.22B**). Furthermore, compared to naïve mice, AOM/DSS treated mice had significantly higher proportions of eosinophils and neutrophils (**Figures 3.22D, 3.22F, 3.22G and 3.22I**) and they had a trend towards higher total cell counts of these cells (**Figure 3.22E and Figure 3.22H**). Unfortunately, due to the variations in results obtained for mice treated with HES/AOM/DSS, the results were not significant and future studies would have to increase the number of mice in treatment groups.

A

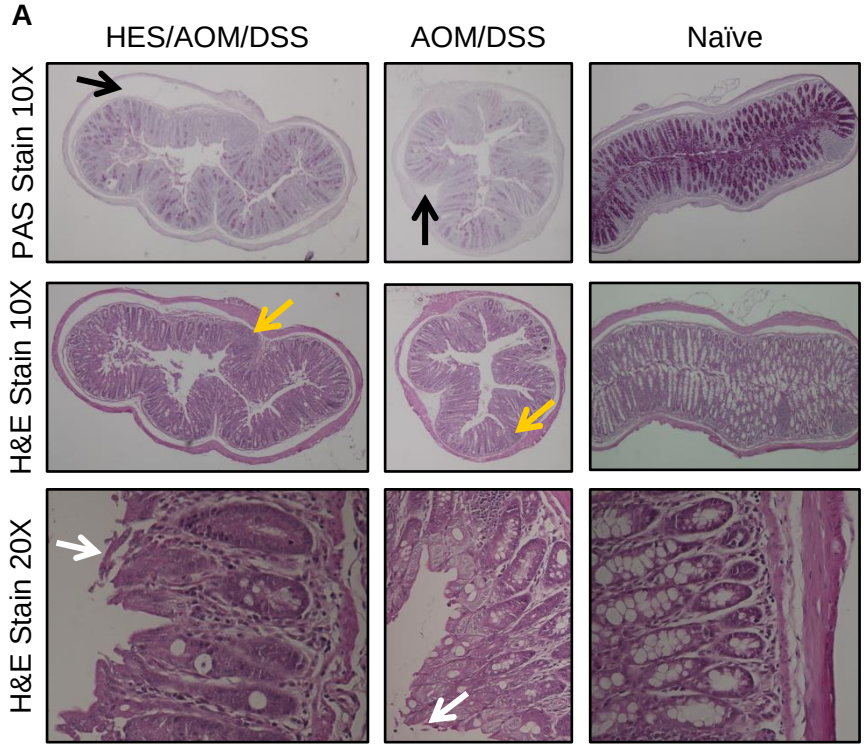

B

Sample	Reduced Goblet Cells	Epithelial Injury	Cell Infiltration	Oedema	Total
Naïve 1	0	0	1	1	2
Naïve 2	0	0	1	1	2
Naïve 3	0	0	0	0	0
AOM/DSS 1	2	0	1	0	3
AOM/DSS 2	2	1	2	1	6
AOM/DSS 3	2	2	2	1	7
AOM/DSS 4	2	2	2	1	7
HES/AOM/DSS 1	3	2	2	2	9
HES/AOM/DSS 2	3	2	2	2	9
HES/AOM/DSS 3	2	1	1	1	5
HES/AOM/DSS 4	2	2	0	2	6
HES/AOM/DSS 5	2	1	1	0	4

C

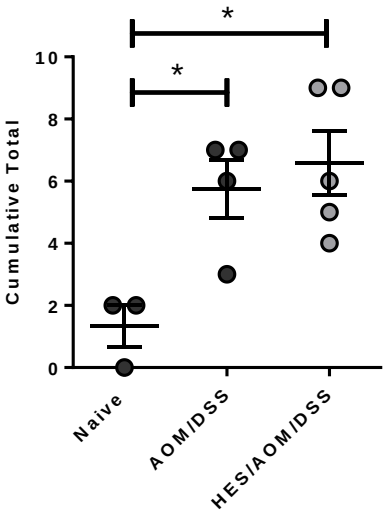

Figure 3.21: HES worsens pathology in a murine model of colitis-associated colorectal cancer (CAC). A. PAS and H&E staining on 5µm thick colon sections. Black arrows indicate oedema, yellow arrows indicate cell infiltration and white arrows indicate epithelial injury. **B.** Histology scores based on goblet cell abundance, epithelial injury, cell infiltration and oedema. Each criterion was scored from 0 to 3. **C.** Graph showing cumulative pathology scores per treatment group. The data were analysed using GraphPad Prism 6.01 and a parametric unpaired t-test was performed *p<0.05 **p<0.01 ***p<0.001 ****p<0.0001. Error bars represent Standard Error of the Mean.

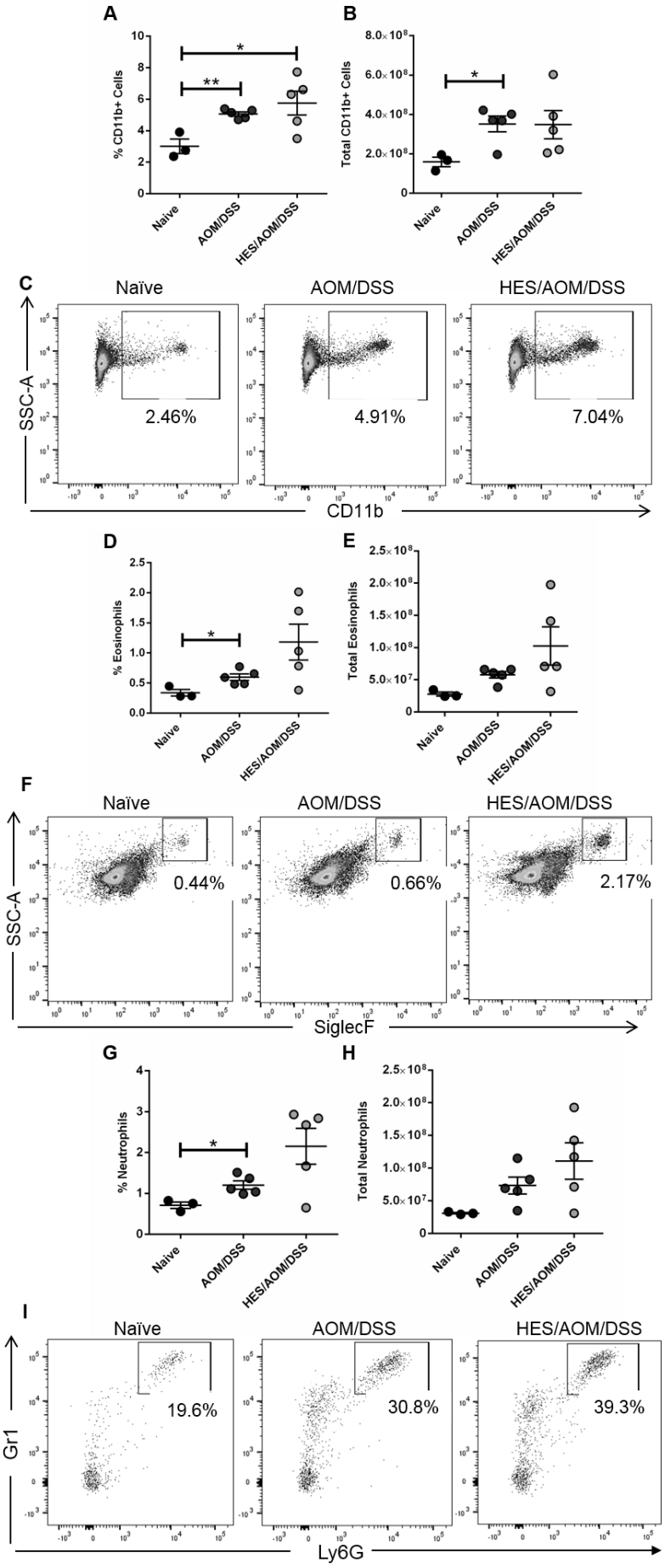
A
% CD11b+ Cells
Naive
AOM/DSS
HES/AOM/DSS
B
Total CD11b+ Cells
C
Naïve
AOM/DSS
HES/AOM/DSS
SSC-A
CD11b
2.46%
4.91%
7.04%
D
% Eosinophils
E
Total Eosinophils
F
SiglecF
0.44%
0.66%
2.17%
G
% Neutrophils
H
Total Neutrophils
I
Gr1
Ly6G
19.6%
30.8%
39.3%

In the case of the adaptive immune system, compared to naïve mice, HES/AOM/DSS treated mice had comparable CD4+ T cell proportions (**Figures 3.23A and 3.23E**) and a trend towards higher total CD4+ T cell counts (**Figure 3.23B**). Similar results were obtained for the AOM/DSS treated mice (**Figure 3.23A, 3.23B and 3.23E**) compared to naïve mice. Lastly, compared to naïve mice, HES/AOM/DSS and AOM/DSS treatment groups had similar CD4- T cell proportions and a trend towards higher total CD4- T cell counts (**Figure 3.23C – 3.23E**).

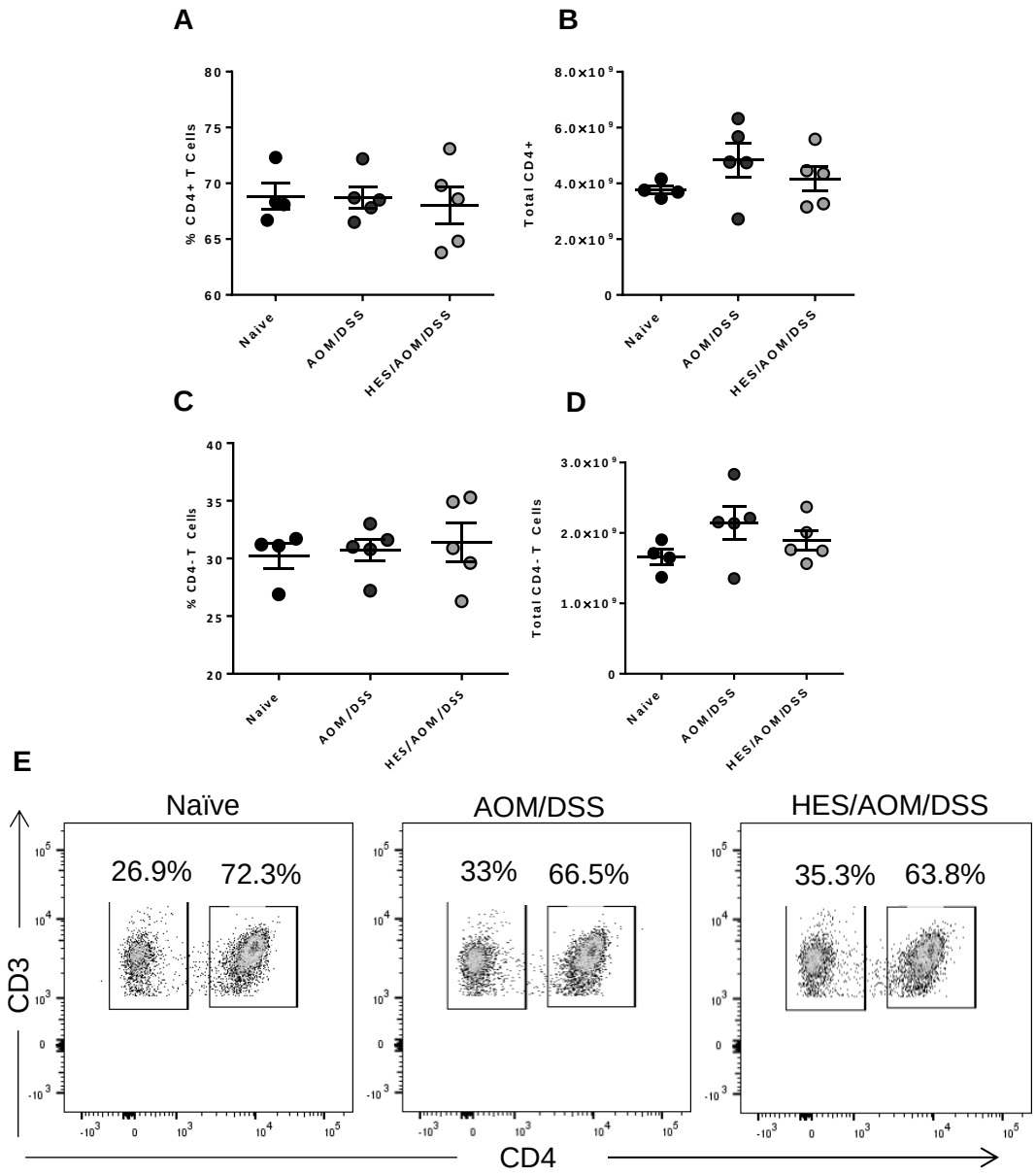

Figure 3.23: HES treatment decreases the total CD4+ and CD4- populations in a murine model of Colitis-Associated Colorectal Cancer (CAC). Splenocytes were seeded at a density of $1x10^5$ cells per well in a 96-well round-bottom plate, labelled and fixed appropriately and analysed by flow cytometry. The **A.** percentage and **B.** Total CD4+ cells, **C.** percentage and **D.** Total CD4- present in each sample. **E.** Representative dot plots showing the CD4+ and CD4- populations for each treatment analysed using FlowJo Version 10. Analysis was performed using GraphPad Prism 6.01 and a parametric unpaired t-test was performed *p<0.05 **p<0.01 ***p<0.001 ****p<0.0001. Error bars represent Standard Error of the Mean.

3.3.2 Increased morbidity and mortality induced by HES treatment is TFG-β dependent

HES contains a structurally distinct TGF-β mimic, which can signal via the canonical TGF-β receptor pathway and be antagonised by TGF-β receptor inhibitors (16, 33). It was speculated that this mimic could be the cause of the increased morbidity experienced by HES/AOM/DSS mice compared to AOM/DSS and naïve mice. To explore this possibility, the above experiments were repeated in the presence or absence of the TGF-β inhibitor, SB-431542 and weight, distress scores, colon lengths and weight and total cell count of the spleen were determined.

Mice treated with HES/AOM/DSS only experienced the most weight loss (**Figure 3.24A and 3.24B**) and mortality (**Figure 3.24C**) and, in the presence of SB-431542 this group of mice had zero mortality and weight loss comparable to the AOM/DSS only treated mice. HES/AOM/DSS only treated mice also had the highest distress scores out of the four groups (**Figure 3.24D**). While there was no difference in colon lengths between that of HES/AOM/DSS and HES/AOM/DSS/SB-431542 treated mice (**Figure 3.24E**), the spleen weights (**Figure 3.24F**) and spleen total cell counts (**Figure 3.24G**) were higher in the HES/AOM/DSS treated group.

To further understand the impact of the TGF-β mimic in the HES/AOM/DSS treated mice, the spleens of the naive and treated mice were removed and analysed by flow cytometry. The results showed that the spleen of HES/AOM/DSS treated mice had a significantly larger proportion (**Figure 3.25A and Figure 3.25B**) and total cell number (**Figure 3.25C**) of CD11b+ cells compared to the other treatment groups. Importantly, HES/AOM/DSS/SB-431542 treated mice had CD11b+ proportions (**Figure 3.25A and Figure 3.25B**) and total CD11b+ cell counts (**Figure 3.25C**) comparable to that of naïve and AOM/DSS treated mice suggesting that the increase in the CD11b+ population, in HES/AOM/DSS treated mice, is TGF-β dependent. Due to an unexpected problem with the staining of the eosinophil and neutrophil populations an analysis of these cells could not be reliably determined.

Figure 3.22: HES treatment increases the CD11b+, eosinophil and neutrophil populations in a murine model of colitis-associated colorectal cancer (CAC). Splenocytes were seeded at a density of $1x10^5$ cells per well in a 96-well round-bottom plate, labelled and fixed appropriately and analysed by flow cytometry. The **A.** percentage and **B.** Total CD11b+ cells, **D.** percentage and **E.** Total eosinophils, **G.** percentage and **H.** Total neutrophils present in each sample. Representative dot plots showing the **C.** CD11b+, **F.** Eosinophil and **I.** Neutrophil populations for each treatment analysed using FlowJo Version 10. Analysis was performed using GraphPad Prism 6.01 and a parametric unpaired t-test was performed *p<0.05 **p<0.01 ***p<0.001 ****p<0.0001. Error bars represent Standard Error of the Mean.

However, the CD4+ and CD4- T cell proportions and total cell counts were not TGF-β dependent and were either lower (CD4+) or higher (CD4-) in all three treatment groups compared to that of naïve mice (**Figure 3.26**).

It is important to note that the experiments in sections 3.3.1 and 3.3.2 were only performed once and would need to be repeated before any conclusive deductions can be made. To reduce inter-group variations, more mice should be included in each group.

The *in vivo* results in this final section suggest that in a model of CAC, HES significantly exacerbates disease in a manner at least partially dependent on TGF-β and the accumulation of CD11b+ cells in the spleen.

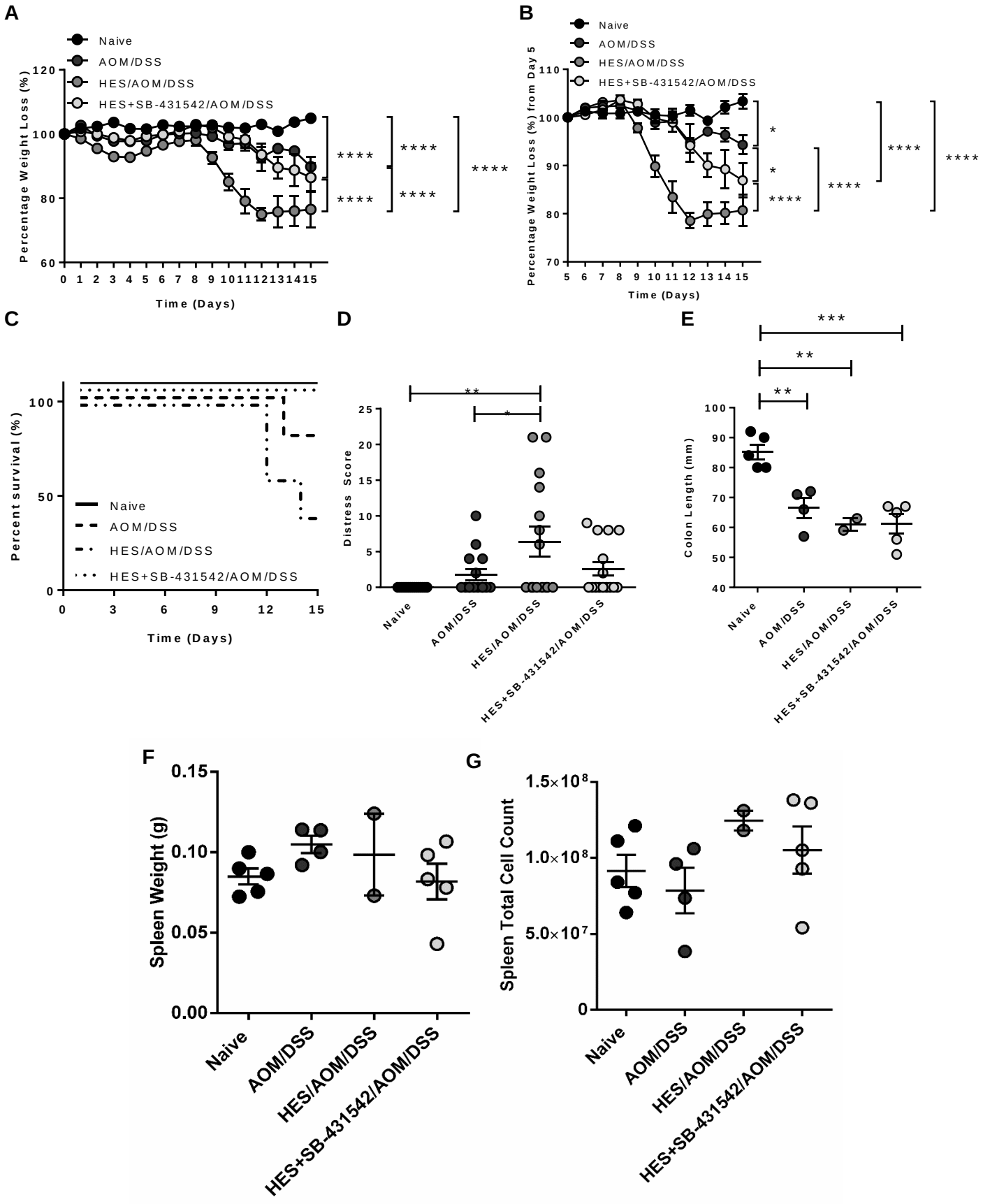

Figure 3.24: Increased morbidity and mortality induced by HES treatment is TFG-β dependent. **A.** Percentage weight loss over 15 days. **B.** Percentage weight loss from Day 5 – start of DSS. **C.** Survival curve over 15 days. **D.** Daily individual distress scores. **E.** Colon length (mm) measured from the end of the cecum to the rectum. **F.** Representative colons from each group **G.** Spleen weight (g). **H.** Spleen total cell counts. The data were analysed using GraphPad Prism 6.01 and a two-way ANOVA with multiple comparisons (**A and B**), a parametric unpaired t-test (**D**) or a one-way ANOVA with multiple comparisons (**E-G**) was performed *p<0.05 **p<0.01 ***p<0.001 ****p<0.0001. Error bars represent Standard Error of the Mean.

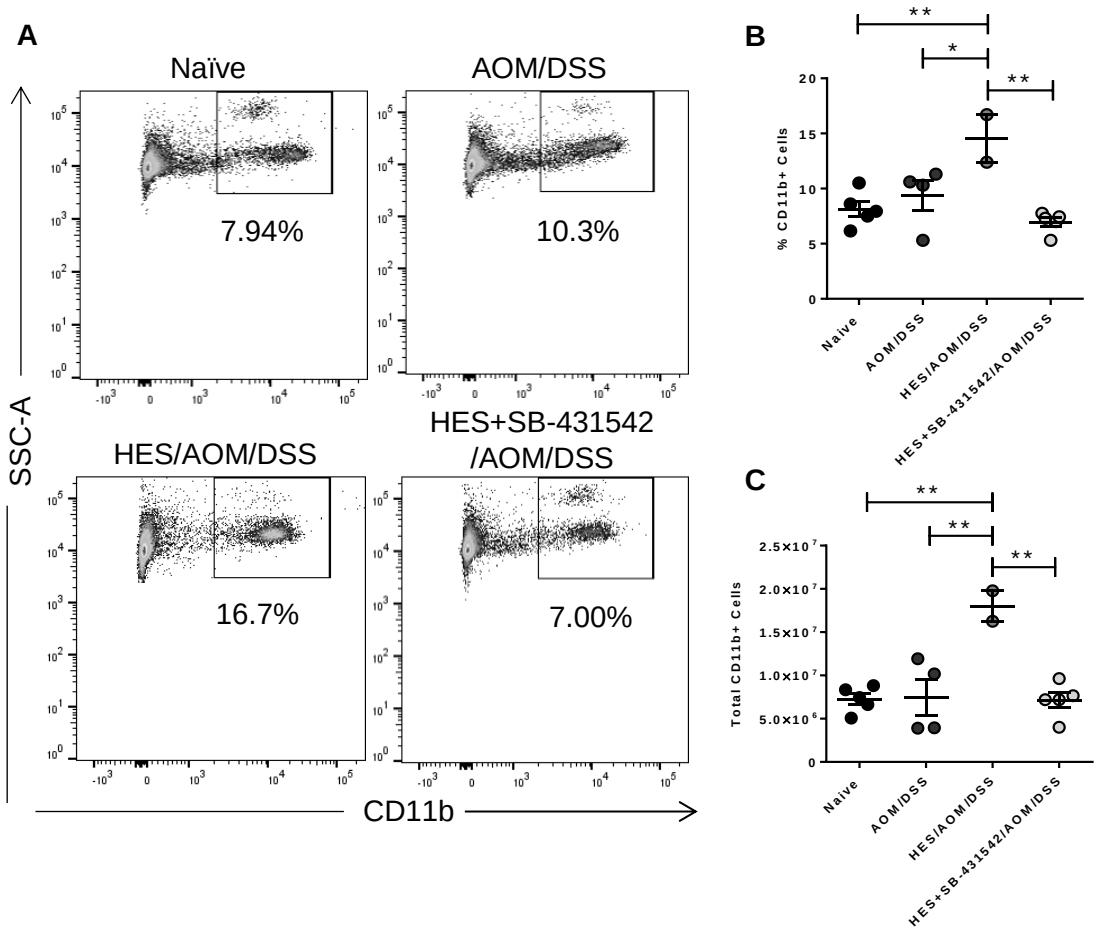

Figure 3.25: Increased CD11b+ proportions and total cell counts, induced by HES treatment, is TFG-β dependent. Splenocytes were seeded at a density of $1x10^5$ cells per well in a 96-well round-bottom plate and labelled and fixed appropriately and **A.** Representative dot plots showing the CD11b+ populations for each treatment analysed using FlowJo Version 10. The **B.** Percentage and **C.** Total CD11b+ cells present in each sample. Analysis was performed using GraphPad 6.01 and a parametric one-way ANOVA with multiple comparisons was performed *p<0.05 **p<0.01 ***p<0.001 ****p<0.0001. Error bars represent Standard Error of the Mean.

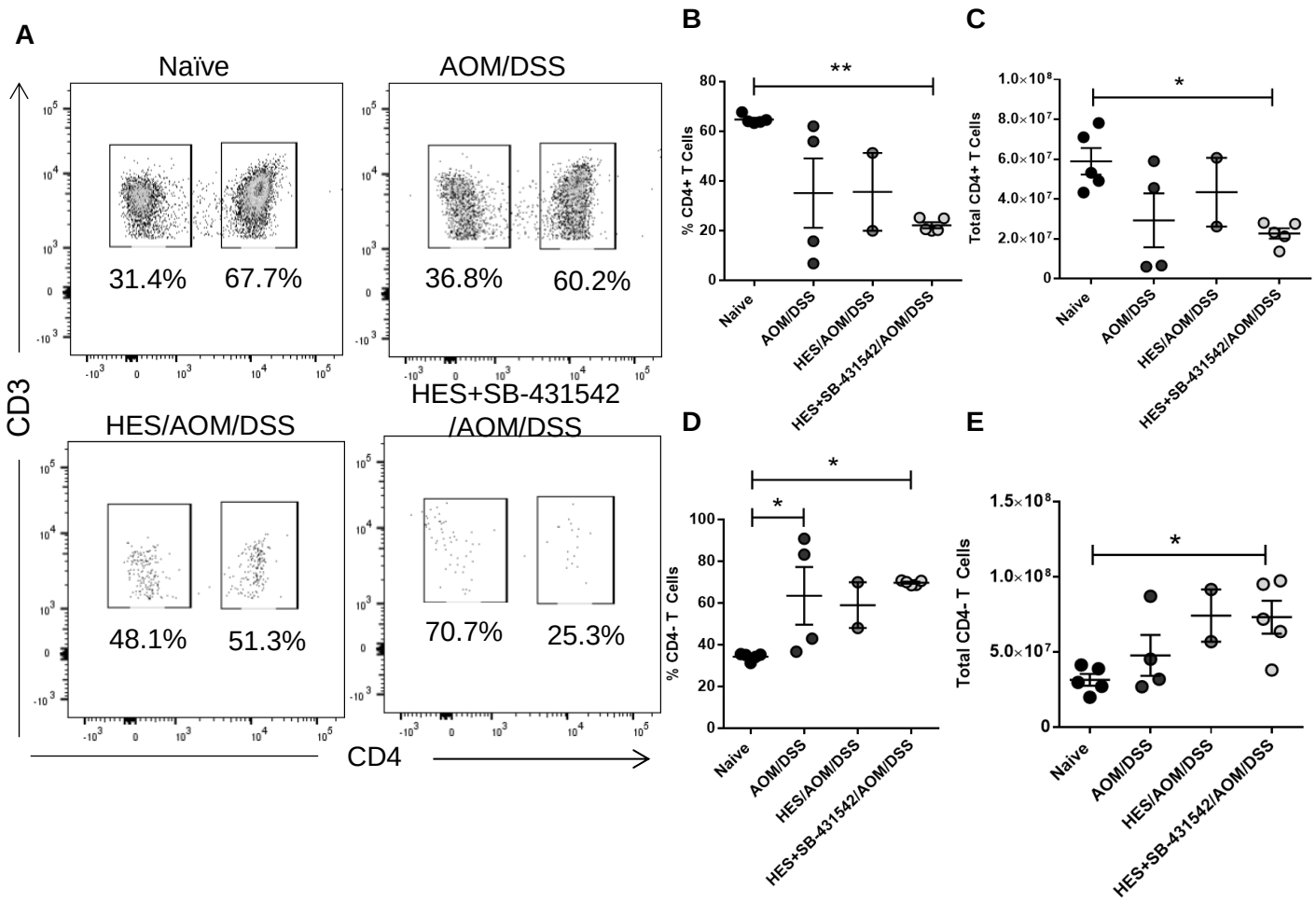

Figure 3.26: The effect of HES treatment on the CD4+ and CD4- T cell population is TFG-β independent. Splenocytes were seeded at a density of $1x10^5$ cells per well in a 96-well round-bottom plate and labelled and fixed appropriately and **A.** Representative dot plots showing the eosinophils population for each treatment analysed using FlowJo Version 10. The **B.** Percentage and **C.** Total CD4+ and **D.** Percentage and **E.** Total CD4- T cells present in each sample. Analysis was performed using GraphPad 6.01 and a parametric one-way ANOVA with multiple comparisons was performed *p<0.05 **p<0.01 ***p<0.001 ****p<0.0001. Error bars represent Standard Error of the Mean.

4. Discussion

Although specific helminths are irrefutable causes of cancer, certain other helminths have been shown to modulate the host immune response by promoting immune suppression (5-7, 67, 75, 107, 173, 174). However, the exact mechanisms that these helminths employ to modify the host immune system and promote immune regulation is largely unclear (105). For this reason, the potential for the use of these parasites in impeding cancer progression is worth thorough investigation. This study, therefore aimed to determine the effect that certain helminths have on cervical and colorectal cancer cell behaviour

4.1 The Role of *N. brasiliensis* in Cervical Cancer Development and Progression

Epidemiological studies have revealed a positive correlation between infection with soil-transmitted helminths (STH) and susceptibility to the oncogenic virus HPV (80). However, whether exposure to STHs can directly influence cervical cancer cell growth and migration is not known. Consequently, this study utilised *N. brasiliensis*, a rodent hookworm commonly used to model infection with the human hookworms *Necator americanus* and *Ancylostoma duodenale*, to investigate the effect of STH exposure on HPV positive and negative cervical cancer behaviour *in vitro* (148).

While *N. brasiliensis* L3 antigen had no significant effect on HPV18 positive HeLa cell proliferation, high concentrations of the antigen significantly decreased cell migration in two-dimensional scratch motility and transwell migration assays. Even though the clinical relevance of the 1.36 fold decrease in HeLa cell migration observed using the transwell migration assay requires further investigation, this result is comparable to what has previously been defined as a significant decrease in HeLa cell migration following drug treatment (175). Although antigen derived from *C. sinensis* and *S. haematobium* has been documented to cause an increase in the migration of cholangiocarcinoma (CCA) and normal epithelial cells respectively, this is the first time a decrease in cervical cancer cell migration following treatment with helminth derived proteins has been observed (176-179). Notably, the inhibitory effect on migration appeared to be hookworm specific as HeLa cells exposed to antigen derived from *H. polygyrus*, a solely gastrointestinal nematode, had no significant changes in cell migration.

The reduction in HeLa cell migration was found to be associated with the lowered expression of EMT markers, N-cadherin and vimentin. N-cadherin, a transmembrane cell adhesion molecule (NCBI Gene ID: 1000), and vimentin, an intermediate filament protein (NCBI Gene ID: 7431), are both expressed by mesenchymal cells and are used as markers of cells which are undergoing, or have undergone, EMT. Indeed, both N-cadherin and vimentin have been

associated with the transition of epithelial cells to a more invasive and metastatic mesenchymal cell type, which is associated with a poor outcome (180-182). Importantly, in accordance with the presented data, previous studies have also shown that helminths can impact the EMT process. *S. haematobium*-induced sarcomas expressed raised levels of vimentin and, when co-administered with a chemical carcinogen into the murine bladder, *S. haematobium* eggs reduced E-cadherin and elevated vimentin expression in urothelial cells (138, 139). Furthermore, infection with *H. polygyrus* or *T. spiralis* has been reported to reduce the expression of E-cadherin and Occludin in the colon respectively (140, 141). Likewise, in humans, infection with *T. trichiura* and *S. mansoni* increased the expression of plasma fibronectin and cellular vimentin respectively (142, 143). The previously described studies all reveal an increased potential for metastasis following helminth exposure, however the results from the current study suggest that *N. brasiliensis* L3 antigen could act as a late-stage cervical cancer treatment by decreasing the proportion of cancer cells progressing to metastasis.

The decline in HeLa cell migration following *N. brasiliensis* L3 antigen treatment was validated in the HPV16 positive cell line, Ca Ski, using two-dimensional scratch motility assays only. Despite numerous attempts, western blotting results which investigated the changes in Ca Ski EMT expression were inconsistent. This was not due to technical error but rather that the results obtained varied between experiments. This may be due to Ca Ski cells having a different level of sensitivity to *N. brasiliensis* L3 antigen compared to HeLa cells, leading to unreliable outcomes. Furthermore, while both the HeLa and Ca Ski cell lines are derived from cancerous epithelial cervical tissue, HeLa cells (ATCC CCL-2) were harvested directly from the cervix and Ca Ski cells (ATCC CRL-1550) were isolated from a metastatic site in the small intestine. Importantly, these cells lines have been reported to respond differently to treatment, therefore it is possible that the vastly different environments from which each cell line originates affects its overall behaviour to external signals and treatments (183).

The reduction in *N. brasiliensis* L3 antigen treated HeLa cell migration and EMT expression was, however confirmed in a HPV negative cell line, C33-A (ATCC HTB-31), which was also harvested directly from the cervix. Interestingly, this cell line appeared to be the most sensitive to *N. brasiliensis* L3 antigen as even low concentrations of the antigen used in the two-dimensional scratch motility assay significantly lowered cell migration. This cell line has been documented to be more sensitive to chemotherapeutic drugs compared to HeLa and Ca Ski cells, however whether this has to do with its HPV status remains to be determined (184, 185). Although the effect of *N. brasiliensis* L3 antigen on cervical cancer cell migration is important to understand, it would also be beneficial to determine whether this antigen can alter the invasive potential of cervical cancer. One possibility to achieve this involves the use of a matrigel which can be added to the apical surface of the transwell hanging-insert membrane,

and the percentage of treated cells which enter the matrigel can then be compared to that of untreated cells (175).

Once the *in vitro* effect of *N. brasiliensis* L3 antigen treatment on cervical cancer cell migration and EMT expression had been determined, the *in vivo* effect of live infection on non-cancerous murine FGT tissue was investigated. The results revealed that *N. brasiliensis* infected mice displayed reduced vimentin and N-cadherin expression in the FGT compared to that of naïve mice. This is significant because *N. brasiliensis* does not enter the genital tissue of the host during its lifecycle, therefore the observed effect on EMT marker expression in the FGT must be systemic and independent of direct contact with the parasite. This is not uncommon as several gastrointestinal helminths, including *N. brasiliensis,* are able to exert non-enteric effects on the immune system (186). Following infection with *N. brasiliensis*, a robust expansion of IL-13-expressing innate cells is observed (187). These cells are abundant in the non-enteric tissue, including the Mesenteric Lymph Node (MLN), spleen and liver, and play a critical role in the Th2 immune response and worm expulsion. It is therefore reasonable to hypothesise that these IL-13-expressing cells may be systemically altering the expression of genital tract EMT markers in a way that impairs cervical cancer progression.

Cell-surface vimentin acts as a cancer-specific EMT marker and has been implicated as a restriction factor for HPV16 pseudovirion entry (137, 163, 188-191). The decrease in cell-surface vimentin expression by *N. brasiliensis* L3 antigen treated HeLa cells was, therefore expected to result in an increase in HPV16 pseudovirion internalisation. This was, however, not the case and instead a significant decrease in pseudovirion internalisation was seen. It is, however, important to note that HPV has multiple receptors and restriction factors and therefore changes in the expression of only one of these proteins may not necessarily have an overall effect on viral internalization (192). It would be beneficial to clarify the effect of changes in cell-surface vimentin expression on HPV infectivity. To achieve this, pseudovirions expressing the luciferase reporter enzyme could be utilised. This would be valuable because only when the luciferase gene has been fully incorporated into the host's genome would luciferase be expressed, and a light signal detected. Differences in the detectable light signal between control and *N. brasiliensis* L3 antigen treated HeLa cells (expressing lowered cell-surface vimentin) could then be used as a measure of successful HPV infection.

Hookworm exposure has never been implicated in reducing cervical cancer cell migration through the modulation of cell-surface EMT markers. A previous study showed that HeLa cells exposed to the ES products derived from the sheep nematodes *Haemonchus contortus* and *Ostertagia circumcincta* had increased vacuolation and loss of cell contact (193). Interestingly, both products were also reported to increase the permeability of CACO-2 (human epithelial

colorectal adenocarcinoma) cell monolayers, through the re-arrangement of tight junction proteins ZO-1 and Occludin (194). It is possible that *N. brasiliensis* L3 antigen alters the migration of cervical cancer cells through the modulation of cell-surface markers common to the formation of tight junctions and the EMT process. However, the effect of *N. brasiliensis* on the expression of tight junction proteins would need to be determined to test whether epithelial permeability is indeed affected.

Another possible explanation for how *N. brasiliensis* L3 antigen modifies the expression of cell-surface receptors and restriction factors involves the action of acetylcholinesterases present in the antigen preparation. Certain nematodes, including *N. brasiliensis*, secrete acetylcholinesterases, which function to suppress the host immune response and promote parasite survival (195-197). Interestingly this enzyme has been shown to increase the expression of the Muscarinic Acetylcholine Receptor M3 (M3 receptor) on rodent intestinal epithelial cells (198). Consequently, perhaps the acetylcholinesterase present in *N. brasiliensis* derived antigen is also able to alter other cell-surface receptors including cell-surface vimentin.

In conclusion, this study suggests that hookworm antigen may limit cervical cancer progression by inhibiting cell migration and reducing the proportion of cancer cells progressing to metastasis.

4.2 The Influence of *H. polygyrus* Derived Antigens on Colorectal Cancer *in vitro*

Despite several studies revealing a favourable role for *H. polygyrus* in the treatment of murine colitis, more recently Pastille *et al.,* reported that infection with *H. polygyrus* exacerbates colitis associated colorectal cancer (CAC) tumour development and intestinal inflammation (103, 124-127). This study therefore sought to determine the effect of antigen derived from this gastrointestinal nematode on CRC behaviour *in vitro*.

The results from growth curve, MTT and BrdU Incorporation assays demonstrated that HES and *H. polygyrus* antigen significantly reduced the *in vitro* proliferation of both mouse (CT26.WT) and human (HCT116) colorectal cancer cells. Western blot analyses showed that this was associated with an upregulation of p53 and p21 expression. p53 and p21 are critical cell cycle regulator proteins, which act as tumour suppressors by preventing the progression from G1 into the S phase of the cell cycle (151). Importantly, other helminths have also been implicated in altering cell cycle progression. The nematode *B. malayi* suppressed the proliferation of several human carcinoma cell lines by inducing a G1 and G2 phase arrest, and *T. spiralis* derived antigen inhibited the proliferation of human myeloid leukemia and hepatoma cells by causing a halt in G1 and S (146, 199). In contrast to these encouraging results, *O.*

viverrini ES product increased *in vitro* proliferation of fibroblasts by causing elevated expression of proteins vital for the progression from G1 to S phase, phosphorylated retinoblastoma (pRB) and cyclin D1 (147). To definitively conclude whether HES and *H. polygyrus* antigen induce a cell cycle arrest, Propidium Iodide could be used to stain the DNA of fixed cells. Propidium Iodide is a dye which proportionately binds to DNA allowing the proportion of cells present in each phase of the cell cycle to be analysed by flow cytometry. Cells in G2, which have been through S phase and replicated their DNA would, therefore stain twice as bright as those in G1, which have not been through S phase or replicated their DNA yet, and cells in S phase would increase in brightness until complete DNA replication has occurred.

Surprisingly, HES and *H. polygyrus* antigen had opposite effects on the migration of each colorectal cancer cell line, causing either a significant increase (CT26.WT) or decrease (HCT116) in cell migration. While unexpected, this differential effect on migration was supported by changes in β-catenin expression. β-catenin (NCBI Gene ID: 1499) forms part of the adherens junctions between cells and is negatively regulated by Adenomatous Polyposis Coli (APC) (200). Significantly, 85% of CRC cancers are associated with mutations in the APC gene, resulting in a loss of its tumour suppressor functions (200, 201). As a result, β-catenin expression becomes upregulated and acts as an oncoprotein. This activation of the Wnt signaling pathway, of which APC and β-catenin are a part, has been implicated in initiating CRC development and is associated with a poor prognosis (100, 166, 200). It is thus anticipated that the elevated level of expression of β-catenin in treated CT26.WT cells coincides with a significant increase in cell migration while the opposite is true for HCT116 cells.

The opposing transwell migration results observed between CT26.WT and HCT116 cells treated with *H. polygyrus* derived antigens could be due to the fact that these cell lines originate from different species. HCT116 (ATCC CCL-247) is a human epithelial colorectal cancer cell line and CT26.WT (ATCC CRL-2368) is a mouse fibroblast colorectal cancer cell line. However, to elucidate whether *H. polygyrus* derived antigens do indeed impact colorectal cancer cell migration in a species-specific manner, additional human and mouse colorectal cancer cell lines could be utilised and the described experiments repeated. Unfortunately, the two-dimensional scratch motility assay was not suitable to measure the migration of CT26.WT and HCT116 cells. CT26.WT cells do not form a monolayer and, therefore do not reach 100% confluency, meaning that one would not be able to reliably measure cell migration into the scratch. In contrast, HCT116 cells form a tight monolayer, which when wounded tears rather than forming a neat scratch. However, a radius cell migration assay may prove more appropriate. This assay similarly measures two-dimensional cell migration while incorporating

a biocompatible hydrogel spot. Cells are seeded in the well of a Radius plate surrounding the hydrogel, and once the cells have adhered the gel is dissolved leaving a gap into which the cells can migrate. The degree of migration into this space can then be quantified.

4.3 *H. polygyrus* Derived Antigens and *in vivo* Colorectal Cancer Tumour Growth

Once it had been determined that antigens derived from *H. polygyrus* were able to affect *in vitro* colorectal cancer cell proliferation and migration, further *in vivo* experiments were performed.

A syngeneic tumour model showed that the growth of tumours derived from HES treated CT26.WT cells was significantly accelerated compared to those derived from untreated and *H. polygyrus* antigen treated CT26.WT cells. This treatment group also had raised levels of CD4+ and CD8+ T cells in the dLN. HES is known to contain a structurally distinct TGF-β mimic, which can signal via the canonical TGF-β receptor pathway and be antagonised by TGF-β receptor inhibitors (16, 33). Furthermore, this mimic can expand the Foxp3+ regulatory T cell (Treg) population in mice and humans. Consequently, the significantly elevated levels of Foxp3+ T cells present in the dLN and tumour of mice bearing tumours derived from HES treated CT26.WT cells was anticipated and confirmed that the HES was functioning as expected. Tregs have been implicated in dampening anti-tumour immunity and as a result are abundant in the tumour microenvironment (170-172). It is therefore possible that the increased growth of tumours in the HES treated CT26.WT group occurred as a result of TGF-β-induced Treg accumulation in the dLN and the tumour microenvironment and the inhibition of an effective anti-tumour immune response.

Interestingly, both HES and *H. polygyrus* antigen increased the total number of CD11b+ cells and neutrophils present in the tumour. These cell populations have both been associated with enhanced colorectal cancer tumour growth and metastasis in mice and human studies, suggesting that the *H. polygyrus* derived antigens may be increasing CT26.WT tumour growth by expanding the CD11b+ and neutrophil populations in the tumour (202-204).

The exact mechanism behind how HES accelerated CT26.WT tumour growth was not determined, however it may involve the Phosphatidlyinositde 3-Kinase (PI3K) pathway. PI3K signaling is an essential regulator of the cell cycle and is important in cell proliferation, survival and differentiation (205). Furthermore, the PI3K pathway has been implicated in the progression of several cancer types with inhibitors of this pathway already being FDA approved for their treatment (206, 207). Inhibiting the PI3K pathway causes an enhanced anti-tumour immune response by depleting Tregs and increasing the amount of CD8+ T cells present in tumours (208-210). Significantly, PI3K inhibitors have been described in controlling

CT26.WT tumour growth by reducing the amount of Tregs present in the tumour (208). This result was however, reversed following the reintroduction of Tregs. Notably, other helminths as well as their derived antigens have been shown to impact the PI3K pathway. *C. sinensis* ES products activated the PI3K pathway, which increased the migration and invasion of CCA and hepatoma cells and elevated the expression of N-cadherin, vimentin and β-catenin and reduced the expression of ZO-1 (178). Similarly, *O. viverrini* exacerbated chemically-induced CCA by inducing PI3K signaling (211). If the PI3K pathway is indeed activated by HES then incorporating an inhibitor of this pathway into the present study may result in reduced CT26.WT tumour growth.

Another possible mechanism behind how HES accelerated CT26.WT tumour growth involves the action of Programmed Cell Death-1 (PD-1), a checkpoint inhibitor protein which plays an active role in immune tolerance (212). Unsurprisingly, both PD-1 and its ligand PD-L1 have been implicated in cancer progression. Certain helminths target host PD-L1 to upregulate its expression and suppress the immune response, thus facilitating their long-term survival in the host (213, 214). It is therefore possible that HES activates PD-L1, to enhance survival of *H. polygyrus,* and in doing so suppresses the host immune system leading to accelerated CT26.WT tumour growth.

It is important to note that the accelerated growth of tumours derived from HES treated CT26.WT cells contradicts what was seen *in vitro* where the proliferation of these cells was significantly reduced following treatment with both HES and *H. polygyrus* antigen. While the exact cause of this is unknown, it may be because the *in vitro* environment lacks critical components found *in vivo.* These include the presence of an intact immune response, high endothelial venules (HEVs) and the tumour microenvironment (215-218). Bearing the above in mind, perhaps the *in vivo* data is more convincing and reliable.

In 2009 Bothelo *et al.,* showed that antigen derived from adult *S. haematobium* accelerated the proliferation of Chinese Hamster Ovary (CHO) tumours, however there is little else known about the effect of helminth derived antigen on *in vivo* tumour growth (138). Therefore, the results obtained from this *in vivo* study are critical in helping to understand the role that helminths may play in cancer progression.

4.4 The Involvement of HES and TGF-β in Colitis-Associated Colorectal Cancer (CAC)

Infection with *H. polygyrus* has been shown to both inhibit and promote the development of colitis *in vivo* (103, 124). However, the role of HES in the development of colitis and CAC has yet to be determined. The results obtained from the model of CAC used in this study suggest that HES exacerbates CAC development.

Mice treated with HES/AOM/DSS had increased morbidity compared to untreated and AOM/DSS only treated mice. This was associated with increased weight loss, shorter colons and higher pathology scores, which coincided with elevated CD11b+, eosinophil and neutrophil cell proportions and total cell numbers in the spleen. Importantly, helminth infections have been shown to alter the CD11b+ population in murine models of CAC. Infection with *T. crassiceps* prevented the up-regulation of markers associated with CAC-tumorigenesis in mice and reduced the numbers of circulating CD11b+ Ly6C (hi) CCR2+ cells (100). Recently, STAT6, a transcription factor critical for the induction of Th2 immune responses, has been shown to exacerbate CAC and tumour development through expansion of the circulating CD11b+ Ly6C (hi) CCR2+ and CD11b+ Ly6C (low) Ly6G+ cell populations (219). HES may therefore, be worsening CAC pathology by activating STAT6 expression and the Th2 response leading to the expansion of CD11b+ immune cell populations.

While *H. polygyrus* derived antigens have not been reported to impact IBD or CAC, the effect that other helminth antigens have on these diseases has been explored. Antigen derived from *T. spiralis* and *H. diminuta* ameliorated DNBS-induced colitis by increasing immune-regulatory and decreasing pro-inflammatory cytokine expression and, similarly TcES inhibited CAC tumour formation by reducing pro-inflammatory cytokine and tumorigenesis marker expression (101, 114, 116, 220). Treatment with *S. mansoni* egg antigen (SEA) modulated disease symptoms in colitic mice through the preferential development of a Th2 response and by expanding the Foxp3+ T cell population, which successfully regulated the inflammatory response characteristic of colitis (26, 221).

Introducing a TGF-β inhibitor (SB-431542) into the study alleviated the symptoms associated with HES/AOM/DSS treatment. This would suggest that the TGF-β mimic present in HES is responsible for the increased morbidity and mortality in the HES/AOM/DSS treated mice. It is proposed that by inhibiting the TGF-β receptor and consequently TGF-β signaling, SB-431542 results in reduced Treg population expansion and, therefore allows for the development of a more effective anti-tumour immune response which limits the morbidity associated with CAC (128, 129).

Mice in the HES/AOM/DSS/SB-431542 treatment group also had CD11b+ cell proportions and numbers comparable to that of the untreated and AOM/DSS only treated groups. This further suggests that the TGF-β mimic present in HES is responsible for expanding the CD11b+ cell population. Interestingly, CD11b+ Gr-1+ cells have been reported to be responsible for the tumour-promoting effects of TGF-β in breast cancer (222, 223). Using the 4T1 breast cancer model, TGF-β neutralization resulted in reduced CD11b+ Gr-1+ cell numbers in the blood and dLN, which directly correlated with a reduction in tumour size. The results from this study,

therefore coincide with the present study, and it is hypothesised that the TGF-β-induced CD11b+ cell accumulation in the spleen of HES/AOM/DSS mice contributes towards the elevated CAC disease severity experience by this group.

A caveat of the present study is the lack of a TGF-β inhibitor only group. TGF-β has a known role in EMT and cancer progression, therefore it cannot be ruled out that the alleviation of symptoms in the HES/AOM/DSS/SB-431542 group is due to the actions of the inhibitor only (224-227). Since only two mice from the HES/AOM/DSS treated group survived to the end of the experiment, no significant conclusions can be drawn from the colon length, spleen weight and spleen total cell count data. Furthermore, from day 12 onwards the HES/AOM/DSS/SB-431542 treated mice started to experience worsened pathology, and this may have skewed the end results. This could be due to SB-431542 having a short half-life and perhaps the compound should have been administered once more towards the end of the experiment to further sustain its protective effect. It is important to repeat this study, including a SB-431542 only group and possibly ending the experiment on day 12 to prevent mortality in the HES/AOM/DSS treated group and increased pathology in the HES/AOM/DSS/SB-431542 treated group.

It is important to note that the DSS used in each of the CAC studies, either with or without the SB-431542 inhibitor, were not from the same batch. The DSS used in the first study, without SB-431542, was found to be less efficient compared to previous and subsequent batches of DSS used. The mice in the first study, therefore experienced less inflammation and consequently were not as susceptible to the immune modulatory effects characteristic of HES. These mice ultimately had reduced morbidity and mortality, which was evident in the HES/AOM/DSS mice in the second study.

These preliminary experiments suggest that exposure to gastrointestinal nematode derived antigen results in a poor outcome in CRC tumour growth and CAC development associated with an expansion of the Treg population. These results align with what is currently known about Tregs and CRC development and progression and implicate Tregs as a key driver of disease as well as a potential target in CRC treatment (128, 129).

5. Conclusion

The data presented here provides compelling evidence that helminth derived antigens can impact cancer development and progression. While hookworm exposure appears to have a protective impact on cervical cancer cell progression through inhibiting migration, EMT marker expression and HPV internalisation (**Figure 4.1**), exposure to gastrointestinal nematode antigens accelerated the development and progression of colorectal cancer by exacerbating

CAC symptoms and accelerating tumour growth (**Figure 4.2**). These findings highlight the complicated nature of cancer and the importance of understanding exactly how helminths can alter the behaviour of this disease. Further in-depth analysis could reveal a preventative and late-stage treatment for cancer using parasitic antigens.

6. Future Work

6.1 *N. brasiliensis* and Cervical Cancer

It is critical to determine the mechanism behind how *N. brasiliensis* systemically alters EMT expression in the murine FGT. This could be achieved in several ways:

Injecting *N. brasiliensis* infected mice with anti-IL-13 would neutralise the function of this cytokine and allow one to determine whether the expression of vimentin and N-cadherin is similarly decreased in the FGT of these mice compared to infected and naïve mice, which did not receive recombinant IL-13. Furthermore, IL-4 Receptor Alpha (IL-4Rα) deficient mice could also be utilised. IL-13 signals via IL-4Rα, therefore mice deficient in this receptor would not be responsive to IL-13 signaling. If *N. brasiliensis* infected IL-4Rα deficient mice have reduced expression of vimentin and N-cadherin in the FGT then one could conclude that IL-13 may be playing a role in systemically reducing EMT expression.

Acetylcholine signals via the M3 receptor, therefore mice deficient in this receptor could be utilised to determine whether this neurotransmitter and the acetylcholinesterase produced by *N. brasiliensis* may play a role in altering EMT expression in the FGT. However, it is important to remember that acetylcholine has multiple receptors, therefore incorporating M3 receptor deficient mice into the study would only provide support for the role of acetylcholinesterase in systemically altering EMT expression and not conclusive evidence. Moreover, treating mice with acetylcholinesterase, instead of *N. brasiliensis,* could also be used to determine whether this enzyme has a similar effect on EMT expression in the FGT compared to live infection alone.

Although the above described experiments would be beneficial in helping to determine the mechanism of action, which *N. brasiliensis* uses to impact cervical cancer development and progression it would be more useful to isolate an individual protein or lipid which directly mediates the observed effects on cervical cancer behaviour. This could be achieved using proteomic analysis, which has been utilised for other helminth derived antigens (228).

6.2 *H. polygyrus* and Colorectal Cancer

A limitation of the syngeneic tumour model used in this study is that the CT26.WT colorectal cancer tumours were not grown in a physiologically relevant location. In future experiments, the cells could be administered intrarectally into the submucosa of mice (229). This is important because C26.WT cells grown in the colon, which contains a more appropriate microenvironment, may behave differently to the CT26.WT cells used in the syngeneic tumour model.

PD-1 has been shown to play a critical role in the negative regulation of ILC-2s, an innate cell population expanded during helminth infection, by causing an increase in ILC-2 cell numbers and facilitating parasite expulsion (13, 230). It is possible that HES activates PD-1 to reduce ILC-2 population numbers and enhance *H. polygyrus* survival in the host. Consequently, the host immune response is suppressed leading to accelerated CT26.WT tumour growth. For this reason, it would be beneficial to determine the changes in the proportion of ILC-2s present in tumours derived from HES treated CT26.WT cells compared to tumours derived from untreated cells.

Interestingly, HES has been reported to contain micro-vesicles encompassing microRNAs (miRNAs) (231). These exosomes can be internalized by mouse cells and play an essential role in host-parasite interactions and dampening the Th2 immune response. It would be fascinating to determine whether these exosomes are able to alter colorectal cancer cell behaviour *in vitro* and *in vivo* as well as the development of CAC in a way similar to that of the *H. polygyrus* derived antigens. To achieve this, the exosomes could be isolated from HES by ultracentrifugation and used in the described *in vitro* and *in vivo* studies.

In addition to the above, it would also be beneficial to determine whether live infection with *H. polygyrus* has similar effects on CRC behaviour and CAC development as observed using HES and *H. polygyrus* antigen.

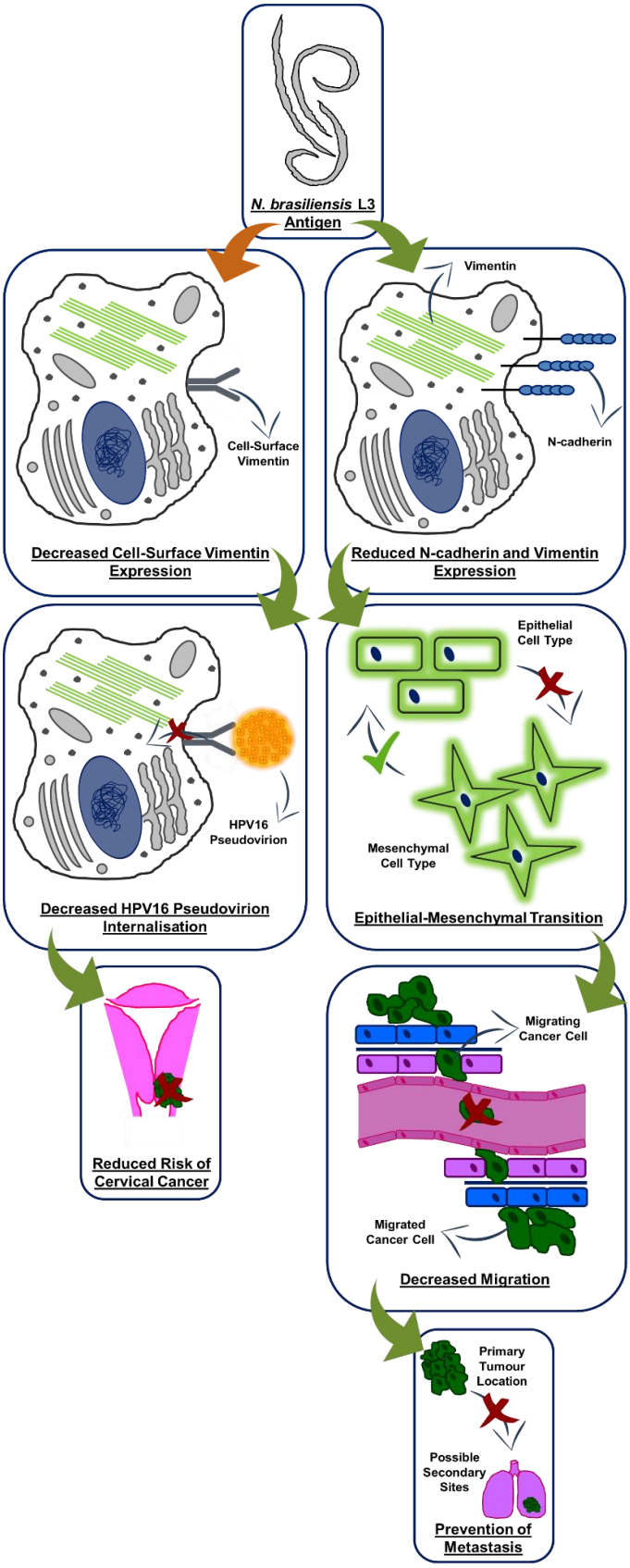

Figure 4.1: Summary of results. *N. brasiliensis* L3 antigen decreased cervical cancer cell migration and EMT expression independent of the HPV status of the cell line. Furthermore, while the L3 antigens decreased cell-surface vimentin expression, HPV16 pseudovirion internalisation was reduced. The results from this study would suggest a reduced risk of cervical cancer development as well as the prevention of possible metastasis. Beneficial outcomes in disease progression are indicated with green arrows and neither beneficial nor detrimental ones with orange arrows.

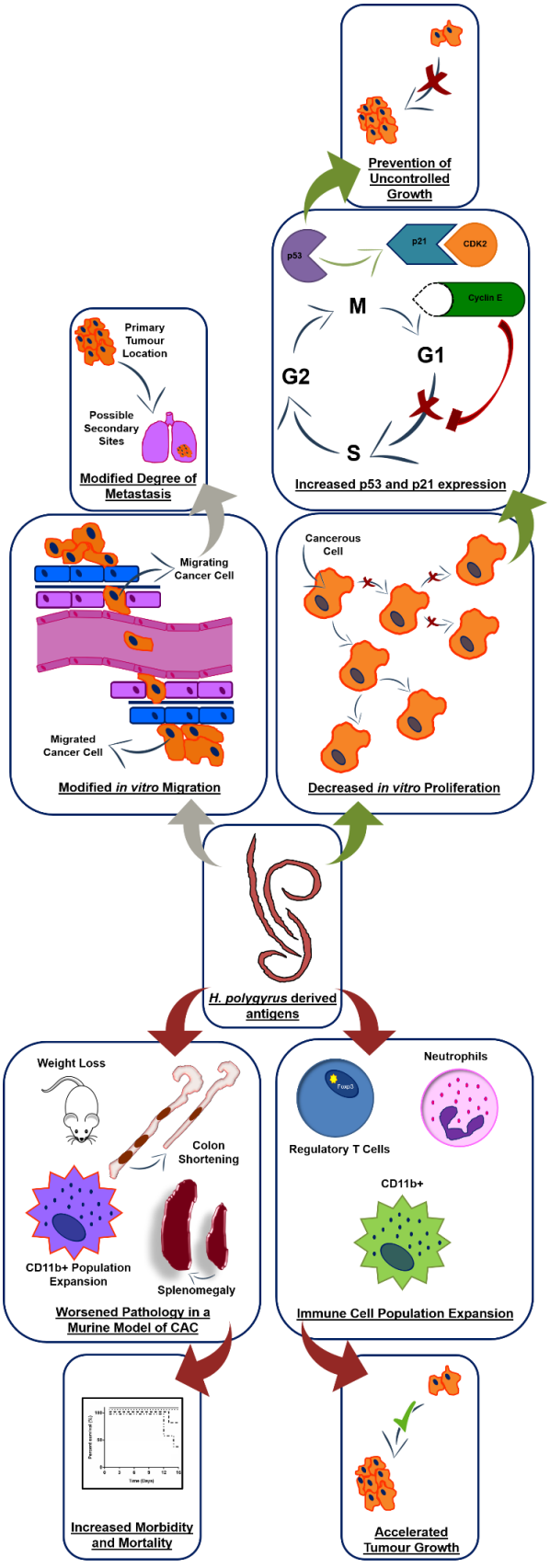

Figure 4.2: Summary of results. *H. polygyrus* derived antigens decreased human and mouse colorectal cancer cell proliferation with an associated increase in cell cycle regulators. These antigens also modified colorectal cancer cell migration in a cell line dependent manner. Tumours derived from HES treated mouse colorectal cancer cells had accelerated growth with an accompanied expansion in Treg, neutrophil and CD11b+ cell populations. Furthermore, in a mouse model of Colitis-Associated Colorectal Cancer (CAC), HES treatment worsened pathology and increased morbidity and mortality. Beneficial outcomes in disease progression are indicated with green arrows and detrimental outcomes with red arrows.

7. References

1. **Coussens LM, Werb Z.** 2002. Inflammation and cancer. Nature **420:**860-867.
2. **Torre LA, Bray F, Siegel RL, Ferlay J, Lortet-Tieulent J, Jemal A.** 2015. Global cancer statistics, 2012. CA: A Cancer Journal for Clinicians **65:**87-108.
3. **de Martel C, Ferlay J, Franceschi S, Vignat J, Bray F, Forman D, Plummer M.** 2012. Global burden of cancers attributable to infections in 2008: a review and synthetic analysis. The Lancet Oncology **13:**607-615.
4. **American Cancer Society.** 2017. The Cancer Atlas. http://canceratlas.cancer.org/risk-factors/infection/. Accessed
5. **Sriamporn S, Pisani P, Pipitgool V, Suwanrungruang K, Kamsa-ard S, Parkin DM.** 2004. Prevalence of Opisthorchis viverrini infection and incidence of cholangiocarcinoma in Khon Kaen, Northeast Thailand. Tropical medicine & international health : TM & IH **9:**588-594.
6. **Choi D, Lim JH, Lee KT, Lee JK, Choi SH, Heo JS, Jang KT, Lee NY, Kim S, Hong ST.** 2006. Cholangiocarcinoma and Clonorchis sinensis infection: a case-control study in Korea. Journal of hepatology **44:**1066-1073.
7. **Rosin MP, El Din Zaki SS, Ward AJ, Anwar WA.** 1994. Involvement of inflammatory reactions and elevated cell proliferation in the development of bladder cancer in schistosomiasis patients. Mutation Research/Fundamental and Molecular Mechanisms of Mutagenesis **305:**283-292.
8. **Hotez PJ, Brindley PJ, Bethony JM, King CH, Pearce EJ, Jacobson J.** 2008. Helminth infections: the great neglected tropical diseases. J Clin Invest **118:**1311-1321.
9. **WHO/TDR.** 2017. Research priorites for helminth infections. http://www.who.int/tdr/publications/helminth_infections/en/. Accessed
10. **Bethony J, Brooker S, Albonico M, Geiger SM, Loukas A, Diemert D, Hotez PJ.** 2006. Soil-transmitted helminth infections: ascariasis, trichuriasis, and hookworm. The Lancet **367:**1521-1532.
11. **Pearce EJ, Caspar P, Grzych JM, Lewis FA, Sher A.** 1991. Downregulation of Th1 cytokine production accompanies induction of Th2 responses by a parasitic helminth, Schistosoma mansoni. The Journal of experimental medicine **173:**159-166.
12. **Elliott DE, Urban Jf JR, Argo CK, Weinstock JV.** 2000. Does the failure to acquire helminthic parasites predispose to Crohn's disease? FASEB journal : official publication of the Federation of American Societies for Experimental Biology **14:**1848-1855.
13. **Allen JE, Maizels RM.** 2011. Diversity and dialogue in immunity to helminths. Nature Reviews Immunology **11:**375.
14. **Watanabe N, Tamauchi H, Ozawa H, Ito M, Ovary Z, Habu S.** 2003. Th2 Immune Responses in GATA-3-Transgenic Mice Infected with Heligmosomoides polygyrus. International archives of allergy and immunology **131(suppl 1):**11-14.
15. **Maizels RM, McSorley HJ.** 2016. Regulation of the host immune system by helminth parasites. The Journal of Allergy and Clinical Immunology **138:**666-675.
16. **Grainger JR, Smith KA, Hewitson JP, McSorley HJ, Harcus Y, Filbey KJ, Finney CA, Greenwood EJ, Knox DP, Wilson MS, Belkaid Y, Rudensky AY, Maizels RM.** 2010. Helminth secretions induce de novo T cell Foxp3 expression and regulatory function through the TGF-beta pathway. The Journal of experimental medicine **207:**2331-2341.
17. **Sartono E, Kruize YCM, Kurniawan A, van der Meide PH, Partono F, Maizels RM, Yazdanbakhsh M.** 1995. Elevated Cellular Immune Responses and Interferon-γ Release after Long-Term Diethylcarbamazine Treatment of Patients with Human Lymphatic Filariasis. The Journal of Infectious Diseases **171:**1683-1687.
18. **Shimon S, Masahiro O, Ruka S, Haruhiko Y, Shohei H, Zoltan F, Jun S, Takeshi T, Takashi N.** 2006. Foxp3+CD25+CD4+ natural regulatory T cells in dominant self-tolerance and autoimmune disease. Immunological Reviews **212:**8-27.
19. **Ehrenstein MR, Evans JG, Singh A, Moore S, Warnes G, Isenberg DA, Mauri C.** 2004. Compromised function of regulatory T cells in rheumatoid arthritis and reversal by anti-TNFalpha therapy. J Exp Med **200:**277-285.
20. **Mucida D, Park Y, Kim G, Turovskaya O, Scott I, Kronenberg M, Cheroutre H.** 2007. Reciprocal TH17 and regulatory T cell differentiation mediated by retinoic acid. Science **317:**256-260.
21. **Hawrylowicz CM, O'Garra A.** 2005. Potential role of interleukin-10-secreting regulatory T cells in allergy and asthma. Nat Rev Immunol **5:**271-283.

22. **Chen W, Jin W, Hardegen N, Lei KJ, Li L, Marinos N, McGrady G, Wahl SM.** 2003. Conversion of peripheral CD4+CD25- naive T cells to CD4+CD25+ regulatory T cells by TGF-beta induction of transcription factor Foxp3. J Exp Med **198:**1875-1886.
23. **Hori S, Nomura T, Sakaguchi S.** 2017. Pillars Article: Control of Regulatory T Cell Development by the Transcription Factor Foxp3. Science 2003. 299: 1057-1061. J Immunol **198:**981-985.
24. **Wang Y, Zhou H, Shen Y, Wu W, Liu H, Yuan Z, Xu Y, Hu Y, Cao J.** 2015. Impairment of dendritic cell function and induction of CD4(+)CD25(+)Foxp3(+) T cells by excretory-secretory products: a potential mechanism of immune evasion adopted by Echinococcus granulosus. BMC immunology **16:**44-015-0110-0113.
25. **McSorley HJ, Harcus YM, Murray J, Taylor MD, Maizels RM.** 2008. Expansion of Foxp3+ regulatory T cells in mice infected with the filarial parasite Brugia malayi. Journal of immunology (Baltimore, Md: 1950) **181:**6456-6466.
26. **Hasby EA, Hasby Saad MA, Shohieb Z, El Noby K.** 2015. FoxP3+ T regulatory cells and immunomodulation after Schistosoma mansoni egg antigen immunization in experimental model of inflammatory bowel disease. Cellular immunology **295:**67-76.
27. **Aranzamendi C, Fransen F, Langelaar M, Franssen F, Van Der Ley P, Van Putten JPM, Rutten V, Pinelli E.** 2012. Trichinella spiralis-secreted products modulate DC functionality and expand regulatory T cells in vitro. Parasite immunology **34:**210-223.
28. **Sawant DV, Gravano DM, Vogel P, Giacomin P, Artis D, Vignali DA.** 2014. Regulatory T cells limit induction of protective immunity and promote immune pathology following intestinal helminth infection. Journal of immunology (Baltimore, Md: 1950) **192:**2904-2912.
29. **Blankenhaus B, Klemm U, Eschbach ML, Sparwasser T, Huehn J, Kuhl AA, Loddenkemper C, Jacobs T, Breloer M.** 2011. Strongyloides ratti infection induces expansion of Foxp3+ regulatory T cells that interfere with immune response and parasite clearance in BALB/c mice. J Immunol **186:**4295-4305.
30. **Blankenhaus B, Reitz M, Brenz Y, Eschbach ML, Hartmann W, Haben I, Sparwasser T, Huehn J, Kuhl A, Feyerabend TB, Rodewald HR, Breloer M.** 2014. Foxp3(+) regulatory T cells delay expulsion of intestinal nematodes by suppression of IL-9-driven mast cell activation in BALB/c but not in C57BL/6 mice. PLoS Pathog **10:**e1003913.
31. **Terrazas CA, Sanchez-Munoz F, Mejia-Dominguez AM, Amezcua-Guerra LM, Terrazas LI, Bojalil R, Gomez-Garcia L.** 2011. Cestode antigens induce a tolerogenic-like phenotype and inhibit LPS inflammatory responses in human dendritic cells. International journal of biological sciences **7:**1391-1400.
32. **Bai X, Wu X, Wang X, Guan Z, Gao F, Yu J, Yu L, Tang B, Liu X, Song Y, Radu B, Boireau P, Wang F, Liu M.** 2012. Regulation of cytokine expression in murine macrophages stimulated by excretory/secretory products from Trichinella spiralis in vitro. Molecular and cellular biochemistry **360:**79-88.
33. **Johnston CJC, Smyth DJ, Kodali RB, White MPJ, Harcus Y, Filbey KJ, Hewitson JP, Hinck CS, Ivens A, Kemter AM, Kildemoes AO, Le Bihan T, Soares DC, Anderton SM, Brenn T, Wigmore SJ, Woodcock HV, Chambers RC, Hinck AP, McSorley HJ, Maizels RM.** 2017. A structurally distinct TGF-beta mimic from an intestinal helminth parasite potently induces regulatory T cells. Nat Commun **8:**1741.
34. **Mulder R, Banete A, Basta S.** 2014. Spleen-derived macrophages are readily polarized into classically activated (M1) or alternatively activated (M2) states. Immunobiology **219:**737-745.
35. **Kreider T, Anthony RM, Urban Jr JF, Gause WC.** 2007. Alternatively activated macrophages in helminth infections. Host-pathogen interactions/Immunological Techniques **19:**448-453.
36. **Broadhurst MJ, Leung JM, Lim KC, Girgis NM, Gundra UM, Fallon PG, Premenko-Lanier M, McKerrow JH, McCune JM, Loke P.** 2012. Upregulation of retinal dehydrogenase 2 in alternatively activated macrophages during retinoid-dependent type-2 immunity to helminth infection in mice. PLoS pathogens **8:**e1002883.
37. **Chen F, Wu W, Millman A, Craft JF, Chen E, Patel N, Boucher JL, Urban JF, Jr., Kim CC, Gause WC.** 2014. Neutrophils prime a long-lived effector macrophage phenotype that mediates accelerated helminth expulsion. Nat Immunol **15:**938-946.
38. **Anthony RM, Urban JF, Alem F, Hamed HA, Rozo CT, Boucher J-L, Van Rooijen N, Gause WC.** 2006. Memory T(H)2 cells induce alternatively activated macrophages to mediate protection against nematode parasites. Nature medicine **12:**955-960.
39. **Zhao A, Urban JF, Jr., Anthony RM, Sun R, Stiltz J, van Rooijen N, Wynn TA, Gause WC, Shea-Donohue T.** 2008. Th2 Cytokine-Induced Alterations in Intestinal Smooth Muscle

Function Depend on Alternatively Activated Macrophages. Gastroenterology **135:**217-225.e211.
40. **Esser-von Bieren J, Mosconi I, Guiet R, Piersgilli A, Volpe B, Chen F, Gause WC, Seitz A, Verbeek JS, Harris NL.** 2013. Antibodies trap tissue migrating helminth larvae and prevent tissue damage by driving IL-4Ralpha-independent alternative differentiation of macrophages. PLoS Pathog **9:**e1003771.
41. **Klose CS, Artis D.** 2016. Innate lymphoid cells as regulators of immunity, inflammation and tissue homeostasis. Nature immunology **17:**765-774.
42. **Spits H, Artis D, Colonna M, Diefenbach A, Di Santo JP, Eberl G, Koyasu S, Locksley RM, McKenzie AN, Mebius RE, Powrie F, Vivier E.** 2013. Innate lymphoid cells--a proposal for uniform nomenclature. Nature reviewsImmunology **13:**145-149.
43. **Neill DR, Wong SH, Bellosi A, Flynn RJ, Daly M, Langford TK, Bucks C, Kane CM, Fallon PG, Pannell R, Jolin HE, McKenzie AN.** 2010. Nuocytes represent a new innate effector leukocyte that mediates type-2 immunity. Nature **464:**1367-1370.
44. **Price AE, Liang H-E, Sullivan BM, Reinhardt RL, Eisley CJ, Erle DJ, Locksley RM.** 2010. Systemically dispersed innate IL-13 expressing cells in type 2 immunity. Proceedings of the National Academy of Sciences **107:**11489-11494.
45. **Walker JA, McKenzie ANJ.** 2013. Development and function of group 2 innate lymphoid cells. Current opinion in immunology; Lymphocyte development / Tumour immunology / Cancer immunology: Clinical translation **25:**148-155.
46. **Howitt MR, Lavoie S, Michaud M, Blum AM, Tran SV, Weinstock JV, Gallini CA, Redding K, Margolskee RF, Osborne LC, Artis D, Garrett WS.** 2016. Tuft cells, taste-chemosensory cells, orchestrate parasite type 2 immunity in the gut. Science **351:**1329-1333.
47. **Grencis RK, Worthington JJ.** 2016. Tuft Cells: A New Flavor in Innate Epithelial Immunity. Trends Parasitol **32:**583-585.
48. **Oliphant CJ, Hwang YY, Walker JA, Salimi M, Wong SH, Brewer JM, Englezakis A, Barlow JL, Hams E, Scanlon ST, Ogg GS, Fallon PG, McKenzie AN.** 2014. MHCII-mediated dialog between group 2 innate lymphoid cells and CD4(+) T cells potentiates type 2 immunity and promotes parasitic helminth expulsion. Immunity **41:**283-295.
49. **Zaiss MM, Maslowski KM, Mosconi I, Guenat N, Marsland BJ, Harris NL.** 2013. IL-1beta suppresses innate IL-25 and IL-33 production and maintains helminth chronicity. PLoS pathogens **9:**e1003531.
50. **McSorley HJ, Blair NF, Smith KA, McKenzie ANJ, Maizels RM.** 2014. Blockade of IL-33 release and suppression of type 2 innate lymphoid cell responses by helminth secreted products in airway allergy. Mucosal Immunol **7:**1068-1078.
51. **Phythian-Adams A, Cook PC, Lundie RJ, Jones LH, Smith KA, Barr TA, Hochweller K, Anderton SM, HÃ¤mmerling GnJ, Maizels RM, MacDonald AS.** 2010. CD11c depletion severely disrupts Th2 induction and development in vivo. The Journal of experimental medicine **207:**2089-2096.
52. **Smith KA, Harcus Y, Garbi N, Hammerling GJ, MacDonald AS, Maizels RM.** 2012. Type 2 innate immunity in helminth infection is induced redundantly and acts autonomously following CD11c(+) cell depletion. Infection and immunity **80:**3481-3489.
53. **Smith KA, Hochweller K, Hammerling GJ, Boon L, MacDonald AS, Maizels RM.** 2011. Chronic helminth infection promotes immune regulation in vivo through dominance of CD11cloCD103- dendritic cells. Journal of immunology (Baltimore, Md: 1950) **186:**7098-7109.
54. **Kane CM, Cervi L, Sun J, McKee AS, Masek KS, Shapira S, Hunter CA, Pearce EJ.** 2004. Helminth Antigens Modulate TLR-Initiated Dendritic Cell Activation. The Journal of Immunology **173:**7454-7461.
55. **Ohnmacht C, Voehringer D.** 2008. Basophil effector function and homeostasis during helminth infection. Blood **113:**2816-2825.
56. **Hepworth MR, DaniÅ‚owicz-Luebert E, Rausch S, Metz M, Klotz C, Maurer M, Hartmann S.** 2012. Mast cells orchestrate type 2 immunity to helminths through regulation of tissue-derived cytokines. Proceedings of the National Academy of Sciences **109:**6644-6649.
57. **Kalinski P.** 2012. Regulation of Immune Responses by Prostaglandin E2. The Journal of Immunology **188:**21-28.
58. **Malhotra I, McKibben M, Mungai P, McKibben E, Wang X, Sutherland LJ, Muchiri EM, King CH, King CL, LaBeaud AD.** 2015. Effect of antenatal parasitic infections on anti-vaccine IgG levels in children: a prospective birth cohort study in Kenya. PLoS Negl Trop Dis **9:**e0003466.

59. **Cooper PJ, Espinel I, Paredes W, Guderian RH, Nutman TB.** 1998. Impaired tetanus-specific cellular and humoral responses following tetanus vaccination in human onchocerciasis: a possible role for interleukin-10. The Journal of infectious diseases **178:**1133-1138.
60. **Morawski BM, Yunus M, Kerukadho E, Turyasingura G, Barbra L, Ojok AM, DiNardo AR, Sowinski S, Boulware DR, Mejia R.** 2017. Hookworm infection is associated with decreased CD4+ T cell counts in HIV-infected adult Ugandans. PLoS Negl Trop Dis **11:**e0005634.
61. **Gazzinelli-Guimaraes PH, de Freitas LF, Gazzinelli-Guimaraes AC, Coelho F, Barbosa FS, Nogueira D, Amorim C, Dhom-Lemos LC, Oliveira LM, da Silveira AB, da Fonseca FG, Bueno LL, Fujiwara RT.** 2017. Concomitant helminth infection downmodulates the Vaccinia virus-specific immune response and potentiates virus-associated pathology. Int J Parasitol **47:**1-10.
62. **McFarlane AJ, McSorley HJ, Davidson DJ, Fitch PM, Errington C, Mackenzie KJ, Gollwitzer ES, Johnston CJC, MacDonald AS, Edwards MR, Harris NL, Marsland BJ, Maizels RM, Schwarze J.** 2017. Enteric helminth-induced type I interferon signaling protects against pulmonary virus infection through interaction with the microbiota. J Allergy Clin Immunol **140:**1068-1078.e1066.
63. **Anuradha R, Munisankar S, Bhootra Y, Dolla C, Kumaran P, Nutman TB, Babu S.** 2017. Modulation of Mycobacterium tuberculosis-specific humoral immune responses is associated with Strongyloides stercoralis co-infection. PLoS Negl Trop Dis **11:**e0005569.
64. **Chen CC, Louie S, McCormick B, Walker WA, Shi HN.** 2005. Concurrent infection with an intestinal helminth parasite impairs host resistance to enteric Citrobacter rodentium and enhances Citrobacter-induced colitis in mice. Infection and immunity **73:**5468-5481.
65. **Su L, Su CW, Qi Y, Yang G, Zhang M, Cherayil BJ, Zhang X, Shi HN.** 2014. Coinfection with an intestinal helminth impairs host innate immunity against Salmonella enterica serovar Typhimurium and exacerbates intestinal inflammation in mice. Infect Immun **82:**3855-3866.
66. **Reynolds LA, Redpath SA, Yurist-Doutsch S, Gill N, Brown EM, van der Heijden J, Brosschot TP, Han J, Marshall NC, Woodward SE, Valdez Y, Borchers CH, Perona-Wright G, Finlay BB.** 2017. Enteric helminths promote Salmonella co-infection by altering the intestinal metabolome. J Infect Dis doi:10.1093/infdis/jix141.
67. **Mishra PK, Patel N, Wu W, Bleich D, Gause WC.** 2013. Prevention of type 1 diabetes through infection with an intestinal nematode parasite requires IL-10 in the absence of a Th2-type response. Mucosal Immunol **6:**297-308.
68. **Morimoto M, Azuma N, Kadowaki H, Abe T, Suto Y.** 2017. Regulation of type 2 diabetes by helminth-induced Th2 immune response. J Vet Med Sci **78:**1855-1864.
69. **Aravindhan V, Mohan V, Surendar J, Rao MM, Ranjani H, Kumaraswami V, Nutman TB, Babu S.** 2010. Decreased prevalence of lymphatic filariasis among subjects with type-1 diabetes. The American Journal of Tropical Medicine and Hygiene **83:**1336-1339.
70. **Hansen CS, Hasseldam H, Bacher IH, Thamsborg SM, Johansen FF, Kringel H.** 2017. Trichuris suis secrete products that reduce disease severity in a multiple sclerosis model. Acta Parasitol **62:**22-28.
71. **Chen Z, Andreev D, Oeser K, Krljanac B, Hueber A, Kleyer A, Voehringer D, Schett G, Bozec A.** 2016. Th2 and eosinophil responses suppress inflammatory arthritis. Nat Commun **7:**11596.
72. **Sarter K, Kulagin M, Schett G, Harris NL, Zaiss MM.** 2017. Inflammatory arthritis and systemic bone loss are attenuated by gastrointestinal helminth parasites. Autoimmunity **50:**151-157.
73. **Kitagaki K, Businga TR, Racila D, Elliott DE, Weinstock JV, Kline JN.** 2006. Intestinal helminths protect in a murine model of asthma. J Immunol **177:**1628-1635.
74. **McSorley HJ, Blair NF, Robertson E, Maizels RM.** 2015. Suppression of OVA-alum induced allergy by Heligmosomoides polygyrus products is MyD88-, TRIF-, regulatory T- and B cell-independent, but is associated with reduced innate lymphoid cell activation. Exp Parasitol **158:**8-17.
75. **McSorley HJ, O'Gorman MT, Blair N, Sutherland TE, Filbey KJ, Maizels RM.** 2012. Suppression of type 2 immunity and allergic airway inflammation by secreted products of the helminth Heligmosomoides polygyrus. Eur J Immunol **42:**2667-2682.
76. **Hartmann S, Schnoeller C, Dahten A, Avagyan A, Rausch S, Lendner M, Bocian C, Pillai S, Loddenkemper C, Lucius R, Worm M, Hamelmann E.** 2009. Gastrointestinal nematode infection interferes with experimental allergic airway inflammation but not atopic dermatitis. Clin Exp Allergy **39:**1585-1596.

77. **Zitvogel L, Apetoh L, Ghiringhelli F, André F, Tesniere A, Kroemer G.** 2008. The anticancer immune response: indispensable for therapeutic success? The Journal of Clinical Investigation **118:**1991-2001.
78. **Medler TR, Cotechini T, Coussens LM.** 2015. Immune response to cancer therapy: mounting an effective antitumor response and mechanisms of resistance. Trends Cancer **1:**66-75.
79. **Ikeda H, Old LJ, Schreiber RD.** 2002. The roles of IFN gamma in protection against tumor development and cancer immunoediting. Cytokine Growth Factor Rev **13:**95-109.
80. **Gravitt PE, Marks M, Kosek M, Huang C, Cabrera L, Olortegui MP, Medrano AM, Trigoso DR, Qureshi S, Bardales GS, Manrique-Hinojosa J, Cardenas AZ, Larraondo MA, Cok J, Qeadan F, Siracusa M, Gilman RH.** 2016. Soil-Transmitted Helminth Infections Are Associated With an Increase in Human Papillomavirus Prevalence and a T-Helper Type 2 Cytokine Signature in Cervical Fluids. J Infect Dis **213:**723-730.
81. **Reese TA, Wakeman BS, Choi HS, Hufford MM, Huang SC, Zhang X, Buck MD, Jezewski A, Kambal A, Liu CY, Goel G, Murray PJ, Xavier RJ, Kaplan MH, Renne R, Speck SH, Artyomov MN, Pearce EJ, Virgin HW.** 2014. Helminth infection reactivates latent gamma-herpesvirus via cytokine competition at a viral promoter. Science (New York, NY) **345:**573-577.
82. **Itthitaetrakool U, Pinlaor P, Pinlaor S, Chomvarin C, Dangtakot R, Chaidee A, Wilailuckana C, Sangka A, Lulitanond A, Yongvanit P.** 2016. Chronic Opisthorchis viverrini Infection Changes the Liver Microbiome and Promotes Helicobacter Growth. PLoS One **11:**e0165798.
83. **Dangtakot R, Pinlaor S, Itthitaetrakool U, Chaidee A, Chomvarin C, Sangka A, Wilailuckana C, Pinlaor P.** 2017. Coinfection with Helicobacter pylori and Opisthorchis viverrini Enhances the Severity of Hepatobiliary Abnormalities in Hamsters. Infect Immun **85**.
84. **Fox JG, Beck P, Dangler CA, Whary MT, Wang TC, Shi HN, Nagler-Anderson C.** 2000. Concurrent enteric helminth infection modulates inflammation and gastric immune responses and reduces helicobacter-induced gastric atrophy. Nature medicine **6:**536-542.
85. **Whary MT, Muthupalani S, Ge Z, Feng Y, Lofgren J, Shi HN, Taylor NS, Correa P, Versalovic J, Wang TC, Fox JG.** 2014. Helminth co-infection in Helicobacter pylori infected INS-GAS mice attenuates gastric premalignant lesions of epithelial dysplasia and glandular atrophy and preserves colonization resistance of the stomach to lower bowel microbiota. Microbes Infect **16:**345-355.
86. **Ek C, Whary MT, Ihrig M, Bravo LE, Correa P, Fox JG.** 2012. Serologic evidence that ascaris and toxoplasma infections impact inflammatory responses to Helicobacter pylori in Colombians. Helicobacter **17:**107-115.
87. **Del Prete G, Chiumiento L, Amedei A, Piazza M, D'Elios MM, Codolo G, de Bernard M, Masetti M, Bruschi F.** 2008. Immunosuppression of TH2 responses in Trichinella spiralis infection by Helicobacter pylori neutrophil-activating protein. J Allergy Clin Immunol **122:**908-913.e905.
88. **Chiumiento L, Del Prete G, Codolo G, De Bernard M, Amedei A, Della Bella C, Piazza M, D'Elios S, Caponi L, D'Elios MM, Bruschi F.** 2011. Stimulation of TH1 response by Helicobacter pylori neutrophil activating protein decreases the protective role of IgE and eosinophils in experimental trichinellosis. Int J Immunopathol Pharmacol **24:**895-903.
89. **Elshal MF, Elsayed IH, El Kady IM, Badra G, El-Refaei A, El-Batanony M, Hendy OM.** 2004. Role of concurrent S. mansoni infection in H. pylori-associated gastritis: a flow cytometric DNA-analysis and oxyradicals correlations. Clinica chimica acta; international journal of clinical chemistry **346:**191-198.
90. **Abou Holw SA, Anwar MM, Bassiouni RB, Hussen NA, Eltaweel HA.** 2008. Impact of coinfection with Schistosoma mansoni on Helicobacter pylori induced disease. J Egypt Soc Parasitol **38:**73-84.
91. **International Agency for Research on Cancer.** 2017. GLOBOCAN 2012: Estimated Cancer Incidence, Mortality and Prevalenve Worldwide in 2012. http://globocan.iarc.fr/Pages/fact_sheets_cancer.aspx. Accessed
92. **Bouvard V, Baan R, Straif K, Grosse Y, Secretan B, El Ghissassi F, Benbrahim-Tallaa L, Guha N, Freeman C, Galichet L.** 2009. A review of human carcinogens—Part B: biological agents. The lancet oncology **10:**321-322.
93. **Pillay P, van Lieshout L, Taylor M, Sebitloane M, Zulu SG, Kleppa E, Roald B, Kjetland EF.** 2016. Cervical cytology as a diagnostic tool for female genital schistosomiasis: Correlation to cervical atypia and Schistosoma polymerase chain reaction. doi:D - NLM: PMC4854169 OTO - NOTNLM.

94. **Hove MM, Javangwe TV.** 2014. Female genital schistosomiasis: pathological features and density infestation. The Central African journal of medicine **60:**13-16.
95. **Petry KU, Scholz U, Hollwitz B, Von Wasielewski R, Meijer CJ.** 2003. Human papillomavirus, coinfection with Schistosoma hematobium, and cervical neoplasia in rural Tanzania. Int J Gynecol Cancer **13:**505-509.
96. **Arnold M, Sierra MS, Laversanne M, Soerjomataram I, Jemal A, Bray F.** 2017. Global patterns and trends in colorectal cancer incidence and mortality. Gut **66:**683-691.
97. **Durko L, Malecka-Panas E.** 2014. Lifestyle Modifications and Colorectal Cancer. Current Colorectal Cancer Reports **10:**45-54.
98. **Song M, Garrett WS, Chan AT.** 2015. Nutrients, foods, and colorectal cancer prevention. Gastroenterology **148:**1244-1260.e1216.
99. **Kinugasa T, Akagi Y.** 2016. Status of colitis-associated cancer in ulcerative colitis. doi:D - NLM: PMC4824713 OTO - NOTNLM.
100. **León-Cabrera S, Callejas BE, Ledesma-Soto Y, Coronel J, Pérez-Plasencia C, Gutiarrez-Cirlos EB, Avila-Moreno F, Rodraguez-Sosa M, Hernandez-Pando R, Marquina-Castillo B, Chirino YI, Terrazas LI.** 2014. Extraintestinal Helminth Infection Reduces the Development of Colitis-Associated Tumorigenesis. International Journal of Biological Sciences **10:**948-956.
101. **Terrazas LI, Callejas B, Reyes S, Ledesma-Soto Y, Olguín EJ, León-Cabrera S, Rodríguez-Sosa M.** 2017. Down-modulation of colitis-associated colorectal cancer development by treatment with helminth-derived molecules. The Journal of Immunology **198:**66.67-66.67.
102. **Hayes KS, Cliffe LJ, Bancroft AJ, Forman SP, Thompson S, Booth C, Grencis RK.** 2017. Chronic Trichuris muris infection causes neoplastic change in the intestine and exacerbates tumour formation in APC min/+ mice. PLoS Negl Trop Dis **11:**e0005708.
103. **Pastille E, Frede A, McSorley HJ, Grab J, Adamczyk A, Kollenda S, Hansen W, Epple M, Buer J, Maizels RM, Klopfleisch R, Westendorf AM.** 2017. Intestinal helminth infection drives carcinogenesis in colitis-associated colon cancer. PLoS Pathog **13:**e1006649.
104. **Madbouly KM, Senagore AJ, Mukerjee A, Hussien AM, Shehata MA, Navine P, Delaney CP, Fazio VW.** 2007. Colorectal cancer in a population with endemic Schistosoma mansoni: is this an at-risk population? International journal of colorectal disease **22:**175-181.
105. **Maizels RM, Balic A, Gomez-Escobar N, Nair M, Taylor MD, Allen JE.** 2004. Helminth parasites - masters of regulation. Immunological reviews **201:**89-116.
106. **Godkin A, Smith KA.** 2017. Chronic infections with viruses or parasites: breaking bad to make good. Immunology **150:**389-396.
107. **Ledesma-Soto Y, Callejas BE, Terrazas CA, Reyes JL, Espinoza-Jimenez A, Gonzalez MI, Leon-Cabrera S, Morales R, Olguin JE, Saavedra R, Oghumu S, Satoskar AR, Terrazas LI.** 2015. Extraintestinal Helminth Infection Limits Pathology and Proinflammatory Cytokine Expression during DSS-Induced Ulcerative Colitis: A Role for Alternatively Activated Macrophages and Prostaglandins. BioMed research international **2015:**563425.
108. **Shaw KA, Bertha M, Hofmekler T, Chopra P, Vatanen T, Srivatsa A, Prince J, Kumar A, Sauer C, Zwick ME, Satten GA, Kostic AD, Mulle JG, Xavier RJ, Kugathasan S.** 2016. Dysbiosis, inflammation, and response to treatment: a longitudinal study of pediatric subjects with newly diagnosed inflammatory bowel disease. Genome medicine **8:**75-016-0331-y.
109. **Brown SJ, Mayer L.** 2007. The Immune Response in Inflammatory Bowel Disease. The American Journal Of Gastroenterology **102:**2058.
110. **Summers RW, Elliott DE, Urban JF, Jr., Thompson R, Weinstock JV.** 2005. Trichuris suis therapy in Crohn's disease. Gut **54:**87-90.
111. **Summers RW, Elliott DE, Qadir K, Urban JF, Thompson R, Weinstock JV.** 2003. Trichuris suis seems to be safe and possibly effective in the treatment of inflammatory bowel disease. The American Journal of Gastroenterology **98:**2034-2041.
112. **Chu KM, Watermeyer G, Shelly L, Janssen J, May TD, Brink K, Benefeld G, Li X.** 2013. Childhood helminth exposure is protective against inflammatory bowel disease: a case control study in South Africa. Inflamm Bowel Dis **19:**614-620.
113. **Kiesler P, Fuss IJ, Strober W.** 2015. Experimental Models of Inflammatory Bowel Diseases. Cellular and Molecular Gastroenterology and Hepatology **1:**154-170.
114. **Motomura Y, Wang H, Deng Y, El-Sharkawy RT, Verdu EF, Khan WI.** 2009. Helminth antigen-based strategy to ameliorate inflammation in an experimental model of colitis. Clinical & Experimental Immunology **155:**88-95.

115. **Hunter MM, Wang A, Parhar KS, Johnston MJ, Van Rooijen N, Beck PL, McKay DM.** 2010. In vitro-derived alternatively activated macrophages reduce colonic inflammation in mice. Gastroenterology **138:**1395-1405.
116. **Hunter MM, Wang A, Hirota CL, McKay DM.** 2005. Neutralizing anti-IL-10 antibody blocks the protective effect of tapeworm infection in a murine model of chemically induced colitis. Journal of immunology (Baltimore, Md: 1950) **174:**7368-7375.
117. **Wang A, Fernando M, Leung G, Phan V, Smyth D, McKay DM.** 2010. Exacerbation of oxazolone colitis by infection with the helminth Hymenolepis diminuta: involvement of IL-5 and eosinophils. Am J Pathol **177:**2850-2859.
118. **Hunter MM, Wang A, McKay DM.** 2007. Helminth infection enhances disease in a murine TH2 model of colitis. Gastroenterology **132:**1320-1330.
119. **Xia CM, Zhao Y, Jiang L, Jiang J, Zhang SC.** 2011. Schistosoma japonicum ova maintains epithelial barrier function during experimental colitis. World J Gastroenterol **17:**4810-4816.
120. **Uhlig HH, Coombes J, Mottet C, Izcue A, Thompson C, Fanger A, Tannapfel A, Fontenot JD, Ramsdell F, Powrie F.** 2006. Characterization of Foxp3+CD4+CD25+ and IL-10-secreting CD4+CD25+ T cells during cure of colitis. Journal of immunology (Baltimore, Md: 1950) **177:**5852-5860.
121. **Gao W, Guo Y, Wang C, Lin Y, Yu L, Sheng T, Wu Z, Gong Y.** 2016. Indirubin ameliorates dextran sulfate sodium-induced ulcerative colitis in mice through the inhibition of inflammation and the induction of Foxp3-expressing regulatory T cells. Acta Histochemica doi:S0065-1281(16)30134-9 [pii].
122. **Elliott DE, Li J, Blum A, Metwali A, Qadir K, Urban JF, Weinstock JV.** 2003. Exposure to schistosome eggs protects mice from TNBS-induced colitis. American Journal of Physiology - Gastrointestinal and Liver Physiology **284:**G385-G391.
123. **Ruyssers NE, De Winter BY, De Man JG, Loukas A, Pearson MS, Weinstock JV, Van dB, Martinet W, Pelckmans PA, Moreels TG.** 2009. Therapeutic potential of helminth soluble proteins in TNBS-induced colitis in mice. Inflammatory bowel diseases **15:**491-500.
124. **Elliott DE, Setiawan T, Metwali A, Blum A, Urban JF, Jr., Weinstock JV.** 2004. Heligmosomoides polygyrus inhibits established colitis in IL-10-deficient mice. Eur J Immunol **34:**2690-2698.
125. **Blum AM, Hang L, Setiawan T, Urban JP, Jr., Stoyanoff KM, Leung J, Weinstock JV.** 2012. Heligmosomoides polygyrus bakeri induces tolerogenic dendritic cells that block colitis and prevent antigen-specific gut T cell responses. J Immunol **189:**2512-2520.
126. **Hang L, Setiawan T, Blum AM, Urban J, Stoyanoff K, Arihiro S, Reinecker HC, Weinstock JV.** 2010. Heligmosomoides polygyrus infection can inhibit colitis through direct interaction with innate immunity. J Immunol **185:**3184-3189.
127. **Leung J, Hang L, Blum A, Setiawan T, Stoyanoff K, Weinstock J.** 2012. Heligmosomoides polygyrus abrogates antigen-specific gut injury in a murine model of inflammatory bowel disease. Inflamm Bowel Dis **18:**1447-1455.
128. **Betts G, Jones E, Junaid S, El-Shanawany T, Scurr M, Mizen P, Kumar M, Jones S, Rees B, Williams G, Gallimore A, Godkin A.** 2012. Suppression of tumour-specific CD4(+) T cells by regulatory T cells is associated with progression of human colorectal cancer. Gut **61:**1163-1171.
129. **Clarke SL, Betts GJ, Plant A, Wright KL, El-Shanawany TM, Harrop R, Torkington J, Rees BI, Williams GT, Gallimore AM, Godkin AJ.** 2006. CD4+CD25+FOXP3+ Regulatory T Cells Suppress Anti-Tumor Immune Responses in Patients with Colorectal Cancer, p e129. - Public Library of Science.
130. **Reynolds LA, Finlay BB, Maizels RM.** 2015. Cohabitation in the Intestine: Interactions among Helminth Parasites, Bacterial Microbiota, and Host Immunity. J Immunol **195:**4059-4066.
131. **Zaiss MM, Rapin A, Lebon L, Dubey LK, Mosconi I, Sarter K, Piersigilli A, Menin L, Walker AW, Rougemont J, Paerewijck O, Geldhof P, McCoy KD, Macpherson AJ, Croese J, Giacomin PR, Loukas A, Junt T, Marsland BJ, Harris NL.** 2015. The Intestinal Microbiota Contributes to the Ability of Helminths to Modulate Allergic Inflammation. Immunity **43:**998-1010.
132. **Harris NL.** 2016. Intimate gut interactions: helminths and the microbiota. Cell Res **26:**861-862.
133. **Ramanan D, Bowcutt R, Lee SC, Tang MS, Kurtz ZD, Ding Y, Honda K, Gause WC, Blaser MJ, Bonneau RA, Lim YAL, Loke Pn, Cadwell K.** 2016. Helminth infection promotes colonization resistance via type 2 immunity. Science **352:**608.

134. **Su C, Su L, Li Y, Long SR, Chang J, Zhang W, Walker WA, Xavier RJ, Cherayil BJ, Shi HN.** 2018. Helminth-induced alterations of the gut microbiota exacerbate bacterial colitis. Mucosal Immunol **11:**144-157.
135. **Reynolds LA, Smith KA, Filbey KJ, Harcus Y, Hewitson JP, Redpath SA, Valdez Y, Yebra MJ, Finlay BB, Maizels RM.** 2014. Commensal-pathogen interactions in the intestinal tract: lactobacilli promote infection with, and are promoted by, helminth parasites. Gut microbes **5:**522-532.
136. **Hanahan D, Weinberg Robert A.** 2011. Hallmarks of Cancer: The Next Generation. Cell **144:**646-674.
137. **Huber MA, Kraut N, Beug H.** 2005. Molecular requirements for epithelial-mesenchymal transition during tumor progression. Current opinion in cell biology; Cell-to-cell contact and extracellular matrix **17:**548-558.
138. **Botelho M, Oliveira P, Gomes J, Gartner F, Lopes C, da Costa JM, Machado JC.** 2009. Tumourigenic effect of Schistosoma haematobium total antigen in mammalian cells. Int J Exp Pathol **90:**448-453.
139. **Chala B, Choi MH, Moon KC, Kim HS, Kwak C, Hong ST.** 2017. Development of Urinary Bladder Pre-Neoplasia by Schistosoma haematobium Eggs and Chemical Carcinogen in Mice. Korean J Parasitol **55:**21-29.
140. **Su C-w, Cao Y, Kaplan J, Zhang M, Li W, Conroy M, Walker WA, Shi HN.** 2011. Duodenal Helminth Infection Alters Barrier Function of the Colonic Epithelium via Adaptive Immune Activation. Infection and Immunity **79:**2285-2294.
141. **McDermott JR, Bartram RE, Knight PA, Miller HR, Garrod DR, Grencis RK.** 2003. Mast cells disrupt epithelial barrier function during enteric nematode infection. Proc Natl Acad Sci U S A **100:**7761-7766.
142. **Cooper ES, Ramdath DD, Whyte-Alleng C, Howell S, Serjeant BE.** 1997. Plasma proteins in children with trichuris dysentery syndrome. J Clin Pathol **50:**236-240.
143. **Pannain VL, Passos JV, Rocha Filho A, Villela-Nogueira C, Caroli-Bottino A.** 2010. Agressive inflammatory myofibroblastic tumor of the liver with underlying schistosomiasis: a case report. World J Gastroenterol **16:**4233-4236.
144. **Williams GH, Stoeber K.** 2012. The cell cycle and cancer. J Pathol **226:**352-364.
145. **Weinert T, Lydall D.** 1993. Cell cycle checkpoints, genetic instability and cancer. Semin Cancer Biol **4:**129-140.
146. **Loke P, MacDonald AS, Robb A, Maizels RM, Allen JE.** 2000. Alternatively activated macrophages induced by nematode infection inhibit proliferation via cell-to-cell contact. European journal of immunology **30:**2669-2678.
147. **Thuwajit C, Thuwajit P, Kaewkes S, Sripa B, Uchida K, Miwa M, Wongkham S.** 2004. Increased cell proliferation of mouse fibroblast NIH-3T3 in vitro induced by excretory/secretory product(s) from Opisthorchis viverrini. Parasitology **129:**455-464.
148. **Mali Camberis GLG, Joseph Urban.** 2003. Animal Model of Nippostrongylus brasiliensis and Heligmosomoides polygyrus. Current Protocols in Immunology **Unit 19.12**.
149. **Johnston CJC, Robertson E, Harcus Y, Grainger JR, Coakley G, Smyth DJ, McSorley HJ, Maizels R.** 2015. Cultivation of Heligmosomoides Polygyrus: An Immunomodulatory Nematode Parasite and its Secreted Products. Journal of Visualized Experiments : JoVE doi:10.3791/52412**:**52412.
150. **Parish CR.** 1999. Fluorescent dyes for lymphocyte migration and proliferation studies. Immunol Cell Biol **77:**499-508.
151. **Willmer T, Hare S, Peres J, Prince S.** 2016. The T-box transcription factor TBX3 drives proliferation by direct repression of the p21WAF1 cyclin-dependent kinase inhibitor. Cell Division **11:**1-13.
152. **Willmer T, Cooper A, Sims D, Govender D, Prince S.** The T-box transcription factor 3 is a promising biomarker and a key regulator of the oncogenic phenotype of a diverse range of sarcoma subtypes.
153. **Mosmann T.** 1983. Rapid colorimetric assay for cellular growth and survival: application to proliferation and cytotoxicity assays. J Immunol Methods **65:**55-63.
154. **Kee N, Sivalingam S, Boonstra R, Wojtowicz JM.** 2002. The utility of Ki-67 and BrdU as proliferative markers of adult neurogenesis. Journal of Neuroscience Methods **115:**97-105.
155. **Schafer G, Graham LM, Lang DM, Blumenthal MJ, Bergant Marusic M, Katz AA.** 2017. Vimentin Modulates Infectious Internalization of Human Papillomavirus 16 Pseudovirions. J Virol **91**.

156. **Ai W, Li H, Song N, Li L, Chen H.** 2013. Optimal Method to Stimulate Cytokine Production and Its Use in Immunotoxicity Assessment. International Journal of Environmental Research and Public Health **10:**3834-3842.
157. **Lecoeur H.** 2002. Nuclear apoptosis detection by flow cytometry: influence of endogenous endonucleases. Exp Cell Res **277:**1-14.
158. **Thaker AI, Shaker A, Rao MS, Ciorba MA.** 2012. Modeling Colitis-Associated Cancer with Azoxymethane (AOM) and Dextran Sulfate Sodium (DSS). Journal of Visualized Experiments : JoVE doi:10.3791/4100**:**4100.
159. **Laroui H, Ingersoll SA, Liu HC, Baker MT, Ayyadurai S, Charania MA, Laroui F, Yan Y, Sitaraman SV, Merlin D.** 2012. Dextran sodium sulfate (DSS) induces colitis in mice by forming nano-lipocomplexes with medium-chain-length fatty acids in the colon. PLoS One **7:**e32084.
160. **Inman GJ, Nicolas FJ, Callahan JF, Harling JD, Gaster LM, Reith AD, Laping NJ, Hill CS.** 2002. SB-431542 is a potent and specific inhibitor of transforming growth factor-beta superfamily type I activin receptor-like kinase (ALK) receptors ALK4, ALK5, and ALK7. Mol Pharmacol **62:**65-74.
161. **Raingeaud J, Gupta S, Rogers JS, Dickens M, Han J, Ulevitch RJ, Davis RJ.** 1995. Pro-inflammatory cytokines and environmental stress cause p38 mitogen-activated protein kinase activation by dual phosphorylation on tyrosine and threonine. J Biol Chem **270:**7420-7426.
162. **Gravitt PE, Marks M, Kosek M, Huang C, Cabrera L, Olortegui MP, Medrano AM, Trigoso DR, Qureshi S, Bardales GS, Manrique-Hinojosa J, Cardenas AZ, Larraondo MA, Cok J, Qeadan F, Siracusa M, Gilman RH.** 2016. Soil-Transmitted Helminth Infections Are Associated With an Increase in Human Papillomavirus Prevalence and a T-Helper Type 2 Cytokine Signature in Cervical Fluids. The Journal of infectious diseases **213:**723-730.
163. **Shafer et al. ud.** 2016. Vimentin modulates infectious internalisation of HPV16 pseudovirions. Journal of Virology.
164. **Liu W, Zeng HZ, Wang QM, Yi H, Mou Y, Wu CC, Hu B, Tang CW.** 2013. Schistosomiasis combined with colorectal carcinoma diagnosed based on endoscopic findings and clinicopathological characteristics: a report on 32 cases. Asian Pac J Cancer Prev **14:**4839-4842.
165. **Madbouly KM, Senagore AJ, Mukerjee A, Hussien AM, Shehata MA, Navine P, Delaney CP, Fazio VW.** 2007. Colorectal cancer in a population with endemic Schistosoma mansoni: is this an at-risk population? Int J Colorectal Dis **22:**175-181.
166. **Cooper HS, Murthy S, Kido K, Yoshitake H, Flanigan A.** 2000. Dysplasia and cancer in the dextran sulfate sodium mouse colitis model. Relevance to colitis-associated neoplasia in the human: a study of histopathology, B-catenin and p53 expression and the role of inflammation. Carcinogenesis **21:**757-768.
167. **Qi J, Yu Y, Akilli Öztürk Ö, Holland JD, Besser D, Fritzmann J, Wulf-Goldenberg A, Eckert K, Fichtner I, Birchmeier W.** 2016. New Wnt/β-catenin target genes promote experimental metastasis and migration of colorectal cancer cells through different signals. Gut **65:**1690-1701.
168. **Zhang Z, Chang Y, Zhang J, Lu Y, Zheng L, Hu Y, Zhang F, Li X, Zhang W, Li X.** 2017. HMGB3 promotes growth and migration in colorectal cancer by regulating WNT/beta-catenin pathway. PLoS One **12:**e0179741.
169. **Peng K, Su G, Ji J, Yang X, Miao M, Mo P, Li M, Xu J, Li W, Yu C.** 2018. Histone demethylase JMJD1A promotes colorectal cancer growth and metastasis by enhancing Wnt/β-catenin signaling. Journal of Biological Chemistry **293:**10606-10619.
170. **Wang HY, Wang R-F.** 2007. Regulatory T cells and cancer. Lymphocyte development/Tumour immunology **19:**217-223.
171. **Wolf D, Sopper S, Pircher A, Gastl G, Wolf AM.** 2015. Treg(s) in Cancer: Friends or Foe? J Cell Physiol **230:**2598-2605.
172. **Nishikawa H, Sakaguchi S.** 2014. Regulatory T cells in cancer immunotherapy. Curr Opin Immunol **27:**1-7.
173. **Donskow-Lysoniewska K, Krawczak K, Doligalska M.** 2012. Heligmosomoides polygyrus: EAE remission is correlated with different systemic cytokine profiles provoked by L4 and adult nematodes. Exp Parasitol **132:**243-248.
174. **Finlay CM, Stefanska AM, Walsh KP, Kelly PJ, Boon L, Lavelle EC, Walsh PT, Mills KH.** 2016. Helminth Products Protect against Autoimmunity via Innate Type 2 Cytokines IL-5 and IL-33, Which Promote Eosinophilia. Journal of immunology (Baltimore, Md: 1950) **196:**703-714.
175. **Li W, Yu KN, Bao L, Shen J, Cheng C, Han W.** 2016. Non-thermal plasma inhibits human cervical cancer HeLa cells invasiveness by suppressing the MAPK pathway and decreasing matrix metalloproteinase-9 expression. Sci Rep **6:**19720.

176. **Pak JH, Bashir Q, Kim IK, Hong SJ, Maeng S, Bahk YY, Kim TS.** 2017. Clonorchis sinensis excretory-secretory products promote the migration and invasion of cholangiocarcinoma cells by activating the integrin beta4-FAK/Src signaling pathway. Mol Biochem Parasitol **214:**1-9.
177. **Pak JH, Shin J, Song IS, Shim S, Jang SW.** 2017. Clonorchis sinensis excretory-secretory products regulate migration and invasion in cholangiocarcinoma cells via extracellular signal-regulated kinase 1/2/nuclear factor-kappaB-dependent matrix metalloproteinase-9 expression. Int J Parasitol **47:**51-59.
178. **Wang C, Lei H, Tian Y, Shang M, Wu Y, Li Y, Zhao L, Shi M, Tang X, Chen T, Lv Z, Huang Y, Tang X, Yu X, Li X.** 2017. Clonorchis sinensis granulin: identification, immunolocalization, and function in promoting the metastasis of cholangiocarcinoma and hepatocellular carcinoma. Parasit Vectors **10:**262.
179. **Botelho M, Ferreira AC, Oliveira MJ, Domingues A, Machado JC, da Costa JM.** 2009. Schistosoma haematobium total antigen induces increased proliferation, migration and invasion, and decreases apoptosis of normal epithelial cells. Int J Parasitol **39:**1083-1091.
180. **Huber MA, Kraut N, Beug H.** 2005. Molecular requirements for epithelial-mesenchymal transition during tumor progression. Curr Opin Cell Biol **17:**548-558.
181. **Nakajima S, Doi R, Toyoda E, Tsuji S, Wada M, Koizumi M, Tulachan SS, Ito D, Kami K, Mori T, Kawaguchi Y, Fujimoto K, Hosotani R, Imamura M.** 2004. N-cadherin expression and epithelial-mesenchymal transition in pancreatic carcinoma. Clin Cancer Res **10:**4125-4133.
182. **Bhat AA, Ahmad R, Uppada SB, Singh AB, Dhawan P.** 2016. Claudin-1 promotes TNF-alpha-induced epithelial-mesenchymal transition and migration in colorectal adenocarcinoma cells. Exp Cell Res **349:**119-127.
183. **Ahn WS, Han YJ, Bae SM, Kim TH, Rho MS, Lee JM, Namkoong SE, Park YS, Kim CK, Sin JI.** 2002. Differential suppression of human cervical cancer cell growth by adenovirus delivery of p53 in vitro: arrest phase of cell cycle is dependent on cell line. Jpn J Cancer Res **93:**1012-1019.
184. **Koraneekit A, Limpaiboon T, Sangka A, Boonsiri P, Daduang S, Daduang J.** 2018. Synergistic effects of cisplatin-caffeic acid induces apoptosis in human cervical cancer cells via the mitochondrial pathways. Oncol Lett **15:**7397-7402.
185. **Filippova M, Filippov V, Williams VM, Zhang K, Kokoza A, Bashkirova S, Duerksen-Hughes P.** 2014. Cellular Levels of Oxidative Stress Affect the Response of Cervical Cancer Cells to Chemotherapeutic Agents. BioMed Research International **2014:**574659.
186. **Mishra PK, Palma M, Bleich D, Loke P, Gause WC.** 2014. Systemic impact of intestinal helminth infections. Mucosal Immunol **7:**753-762.
187. **Price AE, Liang HE, Sullivan BM, Reinhardt RL, Eisley CJ, Erle DJ, Locksley RM.** 2010. Systemically dispersed innate IL-13-expressing cells in type 2 immunity. Proc Natl Acad Sci U S A **107:**11489-11494.
188. **Satelli A, Batth IS, Brownlee Z, Rojas C, Meng QH, Kopetz S, Li S.** 2016. Potential role of nuclear PD-L1 expression in cell-surface vimentin positive circulating tumor cells as a prognostic marker in cancer patients. Sci Rep **6:**28910.
189. **Satelli A, Brownlee Z, Mitra A, Meng QH, Li S.** 2015. Circulating tumor cell enumeration with a combination of epithelial cell adhesion molecule- and cell-surface vimentin-based methods for monitoring breast cancer therapeutic response. Clin Chem **61:**259-266.
190. **Satelli A, Mitra A, Cutrera JJ, Devarie M, Xia X, Ingram DR, Dibra D, Somaiah N, Torres KE, Ravi V, Ludwig JA, Kleinerman ES, Li S.** 2014. Universal marker and detection tool for human sarcoma circulating tumor cells. Cancer Res **74:**1645-1650.
191. **Mitra A, Satelli A, Xia X, Cutrera J, Mishra L, Li S.** 2015. Cell-surface Vimentin: A mislocalized protein for isolating csVimentin(+) CD133(-) novel stem-like hepatocellular carcinoma cells expressing EMT markers. Int J Cancer **137:**491-496.
192. **Letian T, Tianyu Z.** 2010. Cellular receptor binding and entry of human papillomavirus. Virol J **7:**2.
193. **Przemeck S, Huber A, Brown S, Pedley KC, Simpson HV.** 2005. Excretory/secretory products of sheep abomasal nematode parasites cause vacuolation and increased neutral red uptake by HeLa cells. Parasitol Res **95:**213-217.
194. **Rehman ZU, Deng Q, Umair S, Savoian MS, Knight JS, Pernthaner A, Simpson HV.** 2016. Excretory/secretory products of adult Haemonchus contortus and Teladorsagia circumcincta which increase the permeability of Caco-2 cell monolayers are neutralised by antibodies from immune hosts. Vet Parasitol **221:**104-110.

195. **Vaux R, Schnoeller C, Berkachy R, Roberts LB, Hagen J, Gounaris K, Selkirk ME.** 2016. Modulation of the Immune Response by Nematode Secreted Acetylcholinesterase Revealed by Heterologous Expression in Trypanosoma musculi. PLoS Pathog **12:**e1005998.
196. **Ball G, Selkirk ME, Knox DP.** 2007. The effect of vaccination with a recombinant Nippostrongylus brasiliensis acetylcholinesterase on infection outcome in the rat. Vaccine **25:**3365-3372.
197. **Selkirk ME, Lazari O, Hussein AS, Matthews JB.** 2005. Nematode acetylcholinesterases are encoded by multiple genes and perform non-overlapping functions. Chem Biol Interact **157-158:**263-268.
198. **Russell WS, Henson SM, Hussein AS, Tippins JR, Selkirk ME.** 2000. Nippostrongylus brasiliensis: infection induces upregulation of acetylcholinesterase activity on rat intestinal epithelial cells. Exp Parasitol **96:**222-230.
199. **Wang XL, Fu BQ, Yang SJ, Wu XP, Cui GZ, Liu MF, Zhao Y, Yu YL, Liu XY, Deng HK, Chen QJ, Liu MY.** 2009. Trichinella spiralis--a potential anti-tumor agent. Vet Parasitol **159:**249-252.
200. **Markowitz SD, Bertagnolli MM.** 2009. Molecular Origins of Cancer: Molecular Basis of Colorectal Cancer. The New England journal of medicine **361:**2449-2460.
201. **Morin PJ, Sparks AB, Korinek V, Barker N, Clevers H, Vogelstein B, Kinzler KW.** 1997. Activation of beta-catenin-Tcf signaling in colon cancer by mutations in beta-catenin or APC. Science **275:**1787-1790.
202. **Triner D, Xue X, Schwartz AJ, Jung I, Colacino JA, Shah YM.** 2017. Epithelial Hypoxia-Inducible Factor 2alpha Facilitates the Progression of Colon Tumors through Recruiting Neutrophils. Mol Cell Biol **37**.
203. **Inamoto S, Itatani Y, Yamamoto T, Minamiguchi S, Hirai H, Iwamoto M, Hasegawa S, Taketo MM, Sakai Y, Kawada K.** 2016. Loss of SMAD4 Promotes Colorectal Cancer Progression by Accumulation of Myeloid-Derived Suppressor Cells through the CCL15-CCR1 Chemokine Axis. Clin Cancer Res **22:**492-501.
204. **Caiado F, Carvalho T, Rosa I, Remedio L, Costa A, Matos J, Heissig B, Yagita H, Hattori K, da Silva JP, Fidalgo P, Pereira AD, Dias S.** 2013. Bone marrow-derived CD11b+Jagged2+ cells promote epithelial-to-mesenchymal transition and metastasization in colorectal cancer. Cancer Res **73:**4233-4246.
205. **Chang F, Lee JT, Navolanic PM, Steelman LS, Shelton JG, Blalock WL, Franklin RA, McCubrey JA.** 2003. Involvement of PI3K/Akt pathway in cell cycle progression, apoptosis, and neoplastic transformation: a target for cancer chemotherapy. Leukemia **17:**590.
206. **Liu P, Cheng H, Roberts TM, Zhao JJ.** 2009. Targeting the phosphoinositide 3-kinase (PI3K) pathway in cancer. Nature reviews Drug discovery **8:**627-644.
207. **Janku F, Yap TA, Meric-Bernstam F.** 2018. Targeting the PI3K pathway in cancer: are we making headway? Nature Reviews Clinical Oncology **15:**273.
208. **Abu-Eid R, Samara RN, Ozbun L, Abdalla MY, Berzofsky JA, Friedman KM, Mkrtichyan M, Khleif SN.** 2014. Selective inhibition of regulatory T cells by targeting the PI3K-Akt pathway. Cancer Immunol Res **2:**1080-1089.
209. **Ahmad S, Abu-Eid R, Shrimali R, Webb M, Verma V, Doroodchi A, Berrong Z, Samara R, Rodriguez PC, Mkrtichyan M, Khleif SN.** 2017. Differential PI3Kdelta Signaling in CD4(+) T-cell Subsets Enables Selective Targeting of T Regulatory Cells to Enhance Cancer Immunotherapy. Cancer Res **77:**1892-1904.
210. **Qin A, Wen Z, Zhou Y, Li Y, Li Y, Luo J, Ren T, Xu L.** 2013. MicroRNA-126 regulates the induction and function of CD4(+) Foxp3(+) regulatory T cells through PI3K/AKT pathway. J Cell Mol Med **17:**252-264.
211. **Yothaisong S, Thanee M, Namwat N, Yongvanit P, Boonmars T, Puapairoj A, Loilome W.** 2014. Opisthorchis viverrini infection activates the PI3K/ AKT/PTEN and Wnt/beta-catenin signaling pathways in a Cholangiocarcinogenesis model. Asian Pac J Cancer Prev **15:**10463-10468.
212. **Wang X, Teng F, Kong L, Yu J.** 2016. PD-L1 expression in human cancers and its association with clinical outcomes. OncoTargets and therapy **9:**5023-5039.
213. **Smith P, Walsh CM, Mangan NE, Fallon RE, Sayers JR, McKenzie AN, Fallon PG.** 2004. Schistosoma mansoni worms induce anergy of T cells via selective up-regulation of programmed death ligand 1 on macrophages. J Immunol **173:**1240-1248.
214. **Terrazas LI, Montero D, Terrazas CA, Reyes JL, Rodriguez-Sosa M.** 2005. Role of the programmed Death-1 pathway in the suppressive activity of alternatively activated macrophages in experimental cysticercosis. Int J Parasitol **35:**1349-1358.

215. **Hindley JP, Jones E, Smart K, Bridgeman H, Lauder SN, Ondondo B, Cutting S, Ladell K, Wynn KK, Withers D, Price DA, Ager A, Godkin AJ, Gallimore AM.** 2012. T-cell trafficking facilitated by high endothelial venules is required for tumor control after regulatory T-cell depletion. Cancer Res **72:**5473-5482.
216. **Ager A, May MJ.** 2015. Understanding high endothelial venules: Lessons for cancer immunology. Oncoimmunology **4:**e1008791.
217. **Turley SJ, Cremasco V, Astarita JL.** 2015. Immunological hallmarks of stromal cells in the tumour microenvironment. Nat Rev Immunol **15:**669-682.
218. **Park JH, Richards CH, McMillan DC, Horgan PG, Roxburgh CS.** 2014. The relationship between tumour stroma percentage, the tumour microenvironment and survival in patients with primary operable colorectal cancer. Ann Oncol **25:**644-651.
219. **Leon-Cabrera SA, Molina-Guzman E, Delgado-Ramirez YG, Vazquez-Sandoval A, Ledesma-Soto Y, Perez-Plasencia CG, Chirino YI, Delgado-Buenrostro NL, Rodriguez-Sosa M, Vaca-Paniagua F, Avila-Moreno F, Gutierrez-Cirlos EB, Arias-Romero LE, Terrazas LI.** 2017. Lack of STAT6 Attenuates Inflammation and Drives Protection against Early Steps of Colitis-Associated Colon Cancer. Cancer Immunol Res **5:**385-396.
220. **Du L, Tang H, Ma Z, Xu J, Gao W, Chen J, Gan W, Zhang Z, Yu X, Zhou X, Hu X.** 2011. The protective effect of the recombinant 53-kDa protein of Trichinella spiralis on experimental colitis in mice. Dig Dis Sci **56:**2810-2817.
221. **Heylen M, Ruyssers NE, Nullens S, Schramm G, Pelckmans PA, Moreels TG, De Man JG, De Winter BY.** 2015. Treatment with egg antigens of Schistosoma mansoni ameliorates experimental colitis in mice through a colonic T-cell-dependent mechanism. Inflamm Bowel Dis **21:**48-59.
222. **Li Z, Pang Y, Gara SK, Achyut BR, Heger C, Goldsmith PK, Lonning S, Yang L.** 2012. Gr-1+CD11b+ cells are responsible for tumor promoting effect of TGF-beta in breast cancer progression. Int J Cancer **131:**2584-2595.
223. **Chen X, Yang Y, Zhou Q, Weiss JM, Howard OZ, McPherson JM, Wakefield LM, Oppenheim JJ.** 2014. Effective chemoimmunotherapy with anti-TGFbeta antibody and cyclophosphamide in a mouse model of breast cancer. PLoS One **9:**e85398.
224. **Liang Y, Zhu F, Zhang H, Chen D, Zhang X, Gao Q, Li Y.** 2016. Conditional ablation of TGF-beta signaling inhibits tumor progression and invasion in an induced mouse bladder cancer model. Sci Rep **6:**29479.
225. **Oft M, Heider K-H, Beug H.** TGF-B signaling is necessary for carcinoma cell invasiveness and metastasis. Current Biology **8:**1243-1252.
226. **Shuang ZY, Wu WC, Xu J, Lin G, Liu YC, Lao XM, Zheng L, Li S.** 2014. Transforming growth factor-beta1-induced epithelial-mesenchymal transition generates ALDH-positive cells with stem cell properties in cholangiocarcinoma. Cancer Lett **354:**320-328.
227. **Xu J, Lamouille S, Derynck R.** 2009. TGF-beta-induced epithelial to mesenchymal transition. Cell Res **19:**156-172.
228. **Hewitson JP, Harcus Y, Murray J, van Agtmaal M, Filbey KJ, Grainger JR, Bridgett S, Blaxter ML, Ashton PD, Ashford D, Curwen RS, Wilson RA, Dowle AA, Maizels RM.** 2011. Proteomic analysis of secretory products from the model gastrointestinal nematode Heligmosomoides polygyrus reveals dominance of Venom Allergen-Like (VAL) proteins. Journal of proteomics **74:**1573-1594.
229. **Donigan M, Loh BD, Norcross LS, Li S, Williamson PR, DeJesus S, Ferrara A, Gallagher JT, Baker CH.** 2010. A metastatic colon cancer model using nonoperative transanal rectal injection. Surg Endosc **24:**642-647.
230. **Taylor S, Huang Y, Mallett G, Stathopoulou C, Felizardo TC, Sun M-A, Martin EL, Zhu N, Woodward EL, Elias MS, Scott J, Reynolds NJ, Paul WE, Fowler DH, Amarnath S.** 2017. PD-1 regulates KLRG1(+) group 2 innate lymphoid cells. The Journal of Experimental Medicine **214:**1663-1678.
231. **Buck AH, Coakley G, Simbari F, McSorley HJ, Quintana JF, Le Bihan T, Kumar S, Abreu-Goodger C, Lear M, Harcus Y, Ceroni A, Babayan SA, Blaxter M, Ivens A, Maizels RM.** 2014. Exosomes secreted by nematode parasites transfer small RNAs to mammalian cells and modulate innate immunity. Nature communications **5:**5488.

8. Appendix

8.1 *Heligmosomoides polygyrus* antigen and HES Preparation

Hanks Media:

Supplemented with 100 µg/ml penicillin and 100 µg/ml streptomycin

H. polygyrus Media:

RPMI supplemented with 11.1 ml 25% glucose, 100µg/ml penicillin and 100µg/ml streptomycin, 100 µg/ml L-glutamine and 100 µg/ml Gentomycin

MACs Buffer:

1x PBS supplemented with 0.5%BSA and 2mM EDTA

8.2 Cell Line Culture

Dulbecco's Modified Eagle Medium:

Supplemented with 10% foetal bovine serum (FBS – Gibco No. 10500064), 100 µg/ml penicillin (Sigma-Aldrich-Aldrich No. P032-10MU) and 100 µg/ml streptomycin (Sigma-Aldrich-Aldrich No. S9137-25G)

Roswell Park Memorial Institute Medium-1640:

Supplemented with 10% foetal bovine serum (FBS), 100 µg/ml penicillin and 100 µg/ml streptomycin

McCoy's Modified 5a Medium:

Supplemented with 10% foetal bovine serum (FBS), 100 µg/ml penicillin and 100 µg/ml streptomycin

8.3 Mycoplasma Testing

Fixative:

3:1 Methanol: Acetic Acid

Mounting Fluid:

20mM Citric acid

55mM $Na_2HPO_4.2H_2O$

50% Glycerol

pH5.5 and store at 4°C

8.4 *In vitro* Assays

Trypsin-EDTA:

8g NaCl

1.26g Na_2HPO_4

0.2g KCl

0.2g KH_2PO_4

0.5g -20°C Trypsin (Sigma-Aldrich No. 79794)

0.2g EDTA

Make up to 1L with dH_2O, pH 7.4

Filter-sterilise through 0.2µm filter and autoclave

Phosphate buffered saline (PBS)

10X PBS:

80g NaCl

26.8g $Na_2HPO_4.12H_20$

2g KCl

2.4g KH_2PO_4

Make up to 1L with dH_2O, pH 6.9 and autoclave

For use dilute to 1 X (100ml 10X PBS; make up to 1L with dH20)

PBS/0.1% Tween:

1ml Tween20 to 1X PBS

Carnoy's Fixative

MeOH: Acetic Acid 3:1

2M HCL

60ml dH_2O

40ml 10 N HCL

PBS/0.5% Tween20

200ml of 1X PBS

100µl Tween20

Mix and store at 4°C

0.1M Borate Buffer

7.6g Sodium Borate (borax MW=381.4)

200ml of dH_2O

Mix and pH to 8.5 with HCL

Lidocaine-EDTA:

4mg/ml Lidocaine (Sigma-Aldrich L5647-15G) and 10mM EDTA

8.5 Western Blotting

SDS-PAGE Buffer/Boiling Blue: 10ml

832µl 1.5M Tris-HCl (pH 6.8)

4ml 10% SDS

1ml β-mercaptoethanol

2ml glycerol

2.168ml dH2O

Pinch of bromophenol blue

70µl of boiling blue was added to a 100% confluent well of a 6cm dish

Sodium Dodecyl Sulphate (SDS)-polyacrylamide gels

Acryl-bisacryl-amide mix (30:08):

29 g acrylamide

1g N,N'-methylenebisacrylamide

Make up to 100ml, heat at 37°C to dissolve chemicals.

Store at 4°C, protected from light

10% Sodium dodecyl sulphate (SDS):

100g SDS

Make up to 1L with dH20, pH 7.2

Store at room temperature

10% Ammonium persulphate (APS):

0.1g Ammonium persulphate (Promega No. V3131)

Make solution up to 1ml with dH20

Store at 4°C

4% Stacking gel (1):

3.635ml dH20

625µl 40% Acrylamide

630µl 1.5M Tris (pH 6.8)

50µl 10% SDS

5µl TEMED

50µl 10% Ammonium persulphate

6% Resolving gel:

5.5ml dH20

1.5ml 40% Acrylamide

2.5ml 1.5M Tris (pH 8.8)

100µl 10% SDS

10µl TEMED

100µl 10% Ammonium persulphate

8% Resolving gel:

5.03ml dH20

2ml 40% Acrylamide

2.5ml 1.5M Tris (pH 8.8)

100µl 10% SDS

10µl TEMED

100µl 10% Ammonium persulphate

15% Resolving gel:

3.5ml dH20

3.75ml 40% Acrylamide

2.5ml 1.5M Tris (pH 8.8)

100µl 10% SDS

10µl TEMED

100µl 10% Ammonium persulphate

10X Running buffer:

10g SDS

30g Tris

144g Glycine

pH 8.3 and make solution up to 1L with dH20

For use dilute to 1 X (100ml 10X PBS; make up to 1L with dH20)

10X Transfer buffer:

38g Tris

144g Glycine

Make solution up to 1L with dH_20 and store at 4°C

For use dilute 1 X (100ml 10 X Transfer Buffer, 200ml Methanol and 700ml dH20)
Store at 4°C

Tris buffered saline (TBS)/0.1% Tween20

10X TBS:

6.05g 50mM Tris

8.76g150mM NaCl

Make up to 1L, pH 7.5 and autoclave

For use dilute to 1 X (100ml 10X TBS; make up to 1L with dH20)

TBS/0.1% Tween:

1ml Tween20 to 1X TBS

5% Bovine Serum Albumin (BSA)

2.5g BSA

50ml dH_2O

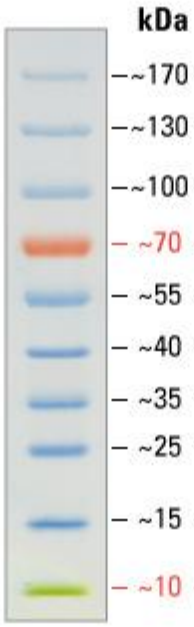

Thermo Scientific PageRuler™ Prestained Protein Marker.

8.6 *In vivo* Experiments

FACs Buffer:

1x PBS supplemented with 5%BSA and 1% Sodium Azide

4% paraformaldehyde

Dilute 37% formaldehyde to 4% using 1X PBS